Slides on r-process enrichment of stars and planets

Joel Primack — UCSC — May 2021

Making the Heaviest Elements in the Universe: A Review of the Rapid Neutron Capture Process - Cowan, Sneden, et al. arXiv:1901.01410

The Origin of r-process Elements in the Milky Way - Benoit Côté, Chris L. Fryer, et al. ApJ, 855, 99, 2018 March 10

STELLAR CHEMICAL SIGNATURES AND HIERARCHICAL GALAXY FORMATION Venn et al. 2004 AJ

Chemical Abundances of Neutron-capture Elements in Exoplanet-hosting Stars - Delgado Mena et al. PASP 130:094202, 2018

Spectral Properties of Cool Stars: Extended Abundance Analysis of Kepler Objects of Interest - Brewer &Fischer ApJ (2018)

Oxygen fugacities of extrasolar rocks: Evidence for an Earth-like geochemistry of exoplanets - Doyle+ Science 2019

SCALING THE EARTH: A SENSITIVITY ANALYSIS OF TERRESTRIAL EXOPLANETARY INTERIOR MODELS - Unterborn et al. - ApJ 2016

THORIUM ABUNDANCES IN SOLAR TWINS AND ANALOGS: IMPLICATIONS FOR HABITABILITY - Unterborn, Johnson, Panero - ApJ (2015)

Thorium in solar twins: implications for habitability in rocky planets - Botelho et al. MNRAS 482, 1690 (2019)

The origin and evolution of r- and s-process elements in the Milky Way stellar disk - Battistini & Bensby, A&A 2016

The GALAH Survey: Temporal Chemical Enrichment of the Galactic Disk - Jane Lin, Martin Asplund, et al. MNRAS 2019

First results from the IllustrisTNG simulations: a tale of two elements - Mg and Eu - Jill P. Naiman+ MNRAS 477, 1206 (2018)

NSMs and rare CCSNe as sources of r-process in simulated galaxies -Freeke van de Voort+ arXiv:1907.01557

COMPREHENSIVE GEONEUTRINO ANALYSIS WITH BOREXINO - M. Agostini et al. arXiv:1909.02257 **PRD.101.012009 (2020)**

A radiogenic heating evolution model for cosmochemically Earth-like exoplanets - Frank et al. - Icarus (2014)

Carbon cycling and habitability of Earth-size stagnant lid planets B. J. Foley & A. J. Smye arXiv:1712.03614v1

Habitability of Earth-like Stagnant Lid Planets: Climate Evolution and Recovery from Snowball States - B.J.Foley ApJ 2019

A nearby neutron-star merger explains the early solar system actinide abundances - I. Bartos & S. Marka - Nature 2019

Reviews: Luongo+2018 on Short-lived Radioisotopes and ESS; Shahar+2019 What Makes a Planet Habitable?

Distribution and Variation of Radioactive Heat Producing Elements Within Meteorites, the Earth, and Planets O'Neill+2020 Space Sci Reviews

Water in Extrasolar Planets and Implications for Habitability - Lena Noack+ Space Sci Reviews 2017

Making the Heaviest Elements in the Universe: A Review of the Rapid Neutron Capture Process

John J. Cowan, Christopher Sneden, et al. arXiv:1901.01410

The production of about half the heavy elements (beyond Fe and Ni) found in nature is assigned to a specific astrophysical nucleosynthesis process: the rapid neutron capture process (r process). Although this idea has been postulated more than six decades ago, the full understanding faces two types of uncertainties/open questions: (a) The nucleosynthesis path in the nuclear chart runs close to the neutron-drip line, where presently only limited experimental information is available, and one has to rely strongly on theoretical predictions for nuclear properties. (b) **While for many years the occurrence of the r process has been associated with supernovae, where the innermost ejecta close to the central neutron star were supposed to be neutron-rich, more recent studies have cast substantial doubts on this environment.** Possibly only a weak r process, not producing the third r-process peak, can be accounted for, while much more neutron-rich conditions, including an r-process path with fission-cycling, are likely responsible for the majority of the heavy r-process elements. Such conditions could result during the ejection of initially highly neutron-rich matter, as found in neutron stars, or during the fast ejection of matter which has prior experienced strong electron-captures at high densities. **Possible scenarios are the mergers of neutron stars, neutron-star black hole mergers, but include also rare classes of supernovae/hypernovae with polar jet ejecta** (and possibly also accretion disk outflows in case of black hole formation) related to the collapse of fast rotating massive stars with high magnetic fields. The composition of the ejecta from each event determines the temporal evolution of the r-process abundances during the "chemical" evolution of the Galaxy. Stellar r-process abundance observations, have provided insights into, and constraints on the frequency of and conditions in the responsible stellar production sites. **One of them, neutron star mergers, was just identified thanks to the observation of the r-process kilonova electromagnetic transient, AT 2017gfo, following the Gravitational wave event GW170817**. These observations, increasingly more precise due to improved experimental atomic data and high resolution observations, have been particularly important in defining the heavy element abundance patterns of the old halo stars, and thus determining the extent, and nature, of the earliest nucleosynthesis in our Galaxy. Combining new results and important breakthroughs in the related nuclear, atomic and astronomical fields of science, this review attempts to provide an answer to the question "How Were the Elements from Iron to Uranium Made?"

Some elements are only formed exclusively or almost so in the r process, such as Eu, Os, Ir, Pt, Th and U (see Figure 2). Their presence in old very metal- poor Galactic halo stars is a clear indication that this neutron process occurred in some violent astrophysical site early in the history of the Galaxy and the Universe (see e.g. Sneden et al., 2008; Thielemann et al., 2017b, and references therein). … **Common r-process elements, like Eu, display an extensive scatter, indicating that they are made in rare events which contribute significant amounts of material, when they occur (see Fig. 8).**

Making the Heaviest Elements in the Universe: A Review of the Rapid Neutron Capture Process

John J. Cowan, Christopher Sneden, et al. arXiv:1901.01410

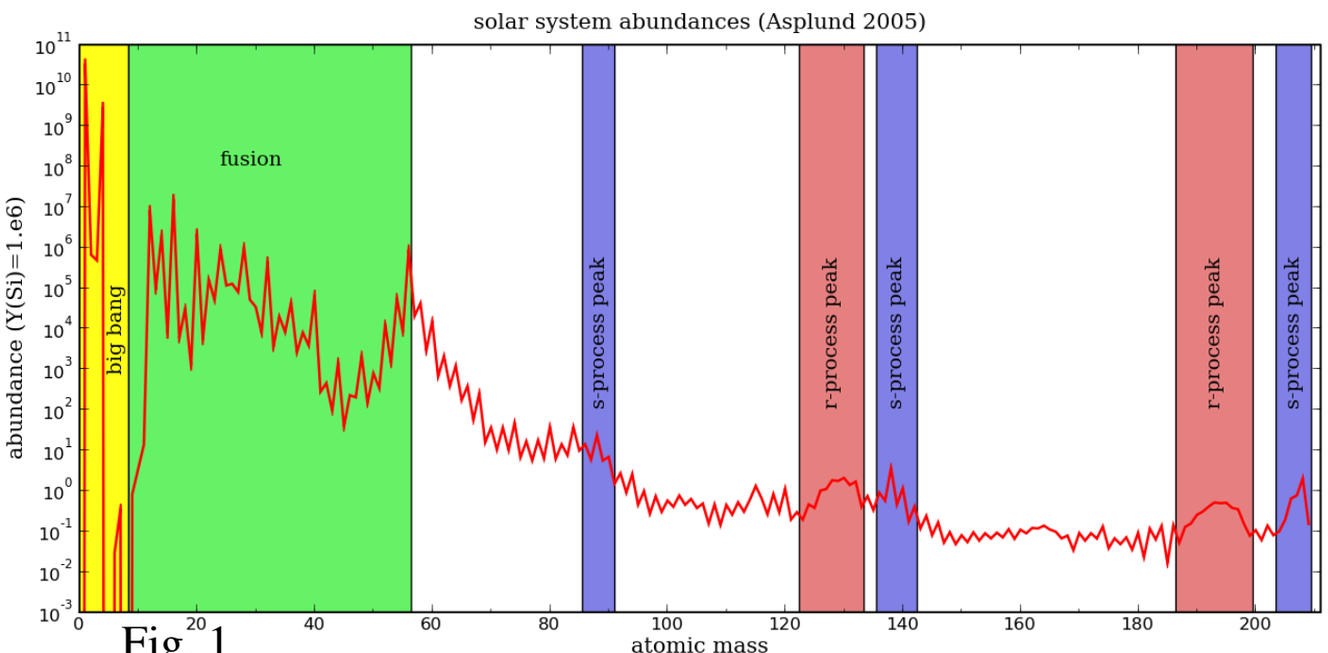

Fig. 1

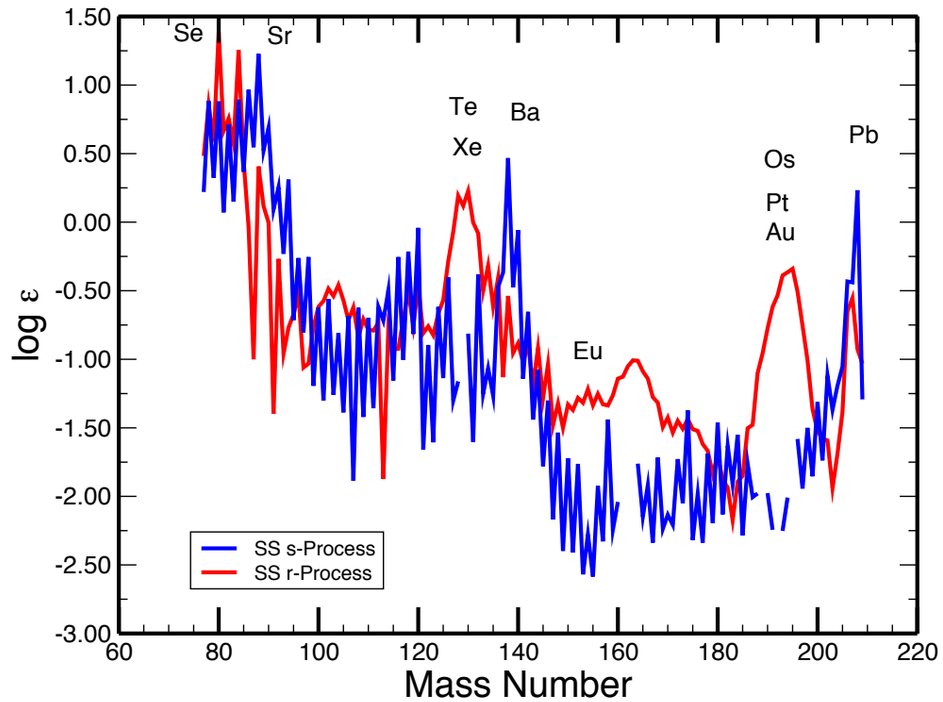

FIG. 2 Breakdown of the solar system abundances into the s and the r process (Cowan and Thielemann, 2004).

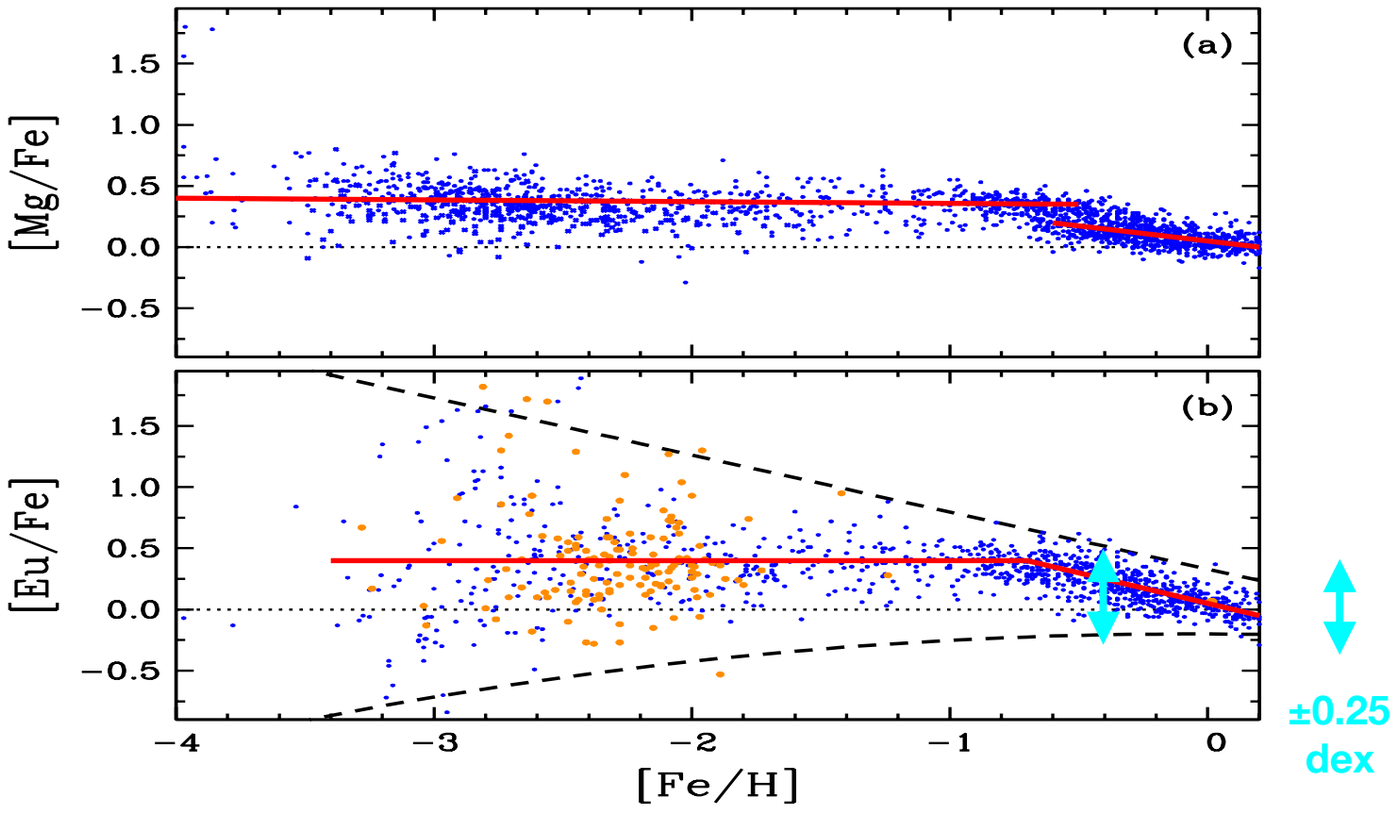

Fig. 8 Abundances as a function of metallicity for [Mg/Fe] (panel a) and [Eu/Fe] (panel b). This is an update of Fig. 14 in (Sneden et al., 2008). Red straight lines are approximate fits to the averages of halo, thick disk, and thin disk stars. Black dashed lines in panel (b) highlight the growing star-to-star scatter in [Eu/Fe] with decreasing metallicity.

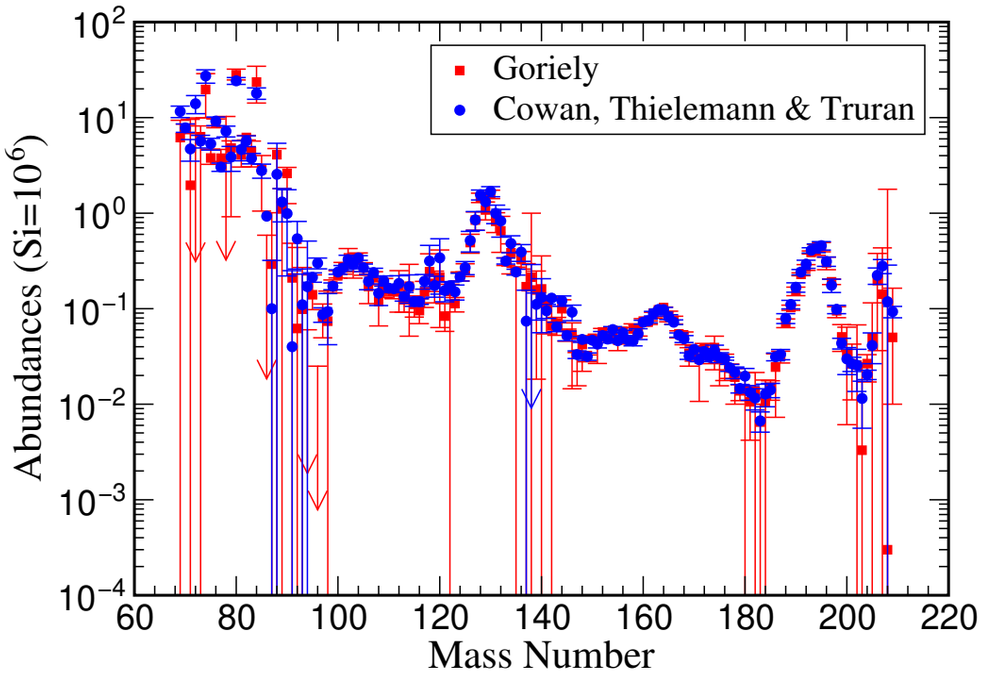

FIG. 3 Solar r-process abundances as determined by Cowan *et al.* (1991) and Goriely (1999). The largest uncertainties are clearly visible for $A \lesssim 100$ (weak s process region) and around lead.

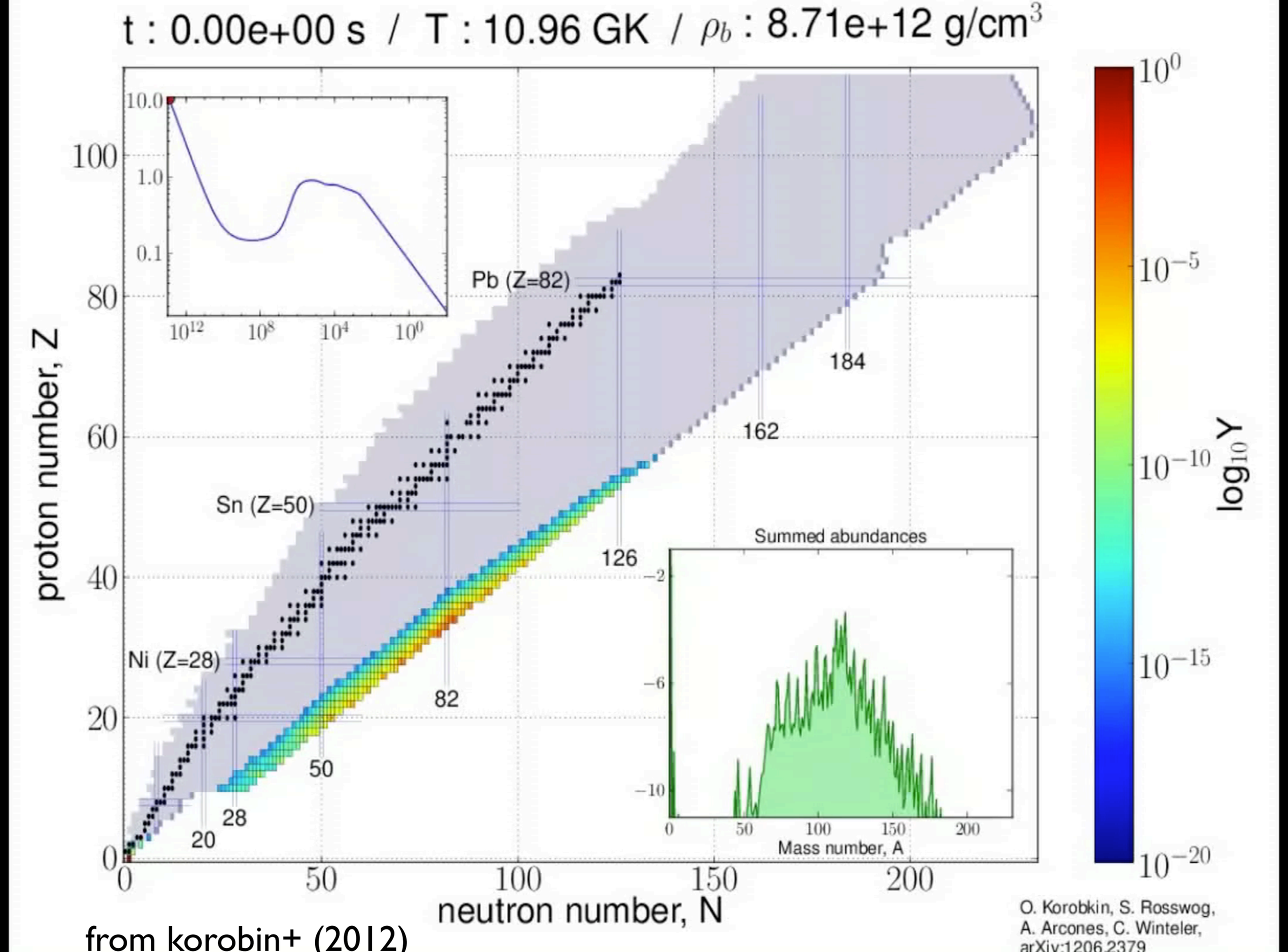

from korobin+ (2012)

The Origin of r-process Elements in the Milky Way - Benoit Côté, Chris L. Fryer, et al. ApJ, 855, 99, 2018 March 10

ABSTRACT Some of the heavy elements, such as gold and europium (Eu), are almost exclusively formed by the rapid neutron capture process (r-process). However, it is still unclear which astrophysical site between core-collapse supernovae and neutron star–neutron star (NS–NS) mergers produced most of the r-process elements in the universe. Galactic chemical evolution (GCE) models can test these scenarios by quantifying the frequency and yields required to reproduce the amount of europium (Eu) observed in galaxies. Although NS–NS mergers have become popular candidates, their required frequency (or rate) needs to be consistent with that obtained from gravitational wave measurements. Here, we address the first NS–NS merger detected by LIGO/Virgo (GW170817) and its associated gamma-ray burst and analyze their implication for the origin of r-process elements. **The range of NS–NS merger rate densities of 320–4740 Gpc^{-3} yr^{-1} provided by LIGO/Virgo is remarkably consistent with the range required by GCE to explain the Eu abundances in the Milky Way with NS–NS mergers, assuming the solar r-process abundance pattern for the ejecta.** Under the same assumption, **this event has produced about 1–5 Earth masses of Eu, and 3–13 Earth masses of gold**. When using theoretical calculations to derive Eu yields, constraining the role of NS–NS mergers becomes more challenging because of nuclear astrophysics uncertainties. This is the first study that directly combines nuclear physics uncertainties with GCE calculations. **If GW170817 is a representative event, NS–NS mergers can produce Eu in sufficient amounts and are likely to be the main r-process site.**

2.2 r-Process Yields. In principle, **the ratio of third to second r-process peaks from GW170817 may not match the solar abundance pattern.** The uncertainties in wind versus dynamical ejecta masses for current light curve fits to GW170817 shown in Table 1 allow for a wide range of ratios of the r-process peaks…

5.5. **Using Europium as the r-process Tracer**. … However, as mentioned in Section 2.2, it is not guaranteed that the third to second r-process peak ratio ejected by GW170817 follows the solar distribution. In the case where the second peak is overestimated relative to the third peak, using Eu from Table 2 with GCE to quantify the role of NS–NS mergers would be irrelevant, as matching Eu would lead to an overestimation of the second peak. On the other hand, if the second peak in the GW170817 ejecta is underestimated, matching Eu with GCE would be reliable, but additional r-process sites would be needed to generate the missing lighter r-process elements (e.g., neutrino-driven winds in CCSNe, Arcones & Thielemann 2013).

STELLAR CHEMICAL SIGNATURES AND HIERARCHICAL GALAXY FORMATION Venn et al. 2004 AJ

To compare the chemistries of stars in the Milky Way dwarf spheroidal (dSph) satellite galaxies with stars in the Galaxy, we have compiled a large sample of Galactic stellar abundances from the literature. When kinematic information is available, we have assigned the stars to standard Galactic components through Bayesian classification based on Gaussian velocity ellipsoids. As found in previous studies, the [/Fe] ratios of most stars in the dSph galaxies are generally lower than similar metallicity Galactic stars in this extended sample. Our kinematically selected stars confirm this for the Galactic halo, thin-disk, and thick-disk components. …

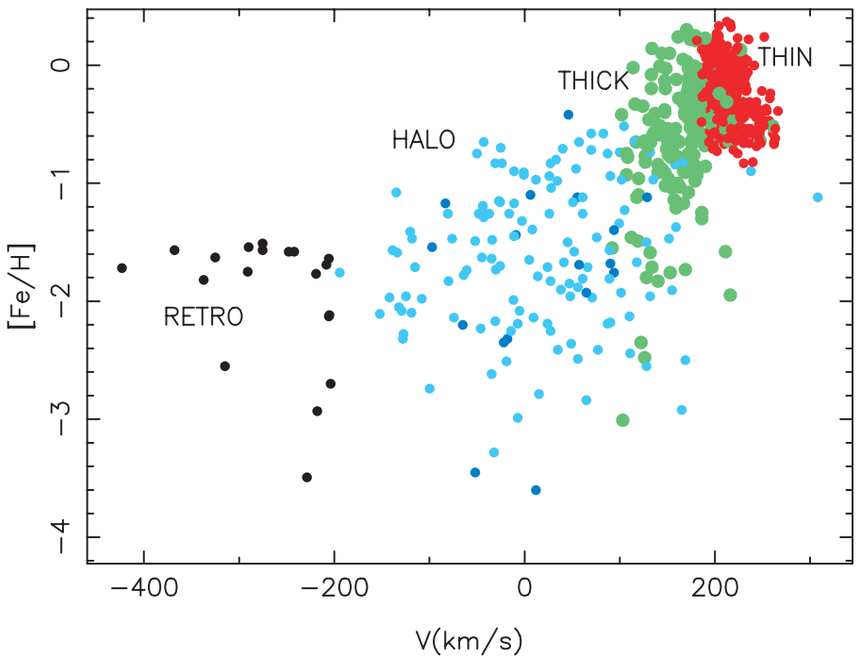

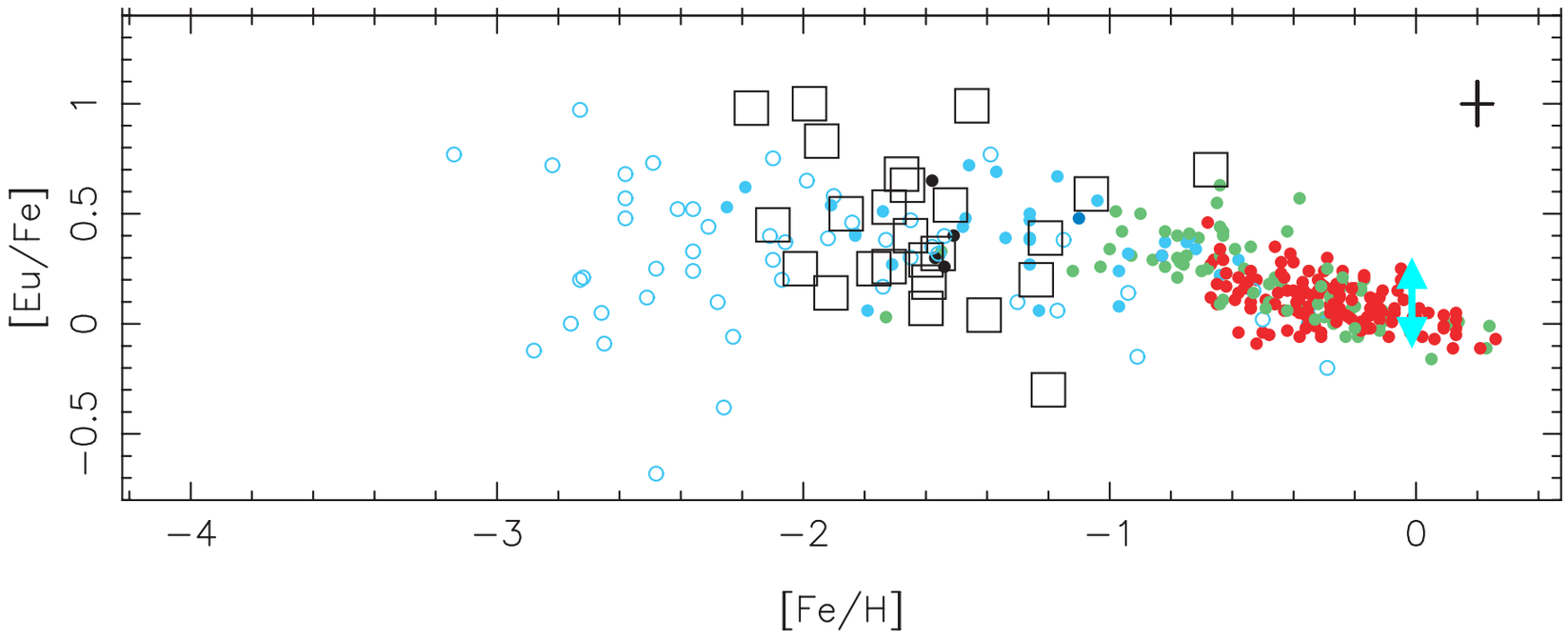

Fig. 3 Stars without kinematic information are plotted as hollow data points. The dSph stars are black squares.

±0.2 dex

E. Delgado Mena et al. 2017, Chemical abundances of 1111 FGK stars from the HARPS GTO planet search program. II. Cu, Zn, Sr, Y, Zr, Ba, Ce, Nd, and Eu https://ui.adsabs.harvard.edu/abs/2017A%26A...606A..94D

We derive chemical abundances of Cu, Zn, Sr, Y, Zr, Ba, Ce, Nd, and Eu for a large sample of more than 1000 FGK dwarf stars with high-resolution (R ~ 115 000) and high-quality spectra from the HARPS-GTO program. . We find that thick disc stars are chemically disjunct for Zn and Eu and also show on average higher Zr but lower Ba and Y than the thin disc stars. We also discovered that the previously identified high-α metal-rich population is also enhanced in Cu, Zn, Nd, and Eu with respect to the thin disc but presents lower Ba and Y abundances on average, following the trend of thick disc stars towards higher metallities and further supporting the different chemical composition of this population. By making a qualitative comparison of O (pure α), Mg, Eu (pure r-process), and s-process elements we can distinguish between the contribution of the more massive stars (SNe II for α and r-process elements) and the lower mass stars (AGBs) whose contribution to the enrichment of the Galaxy is delayed, due to their longer lifetimes. The ratio of heavy-s to light-s elements of thin disc stars presents the expected behaviour (increasing towards lower metallicities) and can be explained by a major contribution of low-mass AGB stars for s-process production at disc metallicities. However, the opposite trend found for thick disc stars suggests that intermediate-mass AGB stars play an important role in the enrichment of the gas from where these stars formed. Previous works in the literature also point to a possible primary production of light-s elements at low metallicities to explain this trend. Finally, we also find an enhancement of light-s elements in the thin disc at super-solar metallicities which could be caused by the contribution of metal-rich AGB stars. This work proves the utility of homogeneous and high-quality data of modest sample sizes. We find some interesting trends that might help to differentiate thin and thick disc population (such as [Zn/Fe] and [Eu/Fe] ratios) and that can also provide useful constraints for Galactic chemical evolution models of the different populations in the Galaxy.

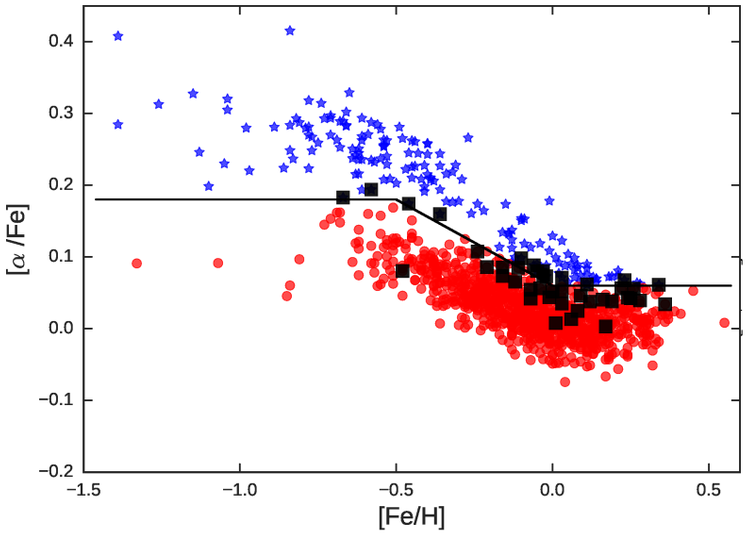

Fig. 9. Updated abundances of α elements (mean abundance of Si, Mg, and Ti) with the new stellar parameters presented in this work. Thin disc stars (red circles) and thick disc stars (blue stars) are chemically separated by their α content (thick line). The *hαmr* stars are the prolongation of thick disc stars at [Fe/H] > –0.2 dex. The stars with a different classification with respect to Adibekyan et al. (2011) are shown as black squares.

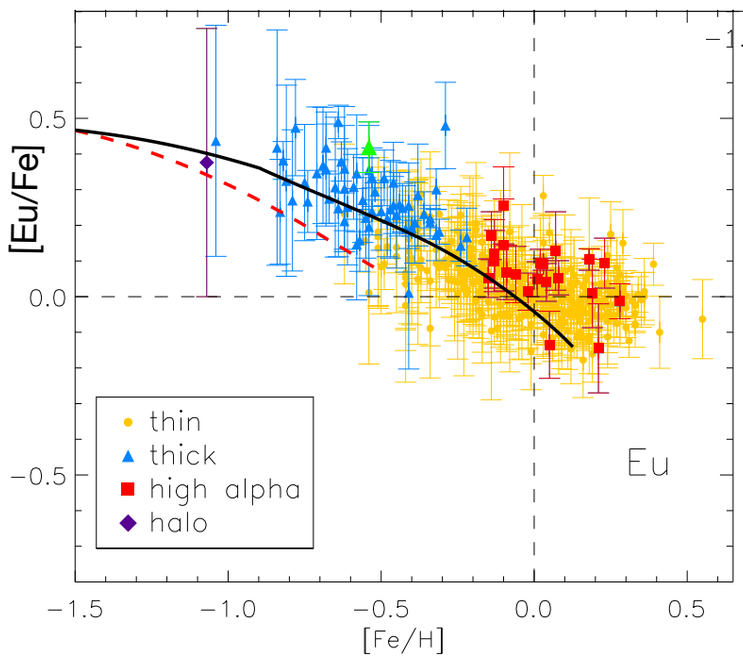

Fig. 10. Final [X/Fe] ratios as a function of [Fe/H] for stars with $T_{\rm eff}$ >5300K and S/N > 100. [The full figures 10, 11, and 12 have many other elements.]

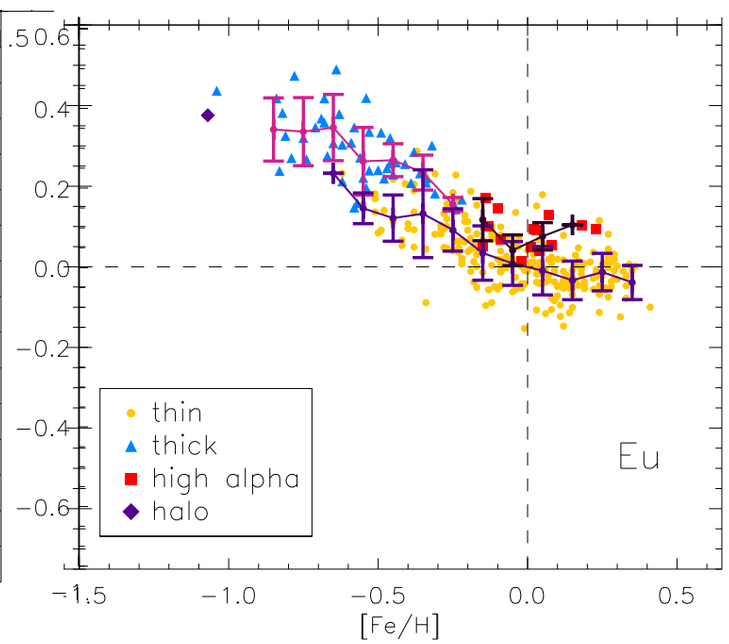

Fig. 11. Final [X/Fe] ratios as a function of [Fe/H] for stars with $T_{\rm eff\,\odot}$ ± 300 K. The different stellar populations are depicted with different colours and symbols as explained in the legend. The mean abundances in each metallicity bin of 0.1 dex are shown together with the standard deviation.

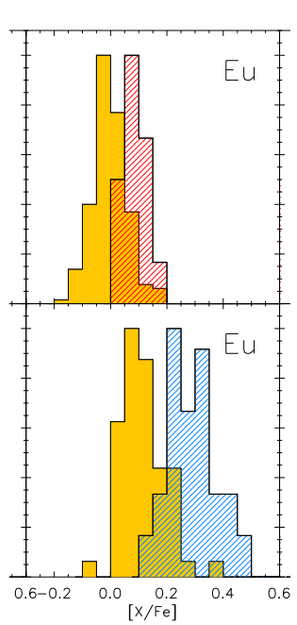

Fig. 12. Yellow: thin disk [Fe/H] ≥ –0.2,
Red: *hαmr* stars,
Blue: thick disk stars

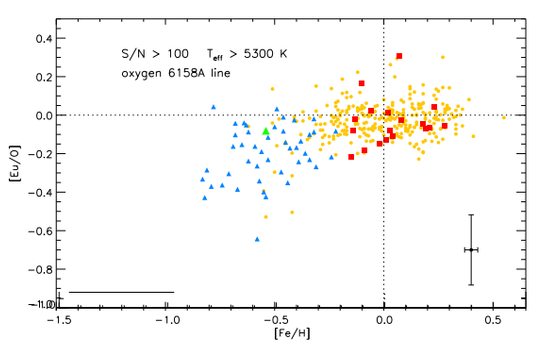

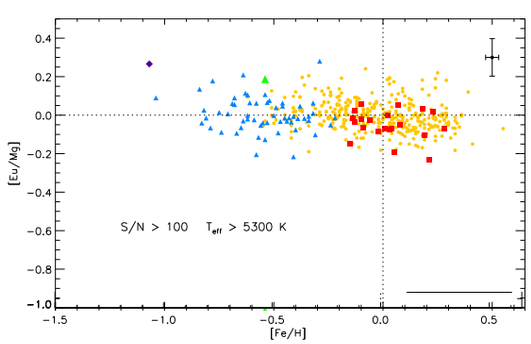

Figs. 14 & 15. [Eu/O] and [Eu/Mg] vs. [Fe/H] for stars with $T_{\rm eff}$ > 5300 K and S/N > 100. Symbols are as in Fig. 10.

Publications of the Astronomical Society of the Pacific, 130:094202 (14pp), 2018 September https://iopscience.iop.org/article/10.1088/1538-3873/aacc1f

Chemical Abundances of Neutron-capture Elements in Exoplanet-hosting Stars

E. Delgado Mena et al. PASP 2018

To understand the formation and composition of planetary systems it is important to study their host stars composition since both are formed in the same stellar nebula. In this work, we analyze the behaviour of chemical abundances of Cu, Zn, Sr, Y, Zr, Ba, Ce, Nd, and Eu in the large and homogeneous HARPS-GTO planet search sample (R ~ 115000). This sample is composed of 120 stars hosting high-mass planets, 29 stars hosting exclusively Neptunians and Super-Earths and 910 stars without detected giant planets. We compare the [X/Fe] ratios of such elements in different metallicity bins and we find that planet hosts present higher abundances of Zn for [Fe/H] < −0.1 dex. On the other hand, Ba, Sr, Ce, and Zr abundances are underabundant in stars with planets, with a bigger difference for stars only hosting low-mass planets. However, most of the offsets found can be explained by differences in stellar parameters and by the fact that planet hosts at low metallicity mostly belong to the Galactic thick disk. Only in the case of Ba we find a statistically significant (3σ) underabundance of 0.03 dex for low-mass planet hosts. The origin of these elements is quite complex due to their evolution during the history of the Galaxy. Therefore, it is necessary to understand and characterize the stellar populations to which planet hosts belong in order to do a fair comparison with stars without detected planets. This work demonstrates that the effects of Galactic chemical evolution and not the presence of planets mostly account for the differences we find.

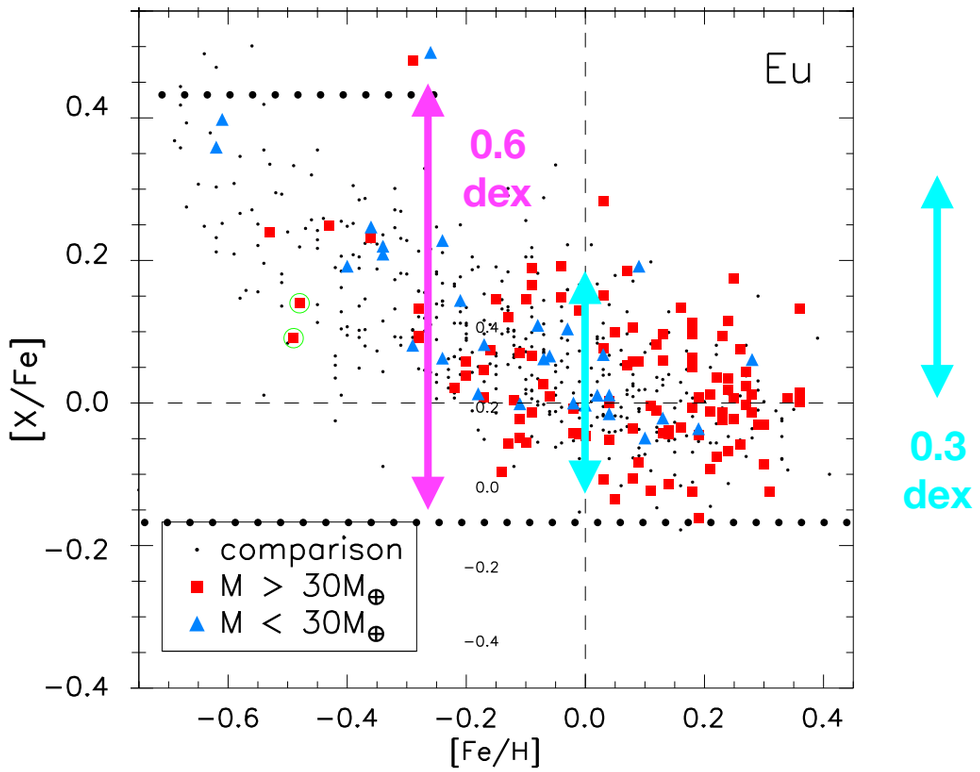

Figure 1. Final [X/Fe] ratios as a function of [Fe/H] for stars in our sample. Low-mass planets are depicted with blue triangles; stars with high-mass planets are shown with red squares. Black dots represent single stars.

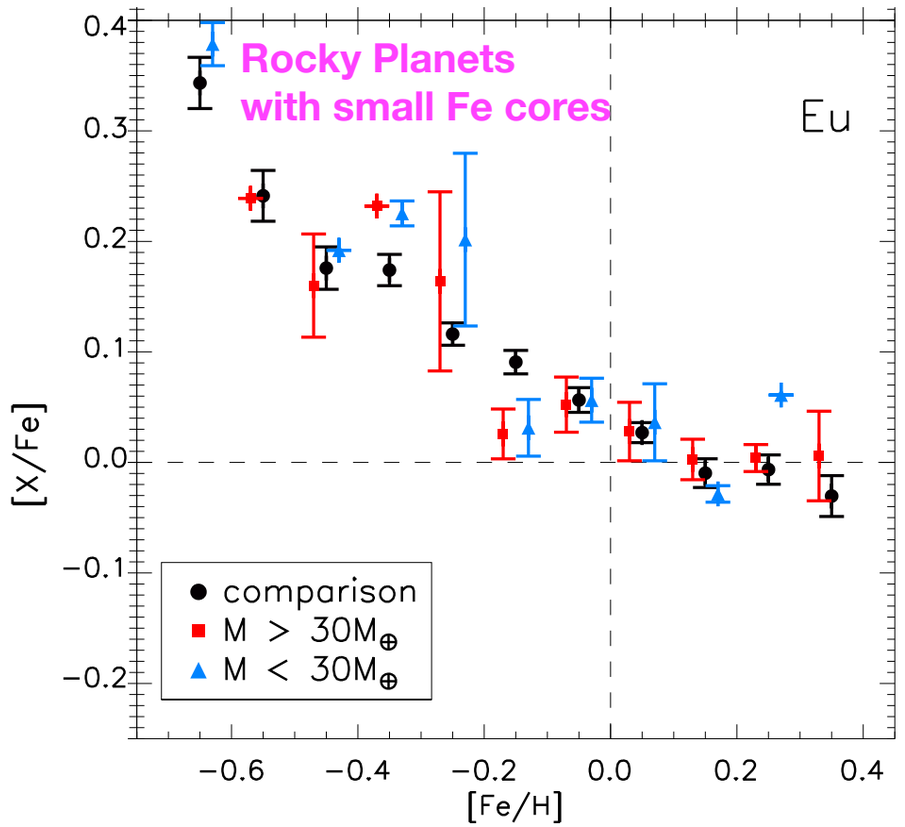

Figure 2. Final [X/Fe] ratios as a function of [Fe/H] for all the stars in our sample. The mean abundances in each metallicity bin of 0.1 dex are shown together with the standard error of the mean.

Publications of the Astronomical Society of the Pacific, 130:094202 (14pp), 2018 September

1. **Introduction** In the last 20 years, the race to search for planets with the radial velocity (RV) method has provided large sets of high quality and high-resolution spectra, allowing the scientific community to explore the chemical abundances of stars with and without planets and search for possible differences among them. After the first discoveries of exoplanets it was soon proposed that stars hosting close-in giant planets present metallicities (defined as iron abundance) higher than stars with no detected planets (Gonzalez 1997; Santos et al. 2001). This finding was further confirmed with larger samples of planet hosts stars (e.g., Santos et al. 2004b; Fischer & Valenti 2005; Sousa et al. 2008) establishing the currently well-known giant planet metallicity [Fe/H] correlation. Interestingly, a recent work by Santos et al. (2017) shows that stars hosting planets more massive than 4 M_J tend to be more metal poor and more massive than stars hosting planets with mass below this threshold. On the other hand, **less massive planets than 4 M_J are preferentially found around metal-rich stars**, following the aforementioned planet-metallicity correlation. This finding might indicate that two different processes of planet formation are at play. On the other hand, **more recent studies have shown that this correlation does not seem to hold for stars hosting less massive planets, those with masses as Neptune or lower** (Sousa et al. 2011; Buchhave et al. 2012; Everett et al. 2013; Buchhave & Latham 2015). **However, other works do find that small planet formation is more probable around metal-rich stars than around metal-poor stars though with a lower factor than giant planet formation (Wang & Fischer 2015).** Moreover, the work by Zhu et al. (2016) claims that the high occurrence rate for low-mass planets and the current small size samples of lowmass planet hosts do not allow to detect the planet metallicity correlation which is however recovered by their theoretical simulations. …
   The aim of this study is to extend our previous works in this field towards heavier elements, since they have not been as extensively studied in the literature as light, iron-peak, or α elements. … Our large and homogeneous sample of stars with and without detected planets gives us the opportunity to study possible correlations between planet occurrence and heavy element abundances in a very detailed way.
2. **Data** The baseline sample used in this work consists of 1111 FGK stars observed within the context of the HARPS-GTO planet search programs (Mayor et al. 2003; Lo Curto et al. 2010; Santos et al. 2011). The final spectra have a resolution of R ∼115000 and high signal-to-noise ratio (S/N) (45% of the spectra have 100 < S/N < 300, 40% of the spectra have S/N > 300 and the mean S/N is 380). The total sample is composed by 151 stars with planets (29 stars with Neptunian-mass planets, 120 stars hosting Jupiter-like planets) and 960 stars without detected planets (hereafter single stars8), although the final sample used here is slightly smaller as explained below.

Abundance to age ratios in the HARPS-GTO sample with Gaia DR2 - Delgado Mena et al. A&A 624, A78 (2019)

More than 1000 FGK dwarf stars with high-resolution ($R \sim 115\,000$) and high-quality spectra from the HARPS-GTO

In Fig. 7 we show the [X/Fe] ratios of the elements presented in DM17 as a function of age for the different populations in our sample together with a linear fit to thin disk stars. …A first look at this figure allows us to see the expected general trends. The ratios of α elements O, Mg, Si, Ca, and Ti respect to Fe show an increasing trend toward older ages with O and Mg showing the steepest trends. ... Since the progenitors of SNeII are more massive than the progenitors of SNeIa, the ratios [α/Fe] will be higher at early ages in the Galaxy because massive stars have shorter lifetimes. It is also clear from Fig. 7 that thick disk stars present a stronger enrichment in α elements when compared to thin disk stars at similar age. This extra enrichment in thick disk stars is also observed for the *r*-process element Eu, which is mainly produced by neutron star mergers (Drout et al. 2017; Côté et al. 2018) and core-collapse supernovae (Travaglio et al. 1999). Both elements have massive progenitors, and in turn [Eu/Fe] also shows a rise toward older ages. Therefore, these trends support the results by Snaith et al. (2015) showing that the star formation rate was more intense in the thick disk than in the thin disk.

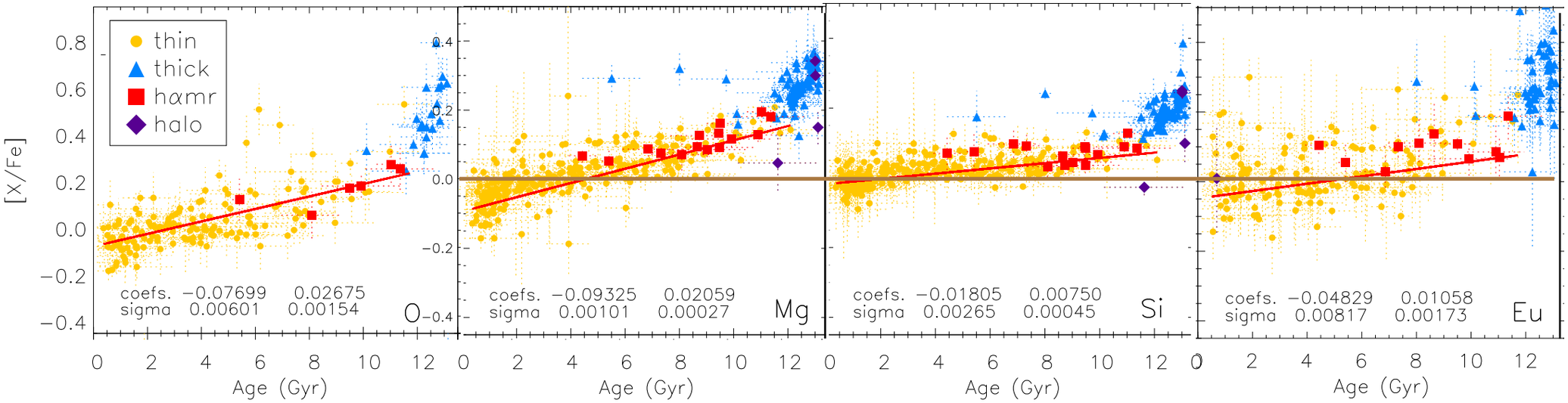

Fig. 7. [X/Fe] as a function of age for stars with an error in age smaller than 1.5 Gyr. The different stellar populations are depicted with different colors and symbols as explained in the legend. We note the different size of y axis for oxygen with respect to the rest of elements. The red line is a weighted linear fit to the thin disk stars to guide the eye on the general behavior of the trends. The *coefs.* values in each panel are the abscissa origin and the slope of the fit, respectively, together with the error (σ) of each coefficient.

Adibekyan et al. 2011 and DM17 revealed the existence of a high-α metal-rich (hereafter **hαmr**) population, with [Fe/H] > –0.2 dex and enhanced [α/Fe] ratios with respect to the thin disk.

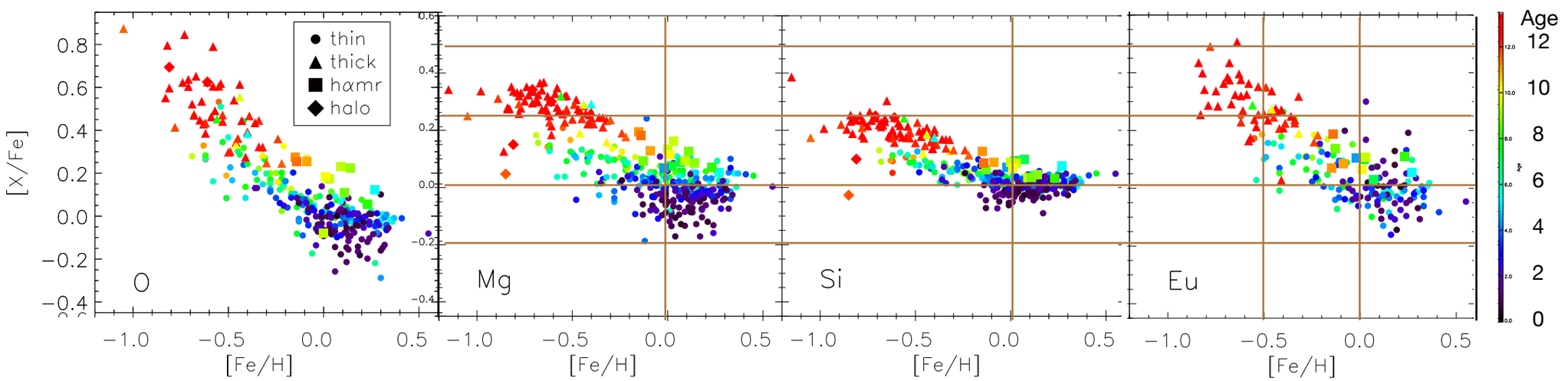

Fig. 8. [X/Fe] as a function of [Fe/H] for stars with an error in age smaller than 1.5 Gyr. We note the different size of *y* axis for oxygen with respect to the rest of elements. The circles, triangles, squares and diamonds are the stars from the thin disk, thick disk, h*α*mr and halo.

It is also clear from Fig. 7 that thick disk stars present a stronger enrichment in α elements when compared to thin disk stars at similar age. This extra enrichment in thick disk stars is also observed for the *r*-process element Eu, which is mainly produced by neutron star mergers (Drout et al. 2017; Côté et al. 2018) and core-collapse supernovae (Travaglio et al. 1999). Both elements have massive progenitors, and in turn [Eu/Fe] also shows a rise toward older ages. Therefore, these trends support the results by Snaith et al. (2015) showing that the star formation rate was more intense in the thick disk than in the thin disk. … In Fig. 8 Eu is higher values as age increases and metallicity decreases, similar to O, but the ages are more mixed due to the larger uncertainties on the abundance derivation of this element.

Abundance to age ratios in the HARPS-GTO sample with Gaia DR2 - Delgado Mena et al. A&A 624, A78 (2019)

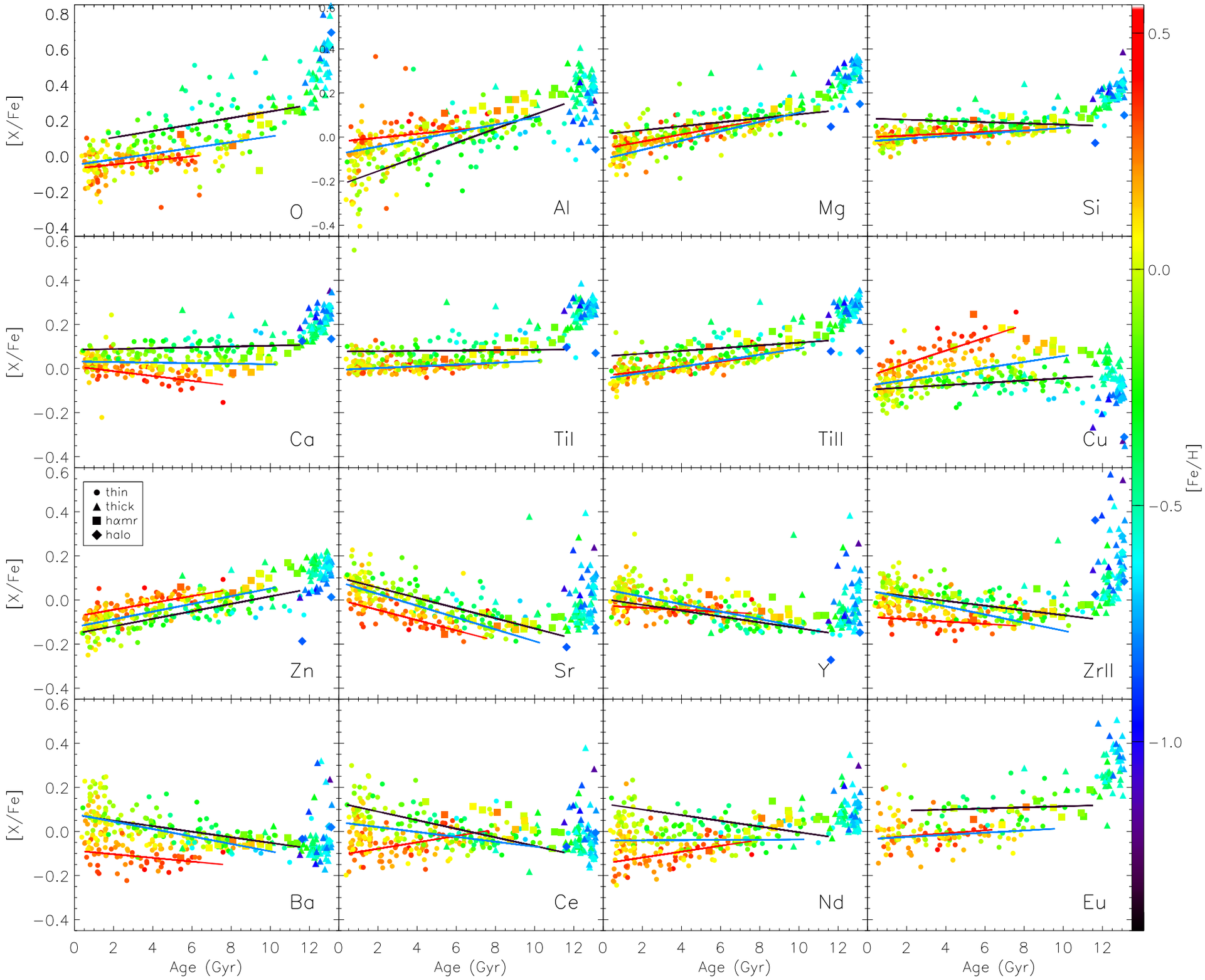

Fig. 9. [X/Fe] as a function of age for stars with an error in age smaller than 1.5 Gyr. We note the different size of y axis for oxygen with respect to the rest of elements. The red, blue, and black lines are weighted linear fits to thin disk stars with [Fe/H] > 0.2 dex, –0.2 < [Fe/H] < 0.2 dex and –0.6 < [Fe/H] < –0.2 dex, respectively.

[Figs.9 and 10 show] *r*-process elements such as Eu presenting a negligible correlation with age.

Spectral Properties of Cool Stars: Extended Abundance Analysis of Kepler Objects of Interest - John M. Brewer[1,2] and Debra A. Fischer[1]

ApJ 237, 38 (2018)

ABSTRACT Accurate stellar parameters and precise elemental abundances are vital pieces to correctly characterize discovered planetary systems, better understand planet formation, and trace galactic chemical evolution. We have performed a uniform spectroscopic analysis for 1127 stars, yielding accurate gravity, temperature, and projected rotational velocity in addition to precise abundances for 15 elements (C, N, O, Na, Mg, Al, Si, Ca, Ti, V, Cr, Mn, Fe, Ni, and Y). Most of the stars in this sample are Kepler Objects of Interest, observed by the California-Kepler Survey, and include 1003 stars hosting 1562 confirmed planets. This catalog extends the uniform analysis of our previous catalog, bringing the total number of homogeneously analyzed stars to almost 2,700 F, G, and K dwarfs. To ensure consistency between the catalogs, we performed an analysis of our ability to recover parameters as a function of signal-to-noise ratio (S/N) and present individual uncertainties as well as functions to calculate uncertainties for parameters derived from lower S/N spectra. With the updated parameters, we used isochrone fitting to derive new radii, masses, and ages for the stars. We use our abundance analysis to support the finding that **the radius gap is likely a result of evolution rather than the result of primordial compositional differences between the two populations.**

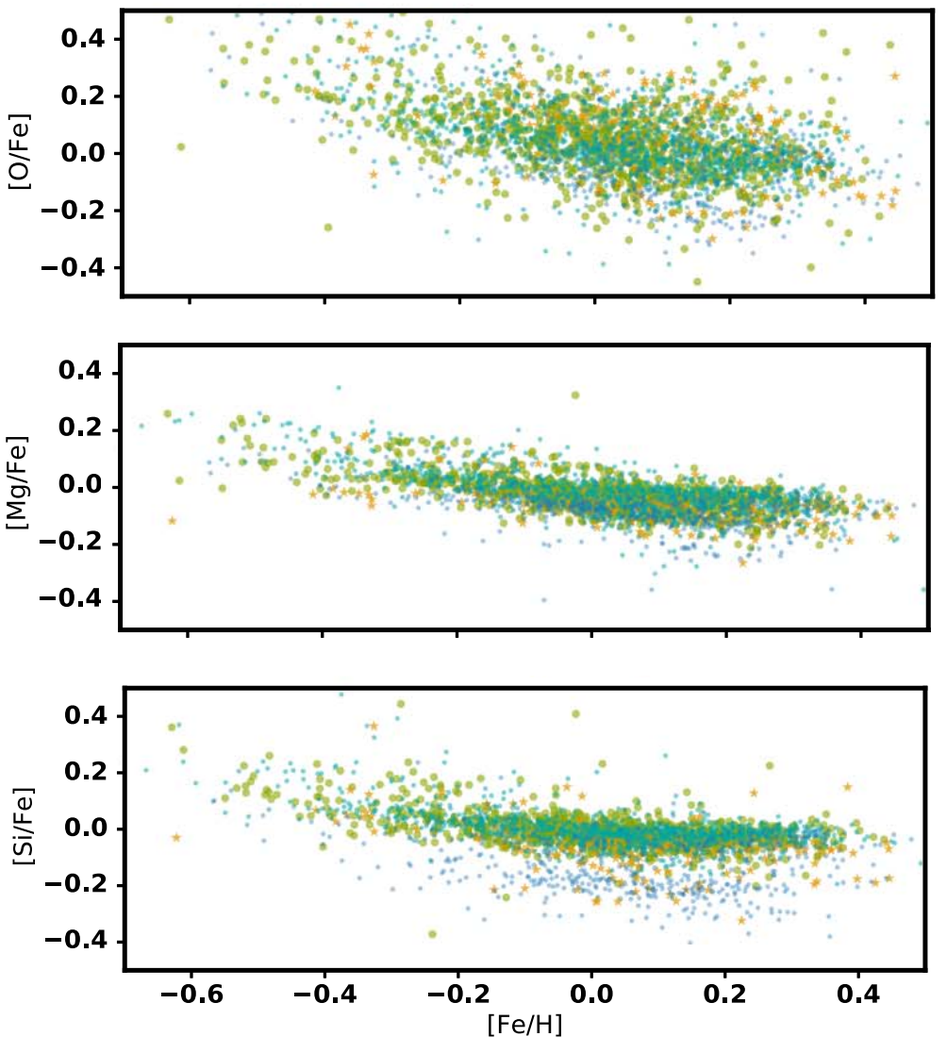

Figure 14. Light elements [X/Fe], after applying empirical correction from B16, plotted against [Fe/H].

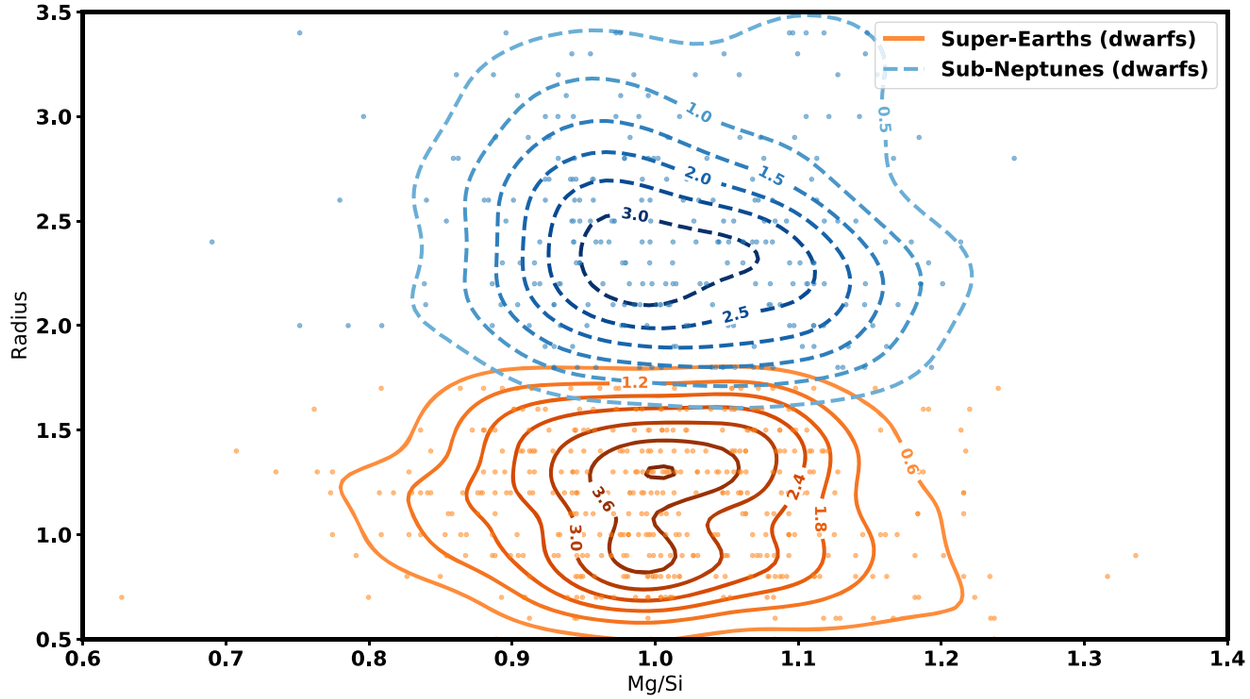

Figure 11. Planet radius as a function of host star Mg/Si ratio for planets around dwarf stars with super-Earth and sub-Neptune planets. The contours represent the two-dimensional PDFs calculated using a Gaussian kernel density estimator as in the one-dimensional PDFs from Figure 10. There is no apparent correlation between the Mg/Si ratio of a planet's host star and the radius of the planet in either the super-Earth or sub-Neptune samples.

Revealing a **Universal Planet-Metallicity Correlation** for Planets of Different Sizes Around Solar-type Stars - Ji Wang & Debra Fisher - AJ 2015

ABSTRACT The metallicity of exoplanet systems serves as a critical diagnostic of planet formation mechanisms. Previous studies have demonstrated the planet–metallicity correlation for large planets (RP E ≥ 4 R); however, a correlation has not been found for smaller planets. With a sample of 406 Kepler objects of interest whose stellar properties are determined spectroscopically, we reveal a universal planet–metallicity correlation: not only gas-giant planets (3.9 - 22.0 R_Earth) but also gas-dwarf (1.7 - 3.9 R_Earth) and terrestrial planets (R_P ≤ 1.7 R_Earth) occur more frequently in metal-rich stars.

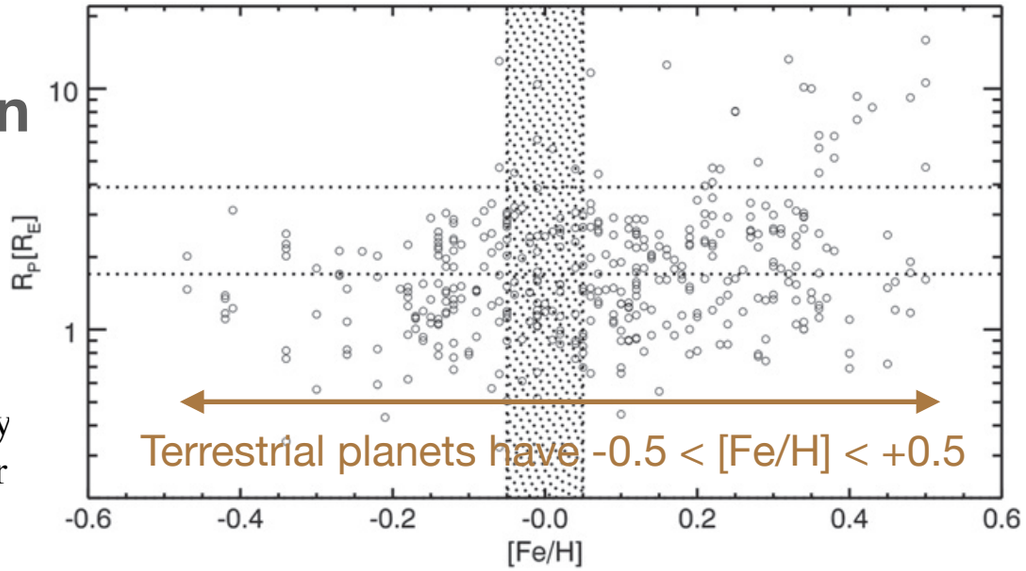

Figure 2. *Kepler* planet candidates on the [Fe/H]–R_P plane. The plane is divided into six sub-regions based on metallicity and planet radius. The dotted area is the metallicity buffer zone ($-0.05 \leqslant$ [Fe/H] $\leqslant 0.05$). Stars in the buffer zone are excluded in our analysis.

KEPLER PLANETS AND METALLICITY - Taylor L. J. Kutra and Yanqin Wu - **arXiv:2003.08431**

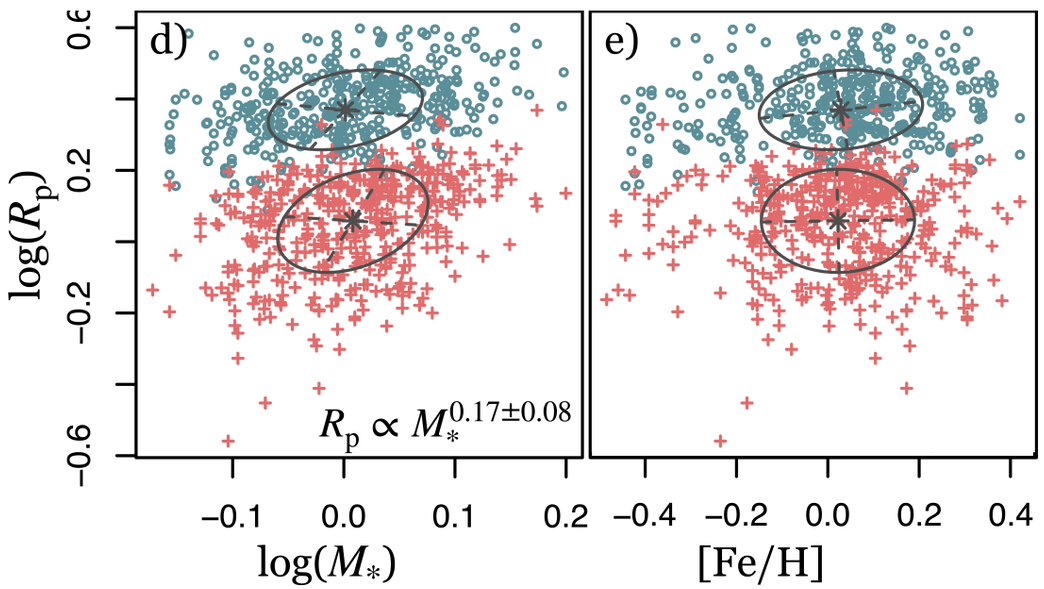

Fig. 1 (excerpt)— Correlation between planet and stellar parameters. … Red crosses and green circles represent the super-Earth and sub-Neptune sub-populations. They have the same [Fe/H] distributions.

Fig. 3 Cumulative fraction of stars with & w/o transiting planets.

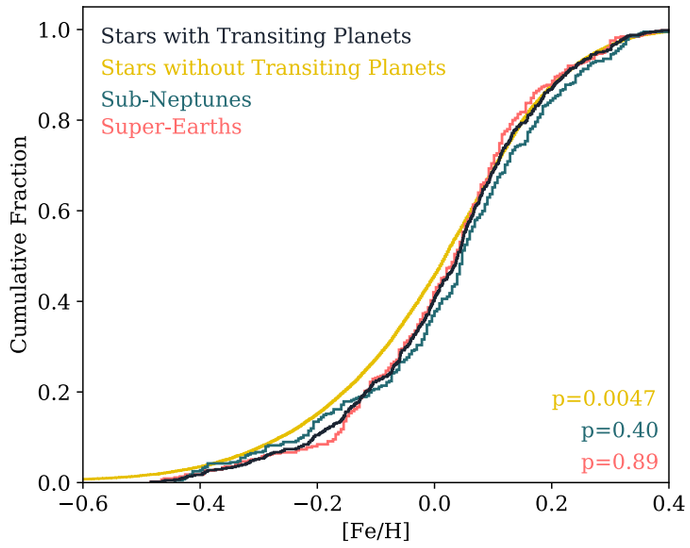

EXOPLANETS

Science 366, 356 (18 October 2019)

Oxygen fugacities of extrasolar rocks: Evidence for an Earth-like geochemistry of exoplanets

Alexandra E. Doyle[1]*, Edward D. Young[1]*, Beth Klein[2], Ben Zuckerman[2], Hilke E. Schlichting[1,2,3]

Oxygen fugacity is a measure of rock oxidation that influences planetary structure and evolution. Most rocky bodies in the Solar System formed at oxygen fugacities approximately five orders of magnitude higher than a hydrogen-rich gas of solar composition. It is unclear whether this oxidation of rocks in the Solar System is typical among other planetary systems. We exploit the elemental abundances observed in six white dwarfs polluted by the accretion of rocky bodies to determine the fraction of oxidized iron in those extrasolar rocky bodies and therefore their oxygen fugacities. The results are consistent with the oxygen fugacities of Earth, Mars, and typical asteroids in the Solar System, suggesting that at least some rocky exoplanets are geophysically and geochemically similar to Earth.

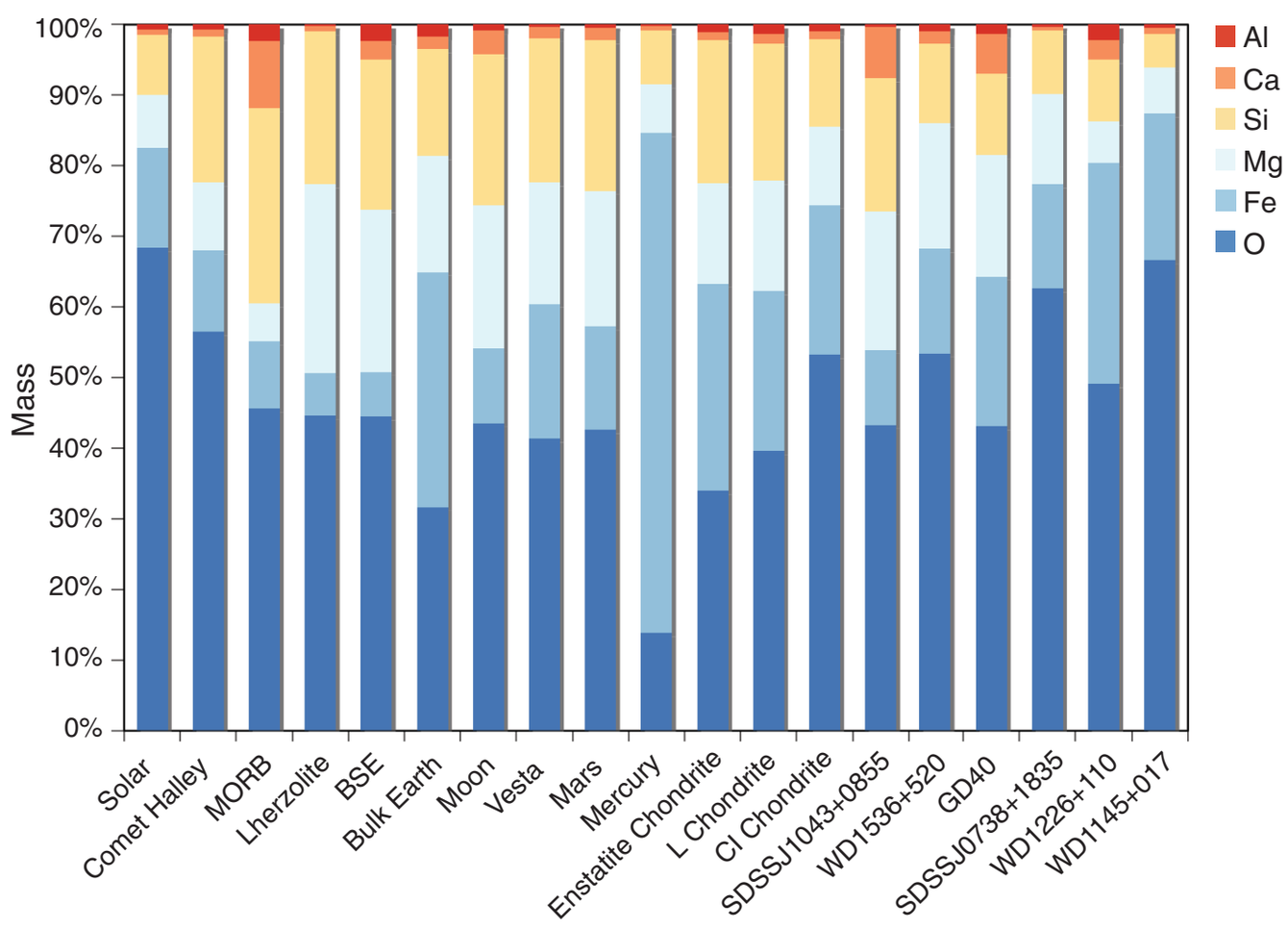

SCALING THE EARTH: A SENSITIVITY ANALYSIS OF TERRESTRIAL EXOPLANETARY INTERIOR MODELS

C. T. Unterborn, E. E. Dismukes, and W. R. Panero - ApJ 2016

ABSTRACT An exoplanet's structure and composition are first-order controls of the planet's habitability. We explore which aspects of bulk terrestrial planet composition and interior structure affect the chief observables of an exoplanet: its mass and radius. We apply these perturbations to the Earth, the planet we know best. Using the mineral physics toolkit BurnMan to self-consistently calculate mass–radius models, we find that the core radius, the presence of light elements in the core, and an upper mantle consisting of low-pressure silicates have the largest effects on the final calculated mass at a given radius, none of which are included in current mass–radius models. We expand these results to provide a self-consistent grid of compositionally as well as structurally constrained terrestrial mass– radius models for quantifying the likelihood of exoplanets being "Earth-like." We further apply this grid to Kepler- 36b, finding that it is only ~20% likely to be structurally similar to the Earth with Si/Fe = 0.9 compared with the Earth's Si/Fe = 1 and the Sun's Si/Fe = 1.19.

Simplified two-layer planet models with a core mass fraction identical to the Earth overpredict the Earth's total mass by ~13% (Zeng & Sasselov 2013). Applying such a simplified model to the Earth would therefore predict a smaller core. Such a difference will erroneously lead to a planet model with more rapid heat loss from the core, limiting the lifetime of a magnetic field and affecting the viability of plate tectonics at the surface assuming a heat budget equal to that of the Earth. These two dynamic processes are likely required to sustain liquid water and life on Earth (Driscoll & Barnes 2015; Foley 2015). While still within the uncertainty of most planet mass measurements, as observational techniques improve, the consequences of these "spherical cow" models will become more and more evident. Here we present a systematic sensitivity analysis of how uncertainties in material properties, core composition, major element chemistry (Mg, Fe, Si, O), and structural transitions in mantle silicates affect the mean density of an Earth-sized, terrestrial planet.

DISCUSSION Of the parameters modeled here we find that core size, the density reduction due to the inclusion of an upper mantle, and the presence of light elements in the core have the largest effects on the final mass of an Earth-radius planet. … As the ratio of mantle to core dominates our determination of mass within mass–radius models, we adopt Si/Fe as a primary compositional constraint on planetary structure. … For a 1 R_{Earth} planet we find that the core density shifts the calculated mass with relatively small changes in Si/Fe. … In this simple "spherical cow" approach to the modeling of an Earth-sized planet interior, we find that there are three major parameters required to account for measured density and composition: the presence of light elements in the core, the radius of the core, and the inclusion of an upper mantle. …The chief difference between the Earth and the other terrestrial planets in our solar system is that the Earth is a habitable dynamic planet with plate tectonics that create a deep water and carbon cycle. These cycles regulate surface C abundances (Sleep & Zahnle 2001), and thus a long-term climate, as well as provide a flux of water into the surface hydrosphere, all of which are vital to Earth being habitable. The driving force behind plate tectonics is the convection of the mantle. The fact that the Earth transports its interior heat via convection is due to a confluence of many factors, including composition, internal budget energy, and planetary structure.

CONCLUSION … As we expand our definition of "Earth-like" beyond one merely of composition toward one based more on chemical and dynamic states, we can begin to limit which of these composition/structure solutions produce planets dynamically unlike Earth, i.e., lacking a mantle convection and the potential for plate tectonics (Unterborn et al. 2014, 2015). Further degeneracy can be reduced by eliminating those core compositions that exceed the amount of light elements soluble in Fe, a topic of great interest in the mineral physics community.

THORIUM ABUNDANCES IN SOLAR TWINS AND ANALOGS: IMPLICATIONS FOR THE HABITABILITY OF EXTRASOLAR PLANETARY SYSTEMS Cayman T. Unterborn, Jennifer A. Johnson, and Wendy R. Panero - ApJ (2015)

ABSTRACT We present the first investigation of Th abundances in solar twins and analogues to understand the possible range of this radioactive element and its effect on rocky planet interior dynamics and potential habitability. The abundances of the radioactive elements Th and U are key components of a planet's energy budget, making up 30%–50% of the Earth's Radiogenic heat drives interior mantle convection and surface plate tectonics, which sustains a deep carbon and water cycle and thereby aides in creating Earth's habitable surface. Unlike other heat sources that are dependent on the planet's specific formation history, the radiogenic heat budget is directly related to the mantle concentration of these nuclides. As a refractory element, the stellar abundance of Th is faithfully reflected in the terrestrial planet's concentration. **We find that log ?$_{Th}$ varies from 59% to 251% that of solar, suggesting extrasolar planetary systems may possess a greater energy budget with which to support surface to interior dynamics and thus increase their likelihood to be habitable compared to our solar system.**

4. CONCLUSION

The measurements presented here are the first measurements of a planetary system's potential energy budget and potential for planetary interior dynamics. Mantle convection, as the underlying mechanism driving plate tectonics on the Earth, recycles and regenerates crustal, oceanic, and atmospheric material (Crowley et al. 2011; Korenaga 2011). This surface- to-interior process regulates the global carbon and water cycles, which in turn, aid in creating a habitable surface (Sleep & Zahnle 2001). **We find that some stellar systems possess a greater Th abundance compared to solar and due to the refractory nature of Th, this increase will be reflected in the mantles and crusts of any resulting terrestrial planets. Planetary systems with higher Th/Si ratios at t = 0 Ga than solar suggest that these systems possess larger energy budgets. This supports interior dynamics and increases the likelihood for carbon and water cycling between the surface crust and planetary interior, thus broadening the range of planets which may support habitable surfaces.**

See also:

Thorium in solar twins: implications for habitability in rocky planets - Botelho et al. MNRAS 482, 1690 (2019)

I found a recent abstract from the Iceland conference: American Astronomical Society, Extreme Solar Systems 4, id. 331.14. Bulletin of the American Astronomical Society, Vol. 51, No. 6, August 2019:

A Matter of Time: The Coupled Role of Stellar Abundances, Exoplanet Radiogenic Heat Budgets and Climatic Evolution

- Unterborn, Cayman; Foley, Bradford; Young, Patrick; Vance, Greg; Chieffle, Lee; Desch, Steve

Abstract

A planet's heat budget is a complex combination of the heat of formation, the energy released during core formation, and decay of the long-lived radionuclides U, Th and 40K. A planet's radiogenic heat budget is solely a function of the total amount of these elements present. Observations of Solar twins show a range of Th abundances between 60 and 250% of the Sun's (Unterborn et al., 2015). We show similar ranges are expected for U and K. If this range is indicative of the span of exoplanet radiogenic heat budgets, an exoplanet's thermal and chemical evolution may be quite different from the Earth's.

We present results of geodynamical models from Foley & Smye 2018 [arXiv:1712.03614v1] for stagnant lid planets with varying radiogenic heat budget. We compile a range of observed radionuclide abundances reported from the literature, adopting a Monte-Carlo approach for determining input abundances in individual models. We focus on stagnant lid planets, as stagnant lid convection is likely to be more common than plate tectonics. We show that changes in a planet's radiogenic heat budget affect the rates of volcanism, surface weathering, and volatile degassing from the interior. This allows us, through the measurement of the host star's abundances of radionuclides, to constrain a planet's thermal history and quantify the timescale over which it can maintain a temperate climate.

In general we find those stagnant lid planets with a greater starting abundance of radionuclides are temperate for a longer period of time. We calculate a conservative estimate of degassing lifetimes for a 1 Earth mass stagnant-lid planet of 1.6±0.6 Gyr across our observationally constrained range of radionuclide abundances. We argue those non-tidally-locked planets orbiting stars older than this are unlikely to be actively degassing in the absence of plate tectonics, including both TRAPPIST-1 (7.6±2.2 Gyr; Burgasser & Mamajek, 2017) and Kepler 444 (10±1.5 Gyr; Mack et al., 2018). These planets therefore are unlikely to have temperate climates, and instead likely lie in a snowball climatic regime, limiting their potential to be habitable and "Earth-like."

Finding "Earth-like" Exoplanets: An Observationally-oriented Exogeoscience Perspective
Unterborn, C. T. (Arizona State University, Tempe, AZ) — AAS Bulletin January 2020 **American Astronomical Society meeting #235, id. 356.01., Vol. 52, No. 1**

Abstract In our search for "Earth-like" planets, we have discovered more than 4000 exoplanets to date with the rate of discovery ever increasing in the current TESS era. In the most idealistic case, we can learn much about an individual exoplanet: its radius, mass, orbital parameters and atmospheric composition. These observations combined with mass-radius models reveal a wide diversity of exoplanets from water worlds to super-Earths, with most being unlike anything in our Solar System. More recent mass-radius work, however, shows that these models are able to at best characterize an exoplanet being broadly rocky, watery or gassy. Given that Venus is nearly the same mass and radius at the Earth, a more detailed understanding of an exoplanet's geology and evolution is necessary to truly characterize a planet as "Earth-like." Critically important parameters for a rocky exoplanet being "Earth-like," such as its composition, structure, mineralogy and thermal state are unknown and unlikely to ever be directly observed. Instead, w**e must turn to other observables such as host-star composition, system age and lab measurements, and combine them with geophysical models to quantify a planet's potential geochemical and geodynamical state.** In this talk, I will provide an overview of the recent work in this new field of exogeoscience. I will pay particular attention to how these direct and indirect observables can provide a useful metric for target selection in future observation campaign when viewed in a geophysical context. I will further argue that it is only through an interdisciplary approach, combining astronomy, astrophysics and geoscience, that we will truly quantify whether a rocky exoplanet is at all Earth-like, habitable and, indeed, hosting life.

see also

Habitability of Earth-like Stagnant Lid Planets: Climate Evolution and Recovery from Snowball States

- Foley, Bradford J. 2019ApJ...875...72F — cited: 2

Scaling the Earth: A Sensitivity Analysis of Terrestrial Exoplanetary Interior Models Unterborn, C. T.; Dismukes, E. E.; Panero, W. R. - 2016ApJ...819...32U - cited: 28

Before Biology: Geologic Habitability and Setting the Chemical and Physical Foundations for Life
Unterborn, Cayman Thomas - 2016PhDT.....12U

and articles listed on the next page

The Devil in the Dark: A Fully Self-Consistent Internal Seismic Model for Venus Unterborn, C. T.; Schmerr, N. C.; Irving, J. C. E. — 2018LPI....49.1768U

Venus: The Making of an Uninhabitable World

- Kane, Stephen R.; Arney, Giada; Crisp, David *and 6 more*

2018arXiv180103146K - cited: 1

The Star-Planet Connection. I. Using Stellar Composition to Observationally Constrain Planetary Mineralogy for the 10 Closest Stars Hinkel, Natalie R.; Unterborn, Cayman T.

2018ApJ...853...83H - cited: 10

To understand the interior of a terrestrial planet, the stellar abundances of planet-building elements (e.g., Mg, Si, and Fe) can be used as a proxy for the planet's composition. We explore the planetary mineralogy and structure for fictive planets around the 10 stars closest to the Sun using stellar abundances from the Hypatia Catalog. Although our sample contains stars that are both sub- and super-solar in their abundances, we find that the mineralogies are very similar for all 10 planets… Nothing about radio…, heating, Th or U.

Redefining "Earth-Like:" Habitable Planet Composition and the Case for Moving Beyond the Mass-Radius Diagram

- Unterborn, C. T.

ExoPlex: A Code for Calculating the Mineralogy and Mass-Radius Relationships for Rocky Planets

- Lorenzo, A. M.; Desch, S. J.; Unterborn, C. *and 2 more*

2017LPICo2042.4107U

Stellar Chemical Clues as to the Rarity of Exoplanetary Tectonics

- Unterborn, C. T.; Hull, S. D.; Stixrude, L. *and 3 more*

2017LPICo2042.4034U - cited: 3

Compositions of Small Planets & Implications for Planetary Dynamics **Johnson, Jennifer; Teske, Johanna; Souto, Diogo; Cunha, Katia M. L.; Unterborn, Cayman T.; Panero, Wendy;**

2017AAS...22941306J Abstract only — no paper

The Potential for Plate Tectonics about Sun-like Stars in the Galaxy as Controlled by Composition **Hull, S. D.; Unterborn, C. T.; Stixrude, L. P.; Panero, W. R.**

2016AGUFM.P41B2077H This is a conf proceeding abstract — no paper

Based on a survey of 1111 Sun-like stars spanning a wide range of refractory element composition, we find that the silica content of the resulting mantle is a controlling factor in the likelihood for exoplantary crusts to sink through combined thermal and compositional factors. Therefore, we estimate that as few as 0.6% of all Sun-like stars are likely to hosting planets that undergo steady-state surface-to-interior crustal cycling. This approach therefore provides a method for identifying the most important planets for time-intensive follow up of atmospheric properties.

BurnMan: Lower mantle mineral physics toolkit

- Cottaar, S.; Heister, T.; Myhill, R.; Rose, I.; Unterborn, C.

2016ascl.soft10010C

Scaling the Earth: A Sensitivity Analysis of Terrestrial Exoplanetary Interior Models **Unterborn, C. T.; Dismukes, E. E.; Panero, W. R.**

2016ApJ...819...32U - cited: 28 No mention of heating, radio…, etc.

Before Biology: Geologic Habitability and Setting the Chemical and Physical Foundations for Life

- Unterborn, Cayman Thomas

2016PhDT.....12U

Thorium in solar twins: implications for habitability in rocky planets - Botelho et al. MNRAS 482, 1690 (2019)

ABSTRACT We have investigated the thorium (Th) abundance in a sample of 53 thin disc solar twins covering a wide range of ages. These data provide constrains on the mantle energy budget of terrestrial planets that can be formed over the evolution of the Galaxy's thin disc. We have estimated Th abundances with an **average precision of 0.025 dex** (in both [Th/H] and [Th/Fe]) through comprehensive spectral synthesis of a Th II line present at 4019.1290 Å, using very high resolution (R = 115 000) high quality HARPS spectra obtained at the ESO La Silla Observatory. We have confirmed that **there is a large energy budget from Th decay for maintaining mantle convection inside potential rocky planets around solar twins, from the Galactic thin disc formation until now, because the pristine [Th/H]$_{ZAMS}$ is super-solar on average** under a uniform dispersion of 0.056 dex (varying from +0.037 up to +0.138 dex based on linear fits against isochrone stellar age). Comparing to neodymium (Nd) and europium (Eu), two others neutron-capture elements, the stellar pristine abundance of **Th follows Eu** along the Galactic thin disc evolution, but it does not follow Nd, probably because neodymium has a significant contribution from the *s*-process (about 60 per cent).

Our results suggest that solar twin stars in the Galactic thin disc are as probable as the Sun to host rocky planets with convective mantles, and perhaps with suitable geological conditions for habitability.

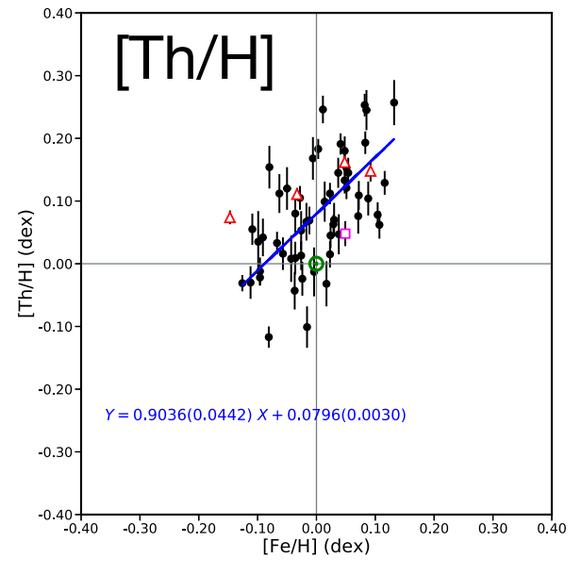

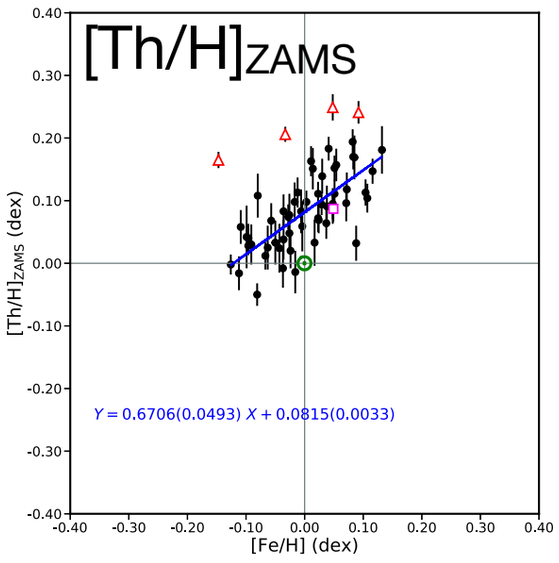

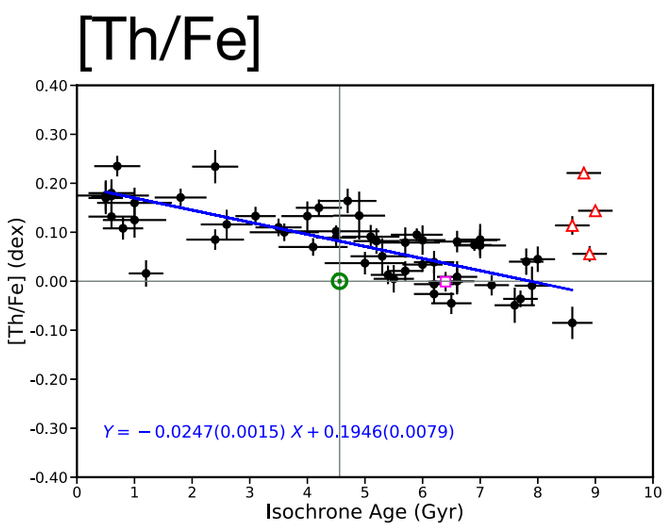

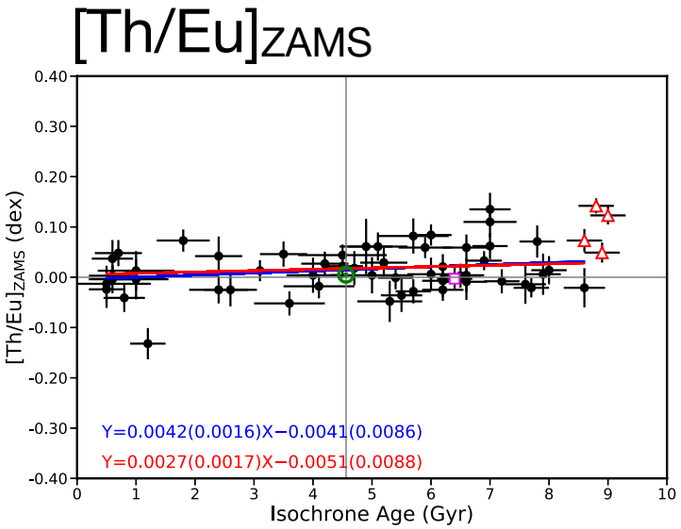

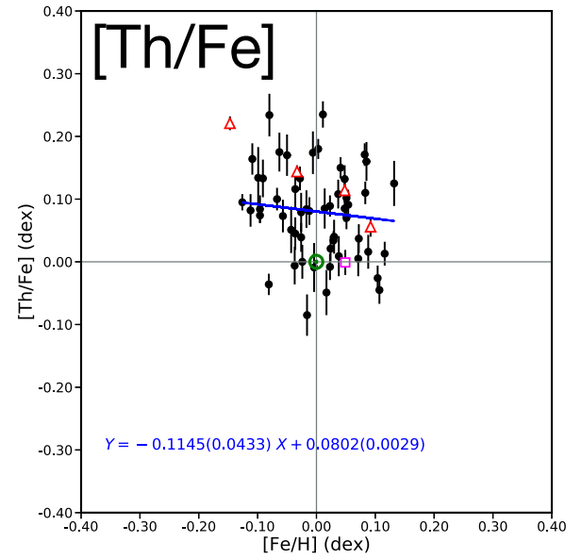

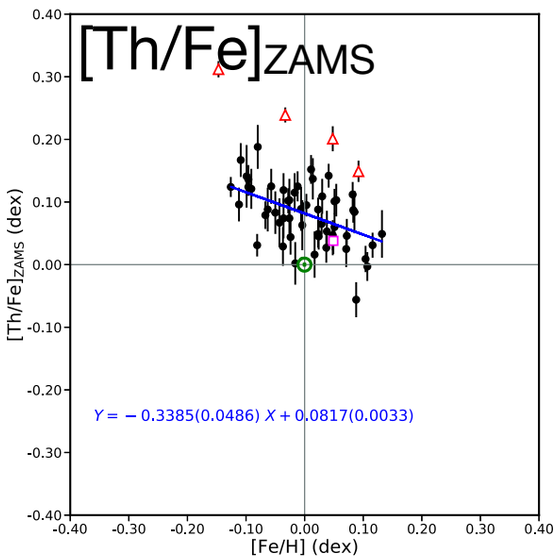

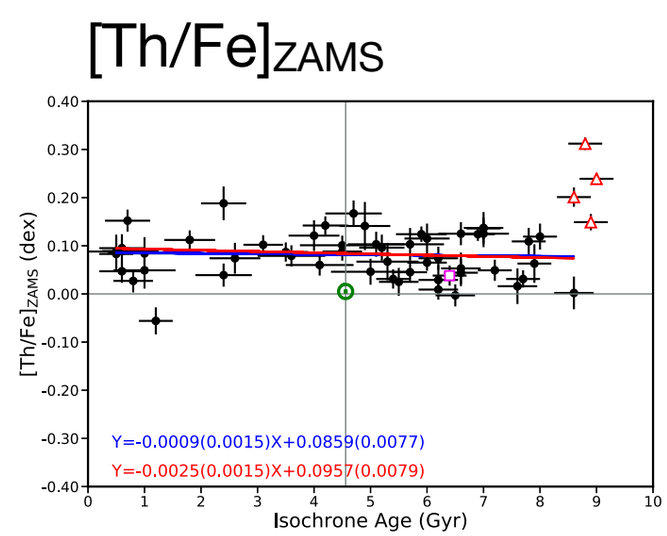

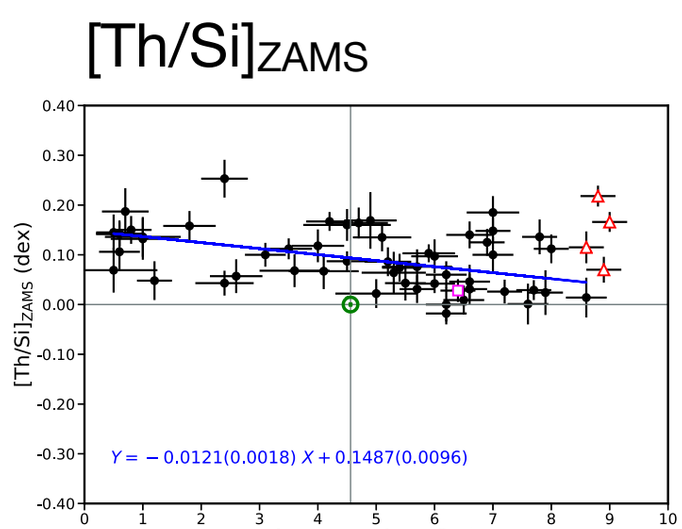

The origin and evolution of r- and s-process elements in the Milky Way stellar disk

Battistini & Bensby, A&A 2016

ABSTRACT Using spectra of high resolution (42 000 R 65 000) and high signal-to-noise (S/N 200) obtained with the MIKE and the FEROS spectrographs, we determine Sr, Zr, La, Ce, Nd, Sm, and Eu abundances for a sample of 593 F and G dwarf stars in the solar neighborhood.

We present abundance results for Sr (156 stars), Zr (311 stars), La (242 stars), Ce (365 stars), Nd (395 stars), Sm (280 stars), and Eu (378 stars). … Europium is almost completely produced by the *r*-process …

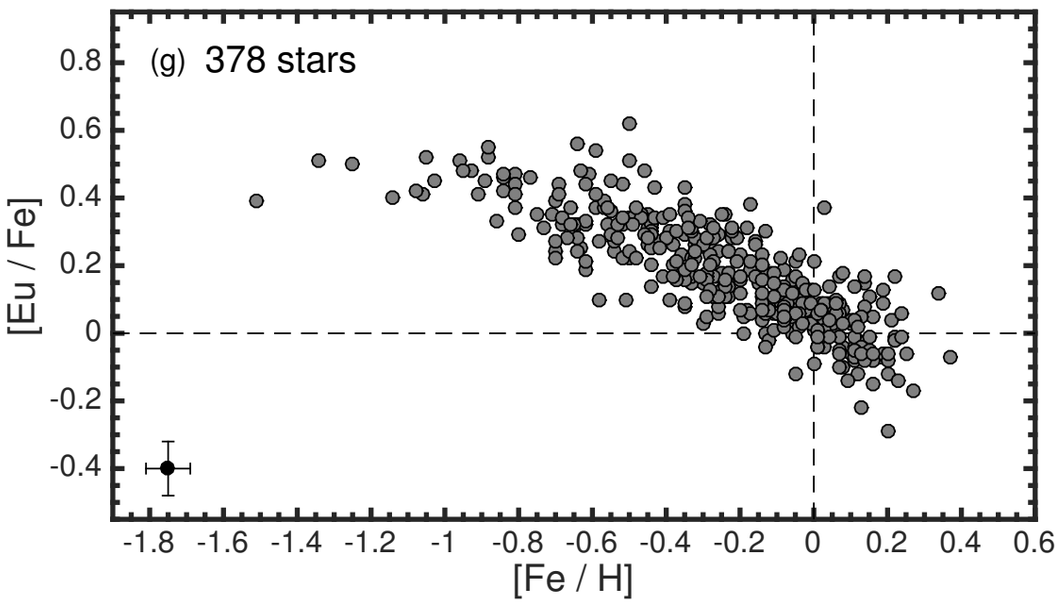

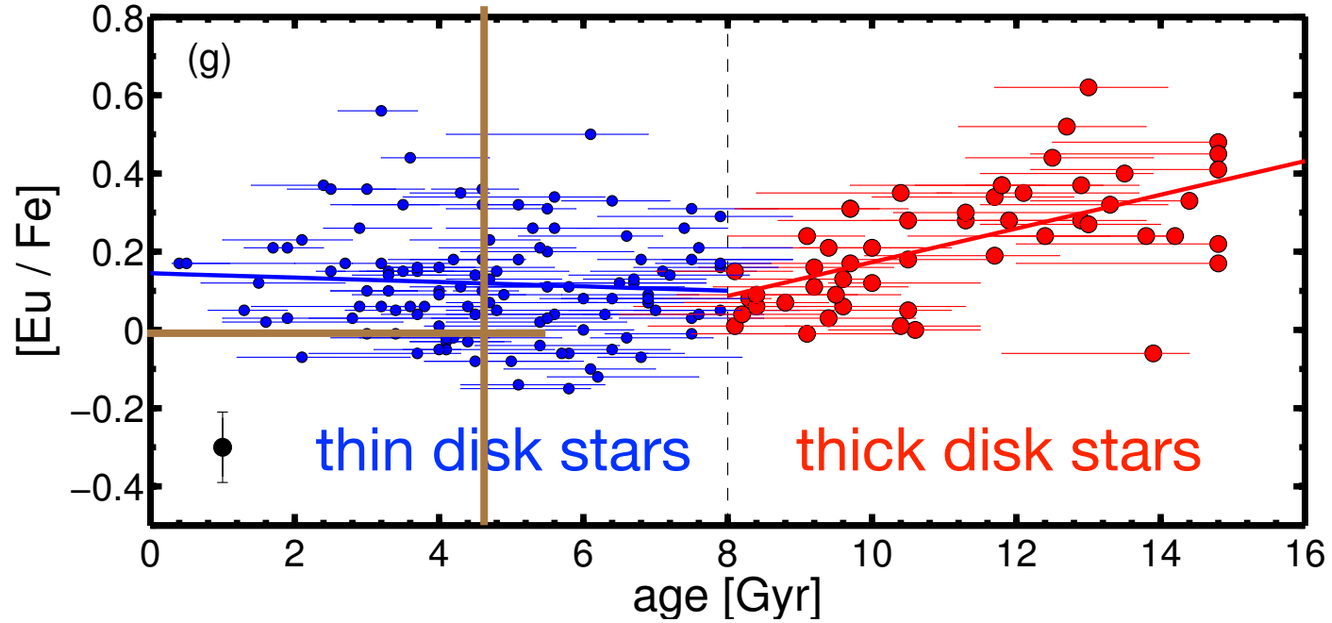

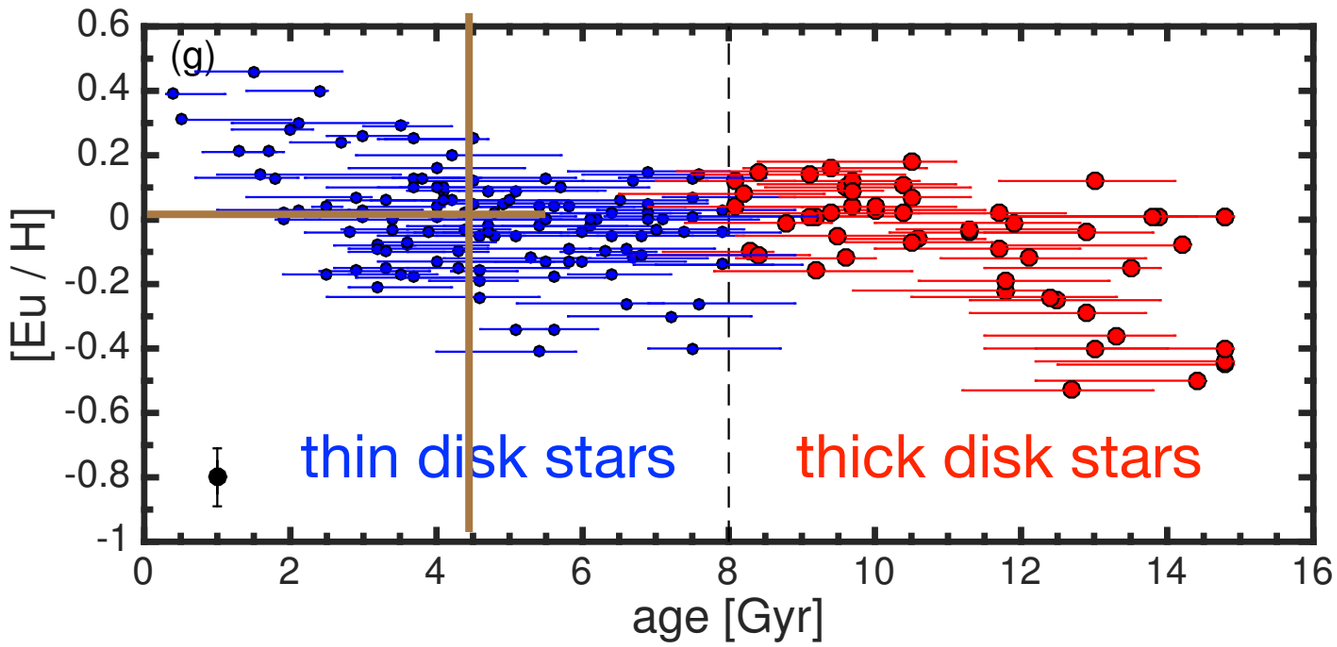

Summary … For the thick disk, there is a decrease in the abundance as age decreases that can be explained by the decrease in SN II events, while Fe production from SN Ia increases. … [The reason for the increase in [Eu/H] in the thin disk] is not completely clear. In theory younger stars should not present such high abundance in Eu, since Eu is almost completely produced in SN II at the beginning of star formation. …

The GALAH Survey: Temporal Chemical Enrichment of the Galactic Disk - Jane Lin, Martin Asplund, et al. MNRAS 2019

We present isochrone ages and initial bulk metallicities ([Fe/H]bulk, by accounting for diffusion) of 163,722 stars from the GALAH Data Release 2, mainly composed of main sequence turn-off stars and subgiants (7000K > Teff > 4000K and logg > 3 dex). The local age-metallicity relationship (AMR) is nearly flat but with significant scatter at all ages; the scatter is even higher when considering the observed surface abundances. After correcting for selection effects, the AMR appear to have intrinsic structures indicative of two star formation events, which we speculate are connected to the thin and thick disks in the solar neighborhood. We also present abundance ratio trends for 16 elements as a function of age, across different [Fe/H]bulk bins. In general, we find the trends in terms of [X/Fe] vs age from our far larger sample to be compatible with studies based on small (~ 100 stars) samples of solar twins but we now extend it to both sub- and super-solar metallicities. The α-elements show differing behaviour: the hydrostatic α-elements O and Mg show a steady decline with time for all metallicities while the explosive α-elements Si, Ca and Ti are nearly constant during the thin disk epoch (ages < ~ 12 Gyr). The s-process elements Y and Ba show increasing [X/Fe] with time while **the r-process element Eu has the opposite trend, thus favouring a primary production from sources with a short time-delay such as core-collapse supernovae over long-delay events such as neutron star mergers.**

Note: > 0.5 dex spread in [Eu/Fe] at < 5 Gyr, and [Eu/Fe] decreases with [Fe/H] increasing, as in Mena+18

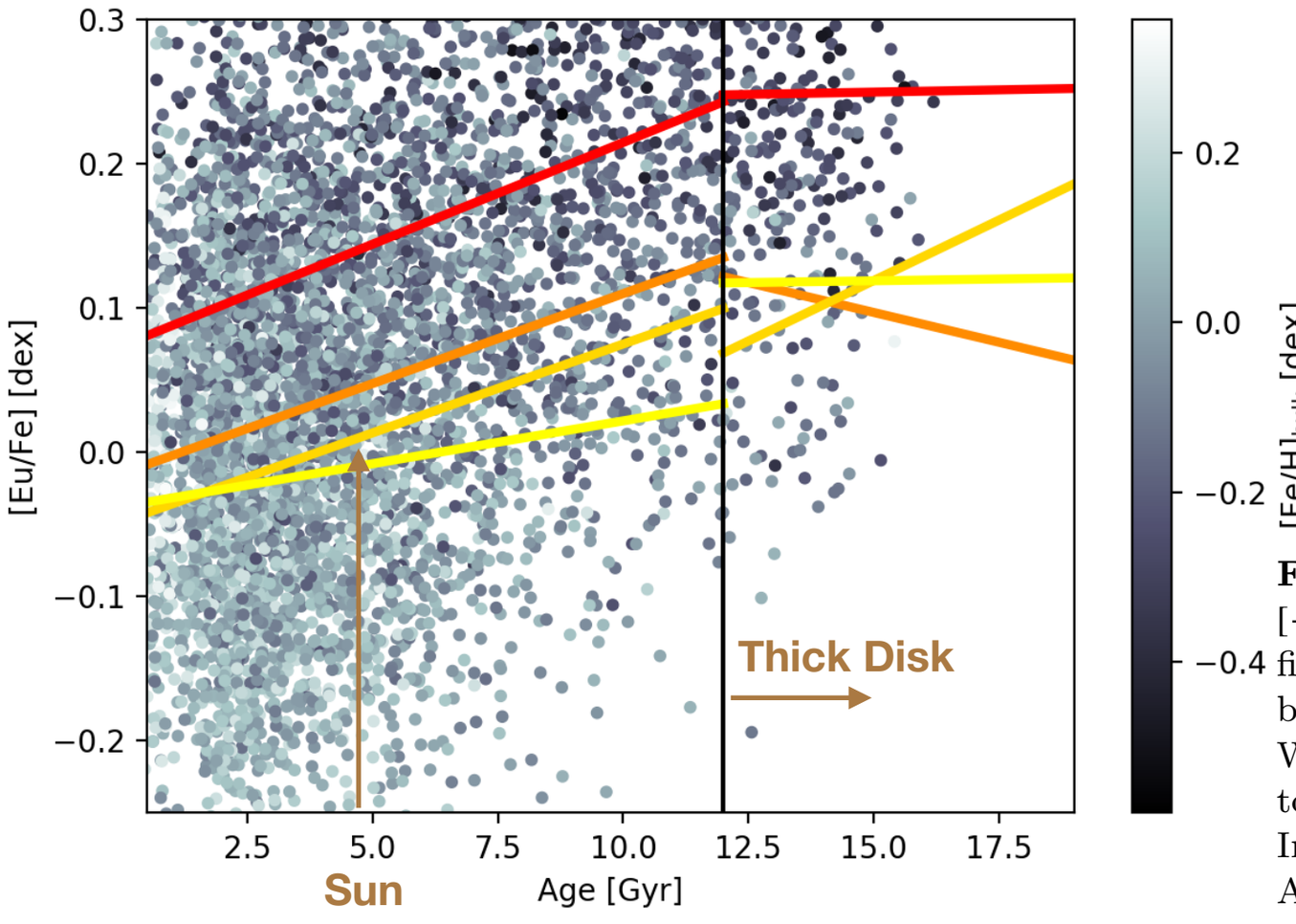

Eu (a r-process element) shows an increase in abundance ratio at higher ages in the thin disk, in contradiction with the other two s-process elements Y and Ba. Some studies have advocated the main production site for r-process elements are neuron star mergers (e.g., Freiburghaus et al. 1999; Wanajo et al. 2014). This should mean that [Eu/Fe] has time-delay features similar to Y and Ba, which is not observed in our data (Figure 13). It has been suggested that production channels with short time-delays have played a role in producing Eu, in addition to neutron star mergers, such as core-collapse SNe (e.g., Ting et al. 2012).

Figure 13. [Eu/Fe] trends over time, across four $[Fe/H]_{bulk}$ bins: [−0.5, −0.1] (red), [−0.1, 0] (orange), [0, 0.1] (gold), [0.1, 0.5] (yellow), fitted linearly and separately for thin/thick disks (above and below 12 Gyr). Points are colour-coded according to $[Fe/H]_{bulk}$. We do not have enough stars with good [Eu/Fe] abundances to make a density plot similar to other elements in Figure 11. Intercepts and gradients of the thin-disk trends are listed in Appendix A.

Abundance ratios in GALAH DR2 and their implications for nucleosynthesis Emily Griffith, Jennifer A. Johnson, and David H. Weinberg - ApJ 2019

Abstract Using a sample of 70,924 stars from the second data release of the GALAH optical spectroscopic survey, we construct median sequences of [X/Mg] versus [Mg/H] for 21 elements, separating the high-α/"low-Ia" and lowα/"high-Ia" stellar populations through cuts in [Mg/Fe]. … The separation of the [Eu/Mg] sequences implies that at least ~30% of Eu enrichment is delayed with respect to star formation.

We adopt the same division as Weinberg+2019 (W19), defining the low-Ia population by

$$\begin{cases} [\mathrm{Mg/Fe}] > 0.12 - 0.13[\mathrm{Fe/H}], & [\mathrm{Fe/H}] < 0 \\ [\mathrm{Mg/Fe}] > 0.12, & [\mathrm{Fe/H}] > 0. \end{cases} \quad (1)$$

(W19 is based on the APOGEE survey, which did not include Eu.)

We then calculate the median absolute deviation between the median trend of a sub-sample and that of the full population to be median(|sub - sample median - full sample median|). Result for Eu is 100% High-α /Low-Ia for 4500<T<6200, which tracks the total population well.

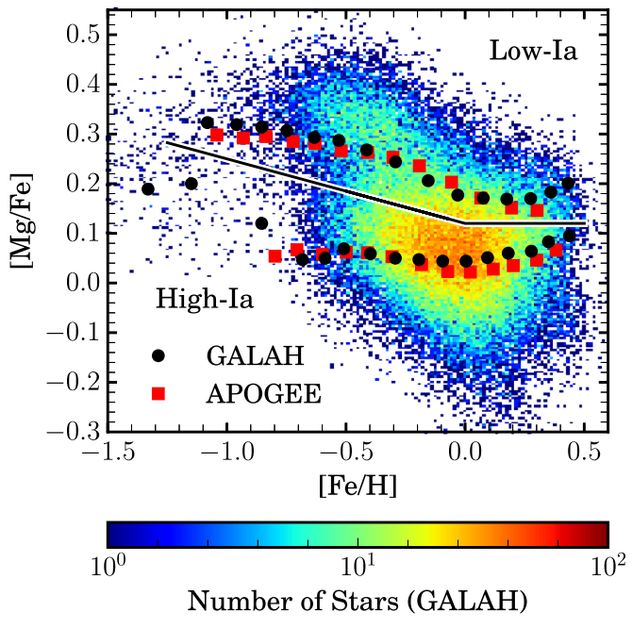

Figure 2. Distribution of 70,924 stars with S/N ⩾ 40 and 4500 K ⩽ $T_{\rm eff}$ ⩽ 6200 K in [Mg/Fe] vs. [Fe/H] space. The dividing line between the high-Ia and low-Ia populations is taken from W19. Black and red markers represent the GALAH and APOGEE median trends, respectively, for high-Ia and low-Ia populations.

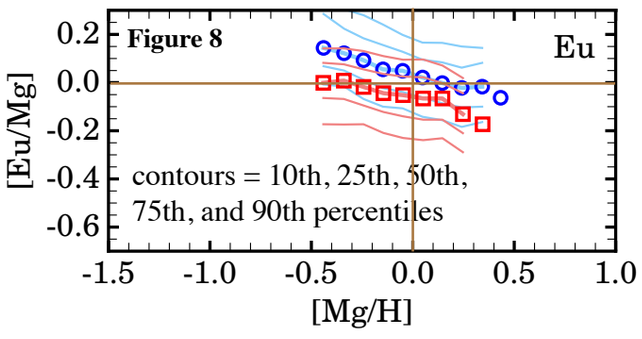

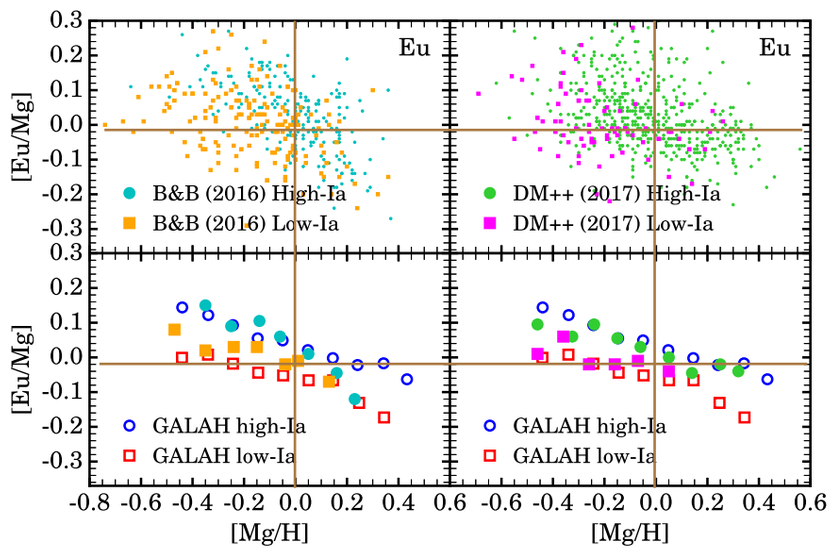

Figure 9. Top left: distribution of Eu abundances in 378 dwarf stars from Battistini & Bensby (2016). Stars classified as high-Ia and low-Ia are colored teal and orange, respectively. Top right: distribution of Eu abundances in 570 FGK stars from Delgado Mena et al. (2017) with green high-Ia and magenta low-Ia stars. Bottom left and right: median abundances of the high-Ia (filled teal/green circles) and low-Ia (filled orange/ magenta squares) populations. GALAH median trends (bottom left panel of Figure 8) are added for comparison.

Eu differs from the other neutron capture elements included in GALAH as the r-process dominates its production (Arlandini et al. 1999; Battistini & Bensby 2016). We see some separation between the high-Ia and low-Ia sequences in Figure 8, suggesting that some Eu is produced by a time-delayed source.

Eu is usually regarded as a nearly pure r-process element, but the separation of [Eu/Mg] in GALAH data implies that some Eu enrichment occurs with a significant time delay relative to star formation ($f_{\rm cc} = 0.70$). As emphasized by Schönrich & Weinberg (2019) who focused on abundance ratios in lower-metallicity stars, some of this time delay could be associated with injection into the hot ISM phase rather than genuinely delayed elemental production. Nonetheless, the gap between the low-Ia and high-Ia [Eu/Mg] sequences suggests that there may be two distinct contributions to Eu enrichment, perhaps one associated with massive star collapse explosions (Siegel et al. 2019) and one with neutron star mergers (Smartt et al. 2017). Neutron star mergers with a short minimum delay time but a power-law DTD (Hotokezaka et al. 2018) might effectively mimic a prompt and delayed combination.

My summary: The High-Ia stars have about 0.2 dex higher [Eu/Mg] than the low-Ia stars, but both show decreases of [Eu/Mg] by ~0.25 dex from [Mg/H] ~ -0.5 to +0.4. From Figs 8 and 9, the 10 to 90 percentile range in [Eu/Mg] is -0.3 to + 0.3 for [Mg/H] > -0.3.

The chemical evolution of r-process elements from neutron star mergers: the role of a 2-phase interstellar medium - Ralph A. Schönrich and David H. Weinberg - MNRAS 487, 580–594 (2019)

ABSTRACT Neutron star mergers (NM) are a plausible source of heavy r-process elements such as Europium, but previous chemical evolution models have either failed to reproduce the observed Europium trends for Milky Way thick disc stars (with [Fe/H] ≈ −1) or have done so only by adopting unrealistically short merger time-scales. Using analytic arguments and numerical simulations, we demonstrate that models with a single-phase interstellar medium (ISM) and metallicity-independent yields cannot reproduce observations showing [Eu/α] > 0 or [Eu/Fe] > [α/Fe] for α-elements such as Mg and Si. However, this problem is easily resolved if we allow for a 2-phase ISM, with hot-phase cooling times τ cool of the order of 1 Gyr and a larger fraction of NM yields injected directly into the cold star-forming phase relative to α-element yields from core-collapse supernovae (ccSNe). We find good agreement with observations in models with a cold phase injection ratio fc,NM/fc,ccSN of the order of 2, and a characteristic merger time-scale τNM = 150 Myr. We show that the observed supersolar [Eu/α] at intermediate metallicities implies that a significant fraction of Eu originates from NM or another source besides ccSNe, and that these non-ccSN yields are preferentially deposited in the star-forming phase of the ISM at early times.

We will argue in this paper that the essential ingredient for resolving this problem is proper accounting for enrichment into different phases of the ISM. While discussions of the ISM often distinguish three or more phases – e.g. cold, warm, and hot – for our purposes we need only distinguish (cold) gas that can immediately form stars from (hot) gas that must first cool on a ∼ Gyr time-scale before entering the star-forming phase.

SAGA = Stellar Abundances for Galactic Archaeology - for low [Fe/H]

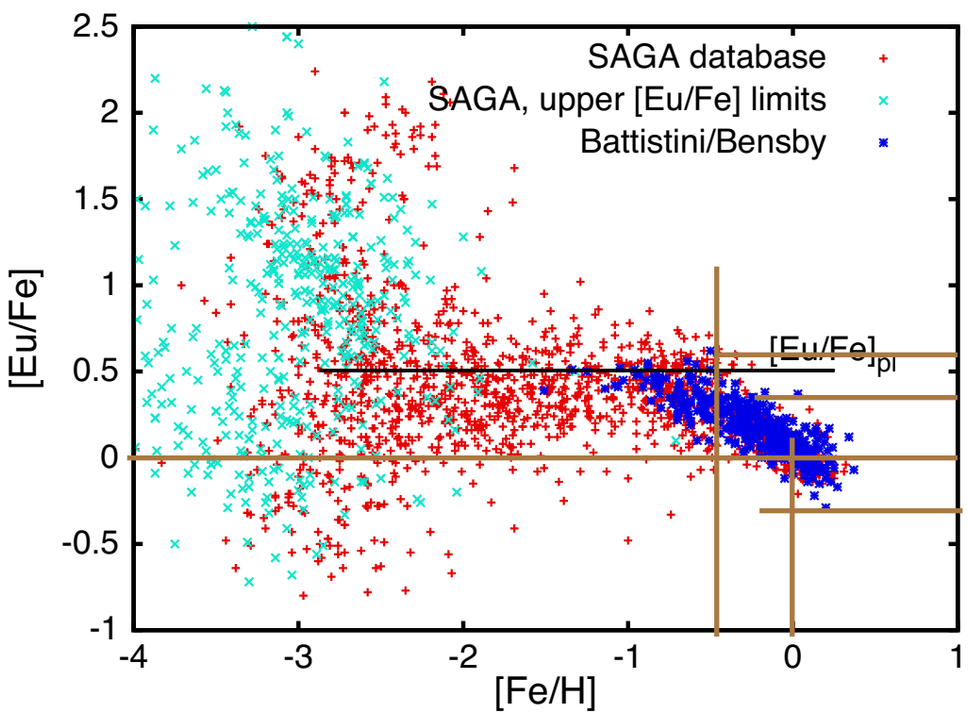

B&B A&A 2016 - Eu in 378 F & G dwarf stars in solar nbh

For [Fe/H] > -0.5 (for stars with planets), [Eu/Fe] range is -0.3 to +0.6, (½ to 4x solar). At [Fe/H] ~ 0 [Eu/Fe] range is -0.3 to +0.4 (½ to 2.5x solar)

7 CONCLUSIONS

We should take three main points from this analysis:

(i) Modelling the different phases of the interstellar medium (hot versus cold star-forming gas) is vital to understand chemical evolution on time-scales smaller than ∼1 Gyr.

(ii) In contrast to 1-phase chemical evolution models, we find that neutron star mergers as source of r-process elements with reasonable DTDs (delay times of the order of 100 Myr) can explain the observed abundance patterns, provided that the fraction of NM yields delivered directly to the cold star-forming phase of the ISM is higher than that of ccSN yields.

(iii) The only other significant sources of r-process elements are (possibly) ccSNe, but we can only explain the [Eu/Si] > 0 and [Eu/Mg] > 0 values in the thick disc if there is a source of r-process elements that differs from a constant ccSN contribution. This implies a significant source of r-process elements besides ccSNe – most naturally neutron star mergers.

The main problem is not as much explaining r-process abundances at the very metal-poor end, where stochastic chemical evolution and the superposition of stellar populations from different accreted dwarf galaxies complicate the picture (and provide freedom in parameter choice). Instead, the challenge is the relatively high-metallicity edge of the high [Eu/Fe] sequence, near the 'knee' of the [Mg/Fe] versus [Fe/H] distribution.

First results from the IllustrisTNG simulations: a tale of two elements – chemical evolution of magnesium and europium

Jill P. Naiman, Annalisa Pillepich, Volker Springel, Enrico Ramirez-Ruiz, et al. **MNRAS 477, 1206 (2018)**

ABSTRACT The distribution of elements in galaxies provides a wealth of information about their production sites and their subsequent mixing into the interstellar medium. Here we investigate the elemental distributions of stars in the IllustrisTNG simulations. We analyse the abundance ratios of magnesium and europium in Milky Way-like galaxies from the TNG100 simulation (stellar masses $\log(M_\star/\mathrm{M}_\odot) \sim 9.7$–$11.2$). Comparison of observed magnesium and europium for individual stars in the Milky Way with the stellar abundances in our more than 850 Milky Way-like galaxies provides stringent constraints on our chemical evolutionary methods. Here, we use the magnesium-to-iron ratio as a proxy for the effects of our SNII (core-collapse supernovae) and SNIa (Type Ia supernovae) metal return prescription and as a comparison to a variety of galactic observations. **The europium-to-iron ratio tracks the rare ejecta from neutron star–neutron star mergers, the assumed primary site of europium production in our models**, and is a sensitive probe of the effects of metal diffusion within the gas in our simulations. We find that europium abundances in Milky Way-like galaxies show no correlation with assembly history, present-day galactic properties, and average galactic stellar population age. We reproduce the europium-to-iron spread at low metallicities observed in the Milky Way, and find it is sensitive to gas properties during redshifts $z \approx 2$–4. We show that **while the overall normalization of [Eu/Fe] is susceptible to resolution and post-processing assumptions, the relatively large spread of [Eu/Fe] at low [Fe/H] when compared to that at high [Fe/H] is quite robust.**

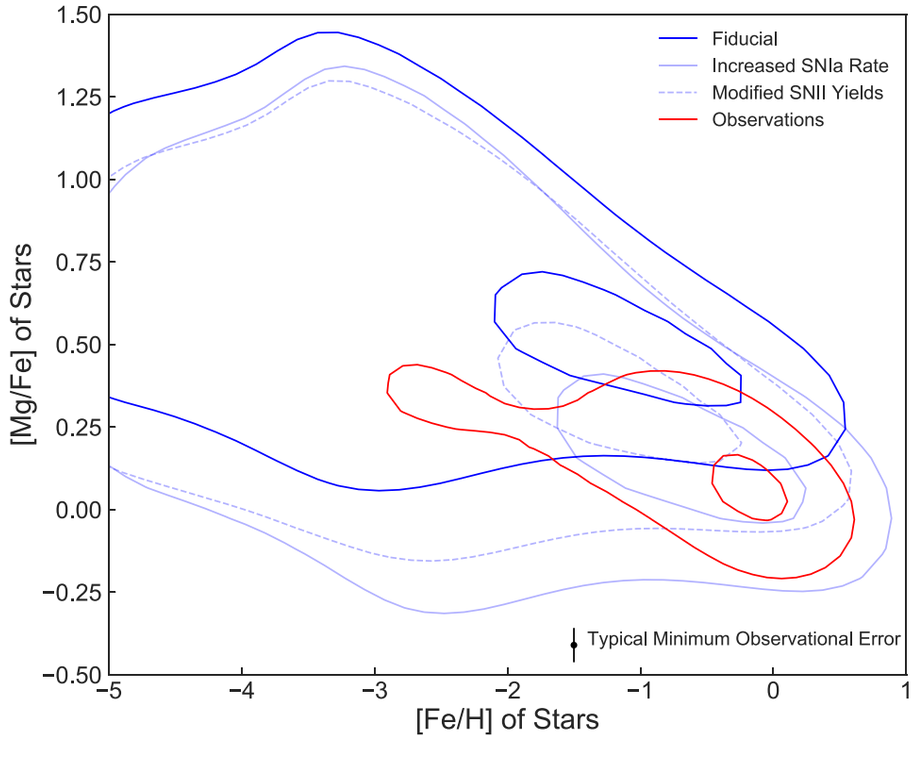

Figure 4. The [Mg/Fe] ratio in stars of both simulated IllustrisTNG MW-sized galaxies (blue contours) and that observed in the MW (red contour).Abundances have been renormalized to the solar values of Asplund, Grevesse & Sauval (2005)….The [Mg/Fe] ratio of simulated star-forming MW-sized galaxies (dark blue lines) is higher than observed (red contours). Besides complications in the comparison of observational and simulated abundance ratios (see Fig. 5), other depicted explanations for the discrepancy are a low rate of SNIa or incorrect SNII yields for Mg and/or Fe. The [Mg/Fe] discrepancy is alleviated in the MW- sized galaxies if the SNIa rate is increased by a factor of 3.5 in post- processing (light blue solid lines; see Fig. 2) or if the SNII Mg and Fe yields are modified (light blue dashed lines, see the text for further details). Contours of each colour are the 50percent and 5percent kernel density estimation levels.

First results from the IllustrisTNG simulations: a tale of two elements – chemical evolution of magnesium and europium Jill P. Naiman, Annalisa Pillepich, Volker Springel, Enrico Ramirez-Ruiz, et al. MNRAS 477, 1206 (2018)

See also galactic simulations of r-process elemental abundances

Christopher J Haynes, Chiaki Kobayashi - MNRAS 2018 claiming NSMs can't explain [Eu/Fe] at low [Fe/H]

and Schonrich & Weinberg MNRAS 2019 saying NSMs can with warm —> cold ISM

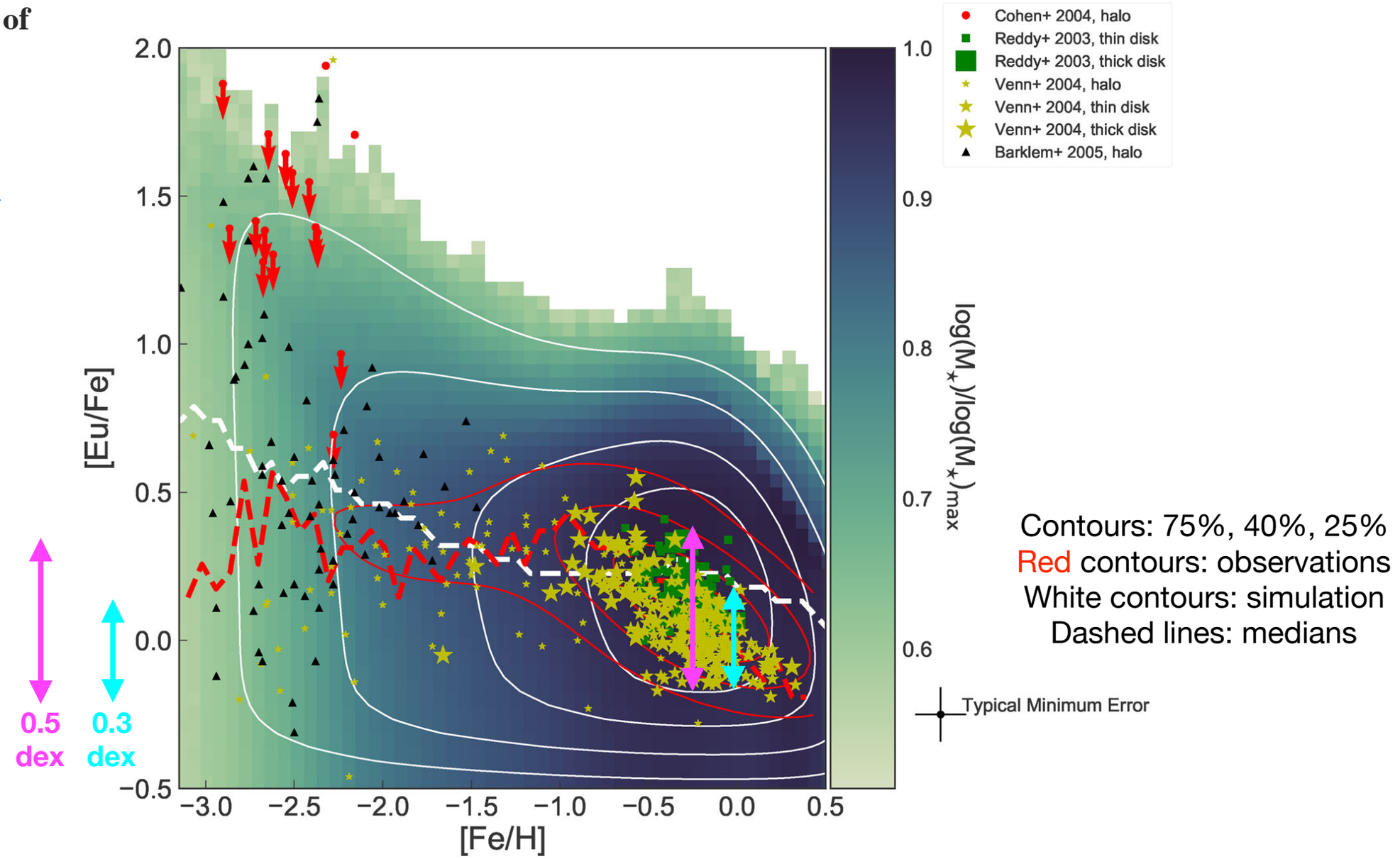

Figure 7. Distribution of [Eu/Fe]versus [Fe/H] for all sub-mass bins of all bound star particles of our simulated MW-like galaxies, binned in a 50 × 50 histogram. Red (white) solid lines denote the 75 per cent, 40 per cent, 25 per cent, and 10 per cent contour levels of the observed (simulated) density of data points while dashed lines show the medians of the distributions in each [Fe/H] bin. Observations denoted with red contour levels are compiled by the NuPyCEE package (Ritter & Côté 2016) and include halo, thick, and thin disc stars (Reddy et al. 2003; Venn et al. 2004; Bensby et al. 2005; Reddy et al. 2006; Aoki & Honda 2008; Lai et al. 2008; Roederer et al. 2009; Frebel 2010; Hansen et al. 2012; Ishigaki et al. 2012; Hinkel et al. 2014; Roederer et al. 2014; Jacobson et al. 2015; Battistini & Bensby 2016). Observationally, MW halo stars dominate the contribution to the [Eu/Fe] ratio at low [Fe/H], as shown by the highlighted observations of Cohen et al. (2004); Venn et al. (2004). In contrast, thin and thick disc stars make up the majority of the contribution at higher metallicities (Reddy et al. 2003; Venn et al. 2004). In the Reddy et al. (2003) observations, membership to the thick disc is denoted by having a line-of-sight velocity $>-40.0\,\mathrm{km\,s^{-1}}$, while membership in any component of the Venn et al. (2004) observations is based on their component membership probability being larger than 0.5. Other sources have selected for halo stars explicitly (Cohen et al. 2004; Barklem et al. 2005). Here, and in following [Eu/Fe]versus [Fe/H] plots, lower confidence interval KDE lines are only approximations to the total [Eu/Fe]versus [Fe/H] distribution as several cuts have been applied to the included star particles due to numerical effects (see the text for details).

Neutron star mergers and rare core-collapse supernovae as sources of r-process enrichment in simulated galaxies

Freeke van de Voort, Rüdiger Pakmor, Robert J. J. Grand, Volker Springel, Facundo A. Gómez, Federico Marinacci arXiv:1907.01557

ABSTRACT

We use cosmological, magnetohydrodynamical simulations of Milky Way-mass galaxies from the Auriga project to study their enrichment with rapid neutron capture (r-process) elements. We implement a variety of enrichment models from both binary neutron star mergers and rare core-collapse supernovae. We focus on the abundances of (extremely) metal-poor stars, most of which were formed during the first ~Gyr of the Universe in external galaxies and later accreted onto the main galaxy. We find that the majority of metal-poor stars are r-process enriched in all our enrichment models. **Neutron star merger models result in a median r-process abundance ratio which increases with metallicity**, whereas the median trend in rare core-collapse supernova models is approximately flat. The scatter in r-process abundance increases for models with longer delay times or lower rates of r-process producing events. Our results are nearly perfectly converged, in part due to the mixing of gas between mesh cells in the simulations. Additionally, different Milky Way-mass galaxies show only small variation in their respective r-process abundance ratios. Current (sparse and potentially biased) observations of metal-poor stars in the Milky Way seem to prefer rare core-collapse supernovae over neutron star mergers as the dominant source of r-process elements. Dwarf galaxies which experience a single r-process event early in their history can show highly enhanced r-process abundances at low metallicity, which is seen both in observations and in our simulations. We discuss possible caveats to our models.

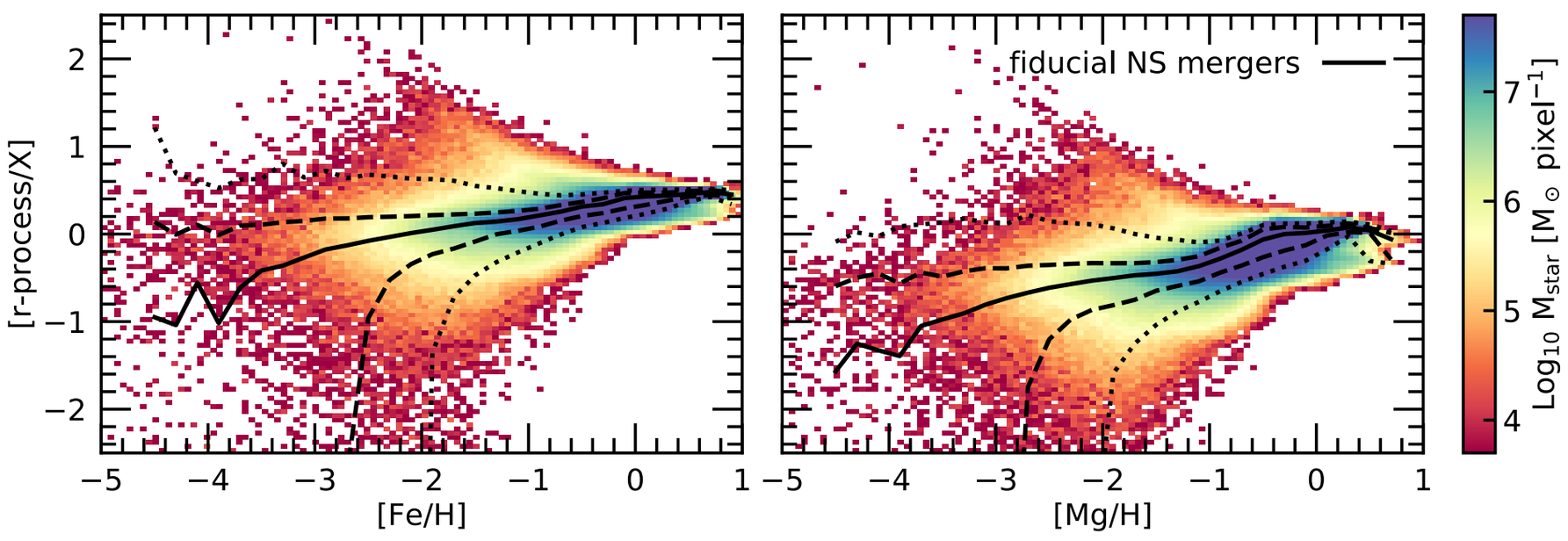

Figure 4. [r-process/Fe] ([r-process/Mg]) as a function of [Fe/H] ([Mg/H]) are shown in the left-hand (right-hand) panel for our fiducial neutron star merger enrichment model. The colour coding of the 200 by 200 pixel images represents the logarithm of the stellar mass per pixel. Black curves show the median (solid curves), the 1σ scatter (dashed curves), and the 2σ scatter (dotted curves). The r-process abundance ratios have been normalized in each panel so that the median is 0.4 (0.0) at [Fe/H] = 0 ([Mg/H] = 0). The median [r-process/Fe] and [r-process/Mg] increase with increasing metallicity. The distribution shows there are many extreme outliers in the metal-poor regime (more than expected from a Gaussian distribution) and the scatter increases towards low metallicity.

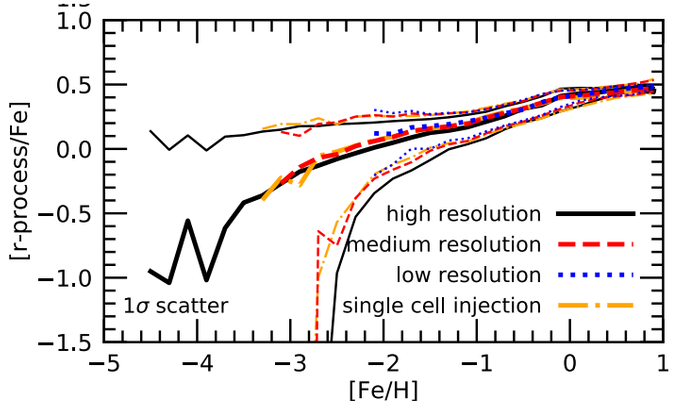

Figure 10. Median (thick curves) and 84th and 16th percentiles (thin curves) of [r-process/Fe] as a function of [Fe/H] using the normalization of the high-resolution simulation (black solid curves).

Shen et al. (2015) used a post-processing enrichment approach, which means they injected r-process elements after the simulation was finished. The results could therefore depend on the spacing between output times of the simulation. Their fiducial model additionally includes a metallicity floor for iron and a subgrid mixing scheme (assigning abundances based on 128 neighbouring gas particles) for both iron and r-process elements. This study found that the median [r-process/Fe] decreases with increasing metallicity, as opposed to the results presented in this work. Unfortunately, whether or not these results depend on resolution is not discussed. We believe the discrepancy with our simulations is likely due to the post-processing approach in Shen et al. (2015) and it would be interesting to see how our results compare when both simulations apply on-the-fly r-process enrichment.

Naiman et al. (2018) used on-the-fly r-process enrichment, which included a metallicity floor for both iron and r-process elements, and a subgrid scheme in post-processing to redistribute r-process elements to only part of the mass contained by a star particle. The latter was necessary because of the limited resolution of the simulation (owing to the much larger volume simulated, yielding many Milky Way-mass galaxies). This study also found that the median [r-process/Fe] decreases with increasing metallicity, again contrary to our current results. We believe the imposed metallicity floor in Naiman et al. (2018) is responsible for this behaviour, because it artificially increases [r-process/Fe] at [Fe/H] < -1.5, as shown by their results without subgrid redistribution model in post-processing.

Because our simulations are well-converged and the r-process enrichment was treated self-consistently and on-the-fly, with no imposed metallicity floor nor subgrid mixing prescription, we believe that **our conclusions of a rising trend in [r-process/Fe] with metallicity for neutron star merger models is robust.** Based on the fact that our r-process results vary little with resolution (see also Section 3.4), we expect that Lagrangian codes with realistic diffusion and on-the-fly r-process enrichment would find an increasing trend of [r-process/Fe] with metallicity as well.

There are a few caveats to our study, however. The ISM model employed by our simulations does not attempt to capture the clumpy multi-phase structure of the Milky Way's ISM. The resulting model ISM is therefore smoother, possibly resulting in metals mixing too efficiently within the ISM (see also Schönrich & Weinberg 2019). Our simulations also do not include neutron star kicks, which could cause a larger fraction of neutron star mergers to occur outside the galaxy, in the low-metallicity halo. This would result in less efficient direct r-process enrichment of the ISM, but potentially higher r- process abundances in accreting gas. Whether or not adding such ingredients improves the match of our neutron star merger models to observations will be explored in future work.

This paper presents a comprehensive geoneutrino measurement using the Borexino detector, located at Laboratori Nazionali del Gran Sasso (LNGS) in Italy. The analysis is the result of 3262.74 days of data between December 2007 and April 2019. The paper describes improved analysis techniques and optimized data selection, which includes enlarged fiducial volume and sophisticated cosmogenic veto. The reported exposure of $(1.29 \pm 0.05)\times10^{32}$ protons × year represents an increase by a factor of two over a previous Borexino analysis reported in 2015. By **observing $52.6^{+9.4}_{-8.6}$ (stat)$^{+2.7}_{-2.1}$(sys) geoneutrinos (68% interval) from ^{238}U and ^{232}Th, a geoneutrino signal of $47.0^{+8.4}_{-7.7}$ (stat)$^{+2.4}_{-1.9}$ (sys) TNU with $^{+18.3}_{-17.2}$% total precision was obtained. This result assumes the same Th/U mass ratio found in chondritic CI meteorites but compatible results were found when contributions from ^{238}U and ^{232}Th were both fit as free parameters.** Antineutrino background from reactors is fit unconstrained and found compatible with the expectations. The null-hypothesis of observing a geoneutrino signal from the mantle is excluded at a 99.0% C.L. when exploiting detailed knowledge of the local crust near the experimental site. Measured mantle signal of $21.2^{+9.6}_{-9.0}$ (stat)$^{+1.1}_{-0.9}$ (sys) TNU corresponds to the production of a radiogenic heat of $24.6^{+11.1}_{-10.4}$ TW (68% interval) from ^{238}U and ^{232}Th in the mantle. Assuming 18% contribution of ^{40}K in the mantle and $8.1^{+1.9}_{-1.4}$ TW of total radiogenic heat of the lithosphere, **the Borexino estimate of the total radiogenic heat of the Earth is $38.2^{+13.6}_{-12.7}$ TW, which corresponds to the convective Urey ratio of $0.78^{+0.41}_{-0.28}$**. These values are compatible with different geological predictions, however there is a ~2.4σ tension with those Earth models which predict the lowest concentration of heat-producing elements in the mantle. In addition, by fitting with a constraint on the number of expected reactor antineutrino events, the existence of a hypothetical georeactor at the center of the Earth having power greater than 2.4 TW at 95% C.L. is excluded. Particular attention is given to the description of all analysis details which should be of interest for the next generation geoneutrino measurements using liquid scintillator detectors.

The expected geo-neutrino signal is expressed in **Terrestrial Neutrino Units**, where 1 TNU corresponds to one event per 10^{32} target protons occurring at the detector per year of exposure time (from ref. 65 M. Coltorti *et al.*, Geochim. Cosmochim. Acta 75, 2271 (2011), arXiv:1102.1335).

The ***Convective Urey Ratio*** **(UR_{CV})** quantifies the ratio of internal heat generation in the mantle over the mantle heat flux:

$$UR_{\mathrm{CV}} = \frac{H_{\mathrm{rad}} - H^{\mathrm{CC}}_{\mathrm{rad}}}{H_{\mathrm{tot}} - H^{\mathrm{CC}}_{\mathrm{rad}}},$$ where H^{CC} is the radiogenic heat produced in the continental crust.

Borexino Radiogenic Heat Flux and Convective Urey Ratio vs. BSE Models

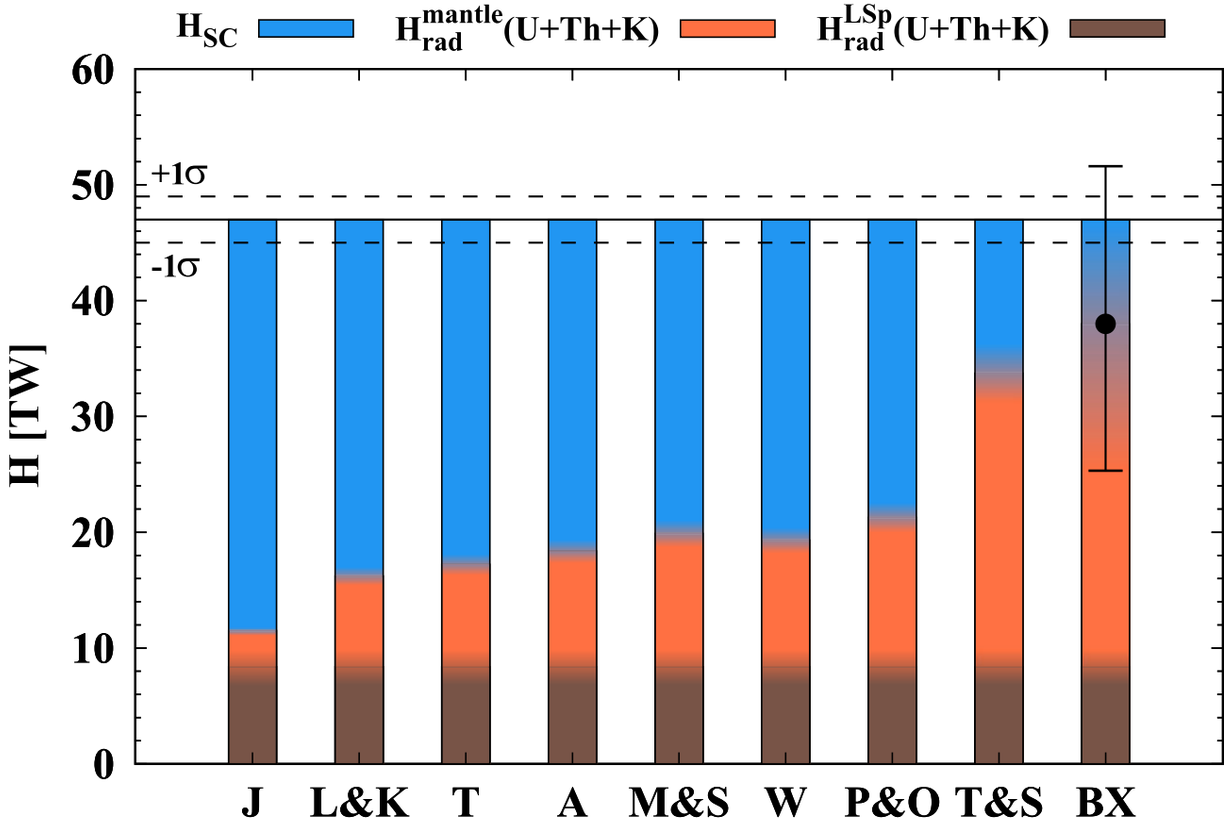

FIG. 55. Decomposition of the Earth's total surface heat flux $H_{tot} = (47 \pm 2)$ TW (horizontal black lines) into its three major contributions—lithospheric (brown) and mantle (orange) radiogenic heat H_{rad}^{LSp} and H_{rad}^{mantle}, respectively, and secular cooling H_{SC} (blue). The labels on the x axis identify different BSE models (Table VII), while the last bar labeled BX represents the Borexino measurement. The lithospheric contribution $H_{rad}^{LSp} = 8.1^{+1.9}_{-1.4}$ TW (Table V) is the same for all bars. The amount of HPEs predicted by BSE models determines the mantle radiogenic heat (Table VII), while for Borexino the value of $30.0^{+13.5}_{-12.7}$ TW is inferred from the extracted mantle signal. The difference between H_{tot} and the respective total radiogenic heat is assigned to the heat from secular cooling of the Earth.

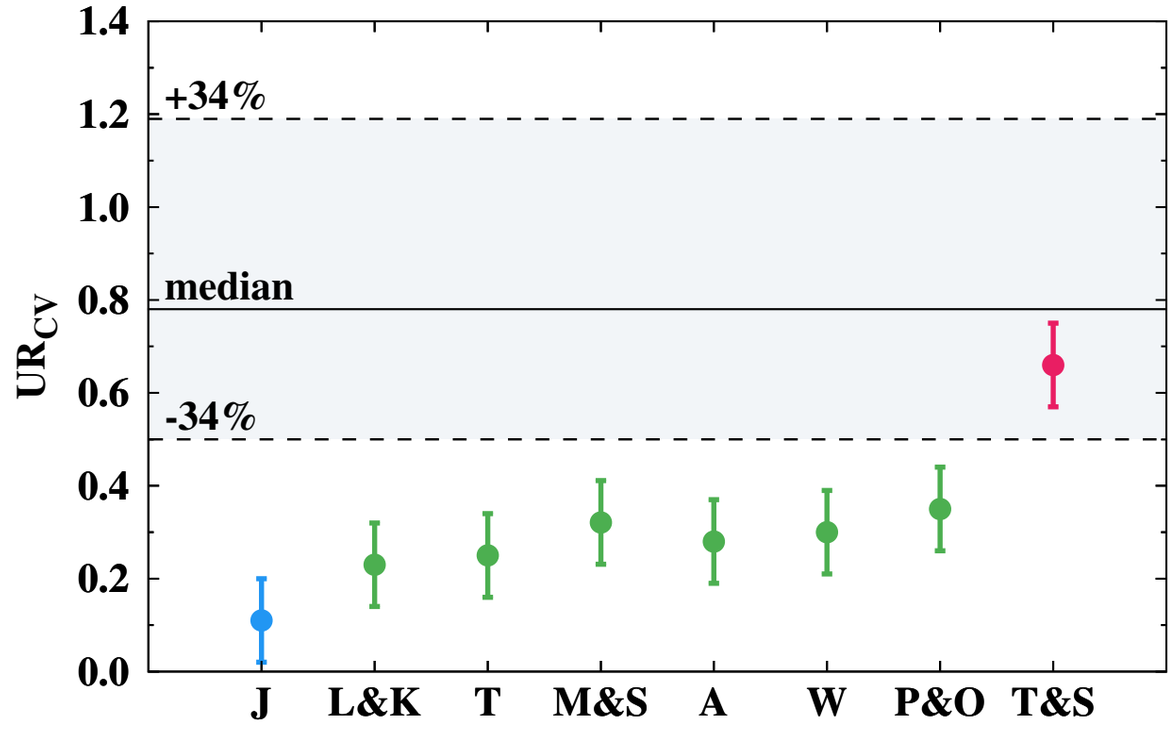

FIG. 56. Comparison of Borexino constraints (horizontal band) with predictions of the BSE models (points with $\pm 3\sigma$ error bars, Table VII) for the convective Urey ratio UR_{CV} [Eq. (6)], assuming the total heat flux $H_{tot} = (47 \pm 2)$ TW and the radiogenic heat of the continental crust $H_{rad}^{CC} = 6.8^{+1.4}_{-1.1}$ TW (Table V). The blue, green, and red colors represent different BSE models (CC, GC, and GD; Table VII, respectively).

- J: Javoy at al., 2010
- L&K: Lyubetskaya and Korenaga, 2007
- T: Taylor, 1980
- A: Anderson, 2007
- M&S: Mc Donough and Sun, 1995
- W: Wang, 2018
- P&O: Palme and O'Neil, 2003
- T&S: Turcotte and Schubert, 2002

An independent method to study the matter composition deep within the Earth, can be provided by geoneutrinos, i.e. (anti)neutrinos emitted by the Earth's radioactive elements. Their detection allows to assess the Earth's heat budget, specifically the heat emitted in the radioactive decays. The latter, the so-called *radiogenic heat* of the present Earth, arises mainly from the decays of isotopes with half-lives comparable to, or longer than Earth's age ($4.543 \cdot 10^9$ years): ^{232}Th ($T_{1/2} = 1.40 \cdot 10^{10}$ years), ^{238}U ($T_{1/2} = 4.468 \cdot 10^9$ years), ^{235}U ($T_{1/2} = 7.040 \cdot 10^8$ years), and ^{40}K ($T_{1/2} = 1.248 \cdot 10^9$ years) [4]. All these isotopes are labeled as *heat-producing elements* (HPEs). The natural Thorium is fully composed of ^{232}Th, while the natural isotopic abundances of ^{238}U, ^{235}U, and ^{40}K are 0.992742, 0.007204, and 1.17×10^{-4}, respectively. In each decay, the emitted radiogenic heat is in a well-known ratio[7] to the number of emitted geoneutrinos [5]:

$$^{238}\mathrm{U} \rightarrow {}^{206}\mathrm{Pb} + 8\alpha + 8e^- + 6\bar{\nu}_e + 51.7\,\mathrm{MeV} \quad (1)$$

$$^{235}\mathrm{U} \rightarrow {}^{207}\mathrm{Pb} + 7\alpha + 4e^- + 4\bar{\nu}_e + 46.4\,\mathrm{MeV} \quad (2)$$

$$^{232}\mathrm{Th} \rightarrow {}^{208}\mathrm{Pb} + 6\alpha + 4e^- + 4\bar{\nu}_e + 42.7\,\mathrm{MeV} \quad (3)$$

$$^{40}\mathrm{K} \rightarrow {}^{40}\mathrm{Ca} + e^- + \bar{\nu}_e + 1.31\,\mathrm{MeV}\ (89.3\%) \quad (4)$$

$$^{40}\mathrm{K} + e^- \rightarrow {}^{40}\mathrm{Ar} + \nu_e + 1.505\,\mathrm{MeV}\ (10.7\%) \quad (5)$$

Obviously, the total amount of emitted geoneutrinos scales with the total mass of HPEs inside the Earth. Hence, geoneutrinos' detection provides us a way of measuring this radiogenic heat.

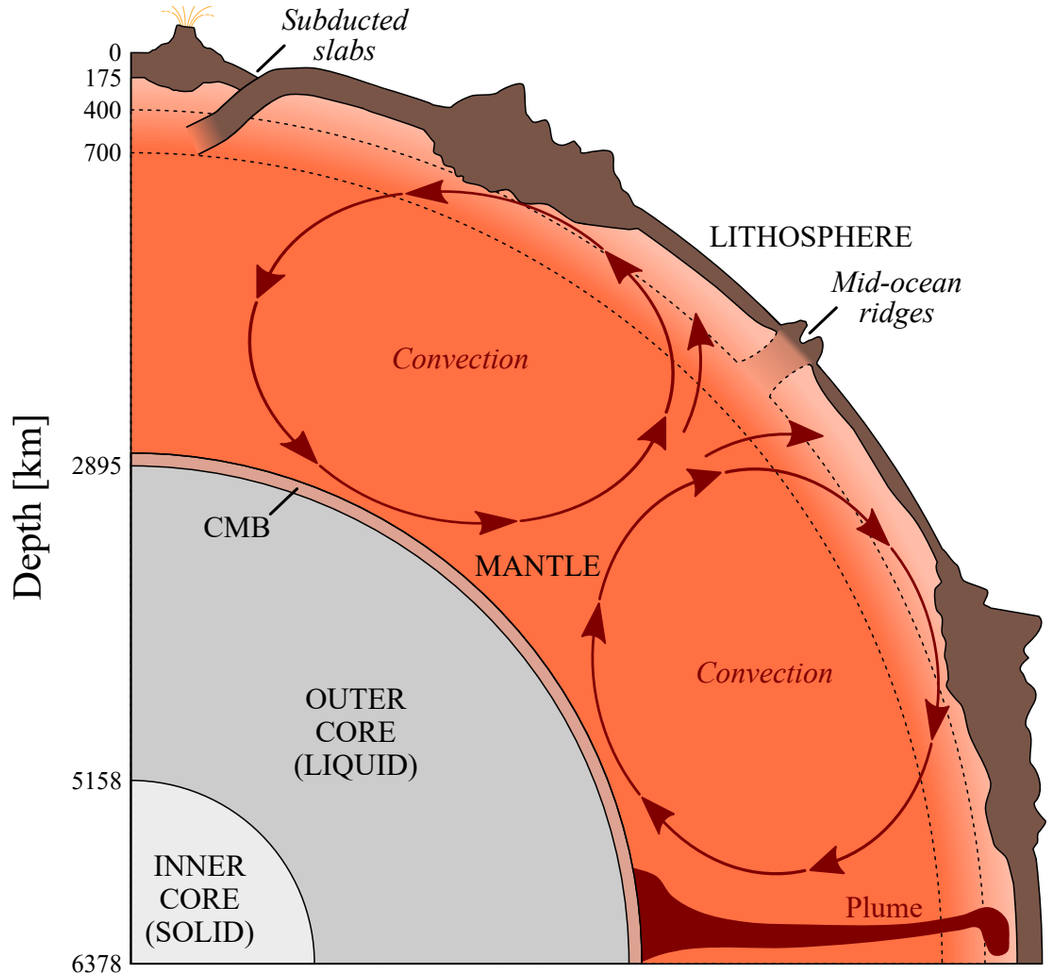

FIG. 1. Schematic cross-section of the Earth. The Earth has a concentrically layered structure with an equatorial radius of 6378 km. The metallic *core* includes an inner solid portion (1220 km radius) and an outer liquid portion which extends to a depth of 2895 km, where the core is isolated from the silicate *mantle* by the *core-mantle boundary* (CMB). Seismic tomography suggests a convection through the whole depth of the viscose mantle, that is driving the movement of the *lithospheric tectonic plates*. The lithosphere, subjected to brittle deformations, is composed of the *crust* and *continental lithospheric mantle*. The *mantle transition zone*, extending from a depth of 400 to 700 km, is affected by partial melting along the mid-oceanic ridges where the *oceanic crust* is formed. The *continetal crust* is more complex and thicker than the oceanic crust.

We assume a $H_{\rm tot}$ =(47±2)TW as the best current estimation. Neglecting the small contribution (<0.5TW) from tidal dissipation and gravitational potential energy released by the differentiation of crust from the mantle, the $H_{\rm tot}$ is typically expected to originate from two main processes: (*i*) *secular cooling* of the Earth, i.e. cooling from the time of the Earth's formation when gravitational binding energy was released due to matter accretion $H_{\rm SC}$, and (*ii*) *radiogenic heat* $H_{\rm rad}$ from heat producing elements (HPEs) radioactive decays in the Earth. The relative contribution of radiogenic heat to the $H_{\rm tot}$ is crucial in understanding the thermal conditions occurring during the formation of the Earth and the energy now available to drive the dynamical processes such as the mantle and outer-core convection. The *Convective Urey Ratio* ($UR_{\rm CV}$) quantifies the ratio of internal heat generation in the mantle over the mantle heat flux, as the following ratio [44]:

$$UR_{\rm CV} = \frac{H_{\rm rad} - H^{\rm CC}_{\rm rad}}{H_{\rm tot} - H^{\rm CC}_{\rm rad}}, \qquad (6)$$

where $H^{\rm CC}$ is the radiogenic heat produced in the continental crust. The secular cooling of the core is expected in the range of [5 - 11] TW [45], while no radiogenic heat is expected to be produced in the core.

Preventing dramatically high temperatures during the initial stages of Earth formation, the present-day $UR_{\rm CV}$ must be in the range between 0.12 to 0.49 [45]. Additionally, HPEs' abundances, and thus Hrad of Eq. 6, are globally representative of *BSE models*, defining the original chemical composition of the Primitive Mantle. The elemental composition of BSE is obtained assuming a common origin for celestial bodies in the solar system. It is supported, for example, by the strong correlation observed between the relative (to Silicon) isotopical abundances in the solar photosphere and in the CI chondrites (Fig. 2 in [32]). Such correlations can be then assumed also for the material from which the Earth was created. The BSE models agree in the prediction of major elemental abundances (e.g. O, Si, Mg, Fe) within 10% [49]. Uranium and Thorium are *refractory* (condensate at high temperatures) and *lithophile* (where silicates over metal are preferred) elements. The relative abundances of the refractory lithophile elements are expected to be stable to volatile loss or core formation during the early stage of the Earth [57]. The content of refractory lithophile elements (e.g. U and Th), which are excluded from the core[11], are assumed based on relative abundances in chondrites, and dramatically differ between different models. In Table II global masses of HPEs and their corresponding radiogenic heat are reported, covering a wide spectrum of BSE compositional models. The contributions to the radiogenic heat of U, Th, and K vary in the range of [39 - 44]%, [40 - 45]%, and [11 - 17]%, respectively.

[11] Recent speculations [58] about possible partitioning of some lithophile elements (including U and Th) into the metallic core are still debated [59, 60]. This would explain the anomalous Sm/Nd ratio observed in the silicate Earth and would represent an additional radiogenic heat source for the geodynamo process.

The most precise estimate of the planetary Th/U mass ratio reference, having a direct application in geoneutrino analysis, has been refined to a value of $M_{\rm Th}/M_{\rm U} = (3.876 \pm 0.016)$ [61]. Recent studies [62], based on measured molar ^{232}Th/^{238}U values and their time integrated Pb isotopic values, are in agreement estimating $M_{\rm Th}/M_{\rm U} = 3.90^{+0.13}_{-0.08}$.

Note: BSE = Bulk Silicate Earth

In future, detection of ^{40}K geoneutrinos might be possible [71, 72]. This would be extremely important, since Potassium is the only semi-volatile HPE. Our planet seems to show ~1/3 [49] to ~1/8 [34] Potassium when compared to chondrites, making its expected bulk mass span of a factor ~2 across different Earth's models. Two theories on the fate of the mysterious "missing K" include loss to space during accretion [49] or segregation into the core [73], but no experimental evidence has been able to confirm or rule out any of the hypotheses, yet. As a consequence, the different BSE class models predict a K/U ratio in the mantle in a relatively wide range from 9700 to 16000 [54]. According to these ratios, the Potassium radiogenic heat of the mantle varies in the range [2.6 – 4.3] TW, which translates to an average contribution of 18% to the mantle radiogenic power. We will use this value in the evaluation of the total Earth radiogenic heat from the Borexino geoneutrino measurement (Sec. 11.6).

5.2 Geoneutrinos The Earth is a planet shining essentially in a flux of antineutrinos with a luminosity $L \sim 10^{25}$ s^{-1}. For a detector placed on the continental crust, the expected U and Th geoneutrino flux is of the order of 10^6 cm^{-2} s^{-1} and is typically dominated by the crustal contribution.

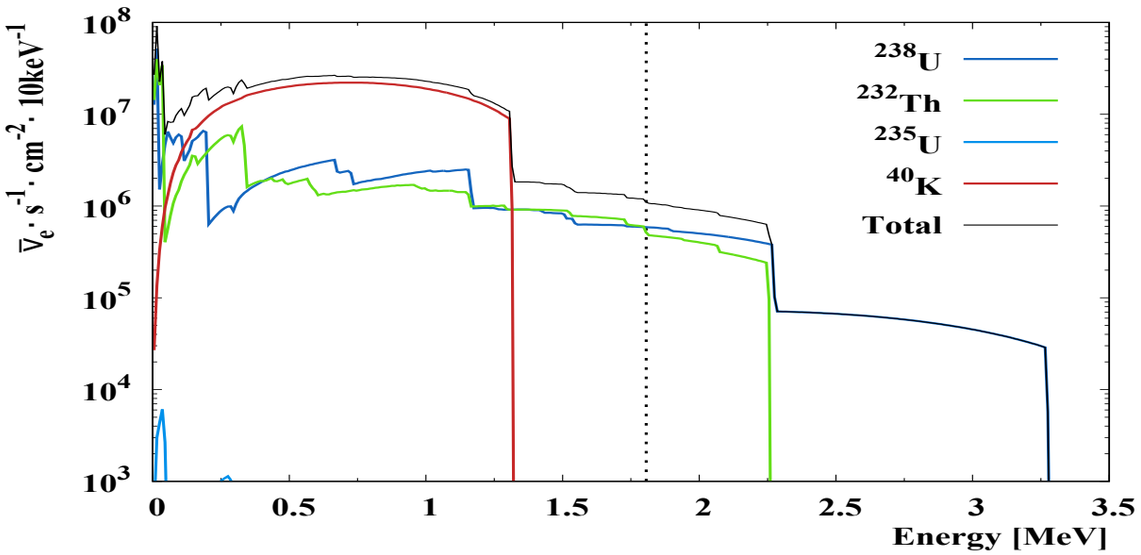

Fig. 15b. Geoneutrino fluxes from different isotopes and their sum at LNGS as a function of geoneutrino energies calculated adopting geophysical and geochemical inputs from [35] for the far-field lithosphere and from [65] for the local crust. The flux from the mantle is calculated assuming a two-layer distribution and adopting HPEs' abundances in BSE according to the GC model. The vertical dashed lines represents the kinematic threshold of the IBD interaction.

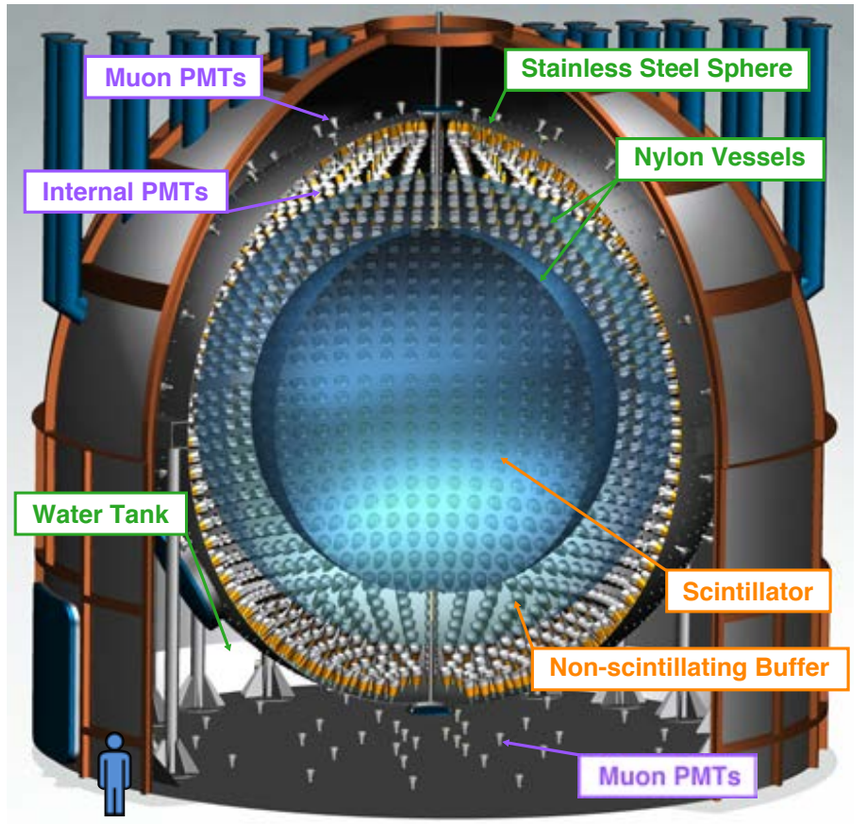

FIG. 2. Scheme of the Borexino detector.

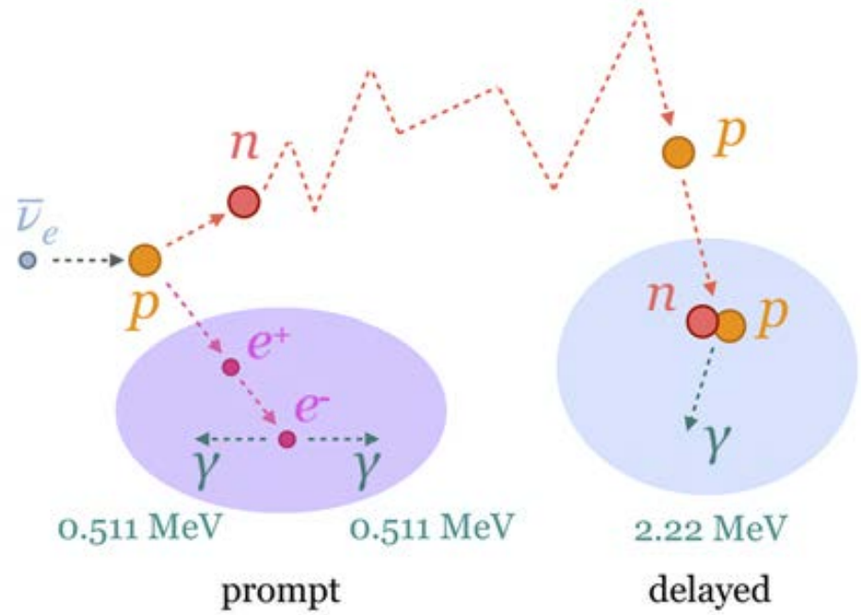

FIG. 12. Schematic of the proton Inverse Beta Decay (IBD) interaction that is used to detect geoneutrinos. The origin of the prompt (positron) and the delayed (gamma from neutron capture) signals is depicted.

A radiogenic heating evolution model for cosmochemically Earth-like exoplanets

Elizabeth A. Frank [a,⇑], Bradley S. Meyer [b], Stephen J. Mojzsis **- Icarus 243 (2014) 274–286**

Discoveries of rocky worlds around other stars have inspired diverse geophysical models of their plausible structures and tectonic regimes. Severe limitations of observable properties require many inexact assumptions about key geophysical characteristics of these planets. We present the output of an **analytical galactic chemical evolution (GCE) model that quantitatively constrains one of those key properties: radiogenic heating. Earth's radiogenic heat generation has evolved since its formation, and the same will apply to exoplanets**. We have fit simulations of the chemical evolution of the interstellar medium in the solar annulus to the chemistry of our Solar System at the time of its formation and then applied the carbonaceous chondrite/Earth's mantle ratio to determine the chemical composition of what we term ''cosmochemically Earth-like'' exoplanets. Through this approach, predictions of exoplanet radiogenic heat productions as a function of age have been derived. The results show that **the later a planet forms in galactic history, the less radiogenic heat it begins with; however, due to radioactive decay, today, old planets have lower heat outputs per unit mass than newly formed worlds**. The long half-life of ^{232}Th allows it to continue providing a small amount of heat in even the most ancient planets, while ^{40}K dominates heating in young worlds. Through constraining the age-dependent heat production in exoplanets, we can infer that **younger, hotter rocky planets are more likely to be geologically active and therefore able to sustain the crustal recycling (e.g. plate tectonics) that may be a requirement for long-term biosphere habitability**. In the search for Earth-like planets, the focus should be made on stars within a billion years or so of the Sun's age.

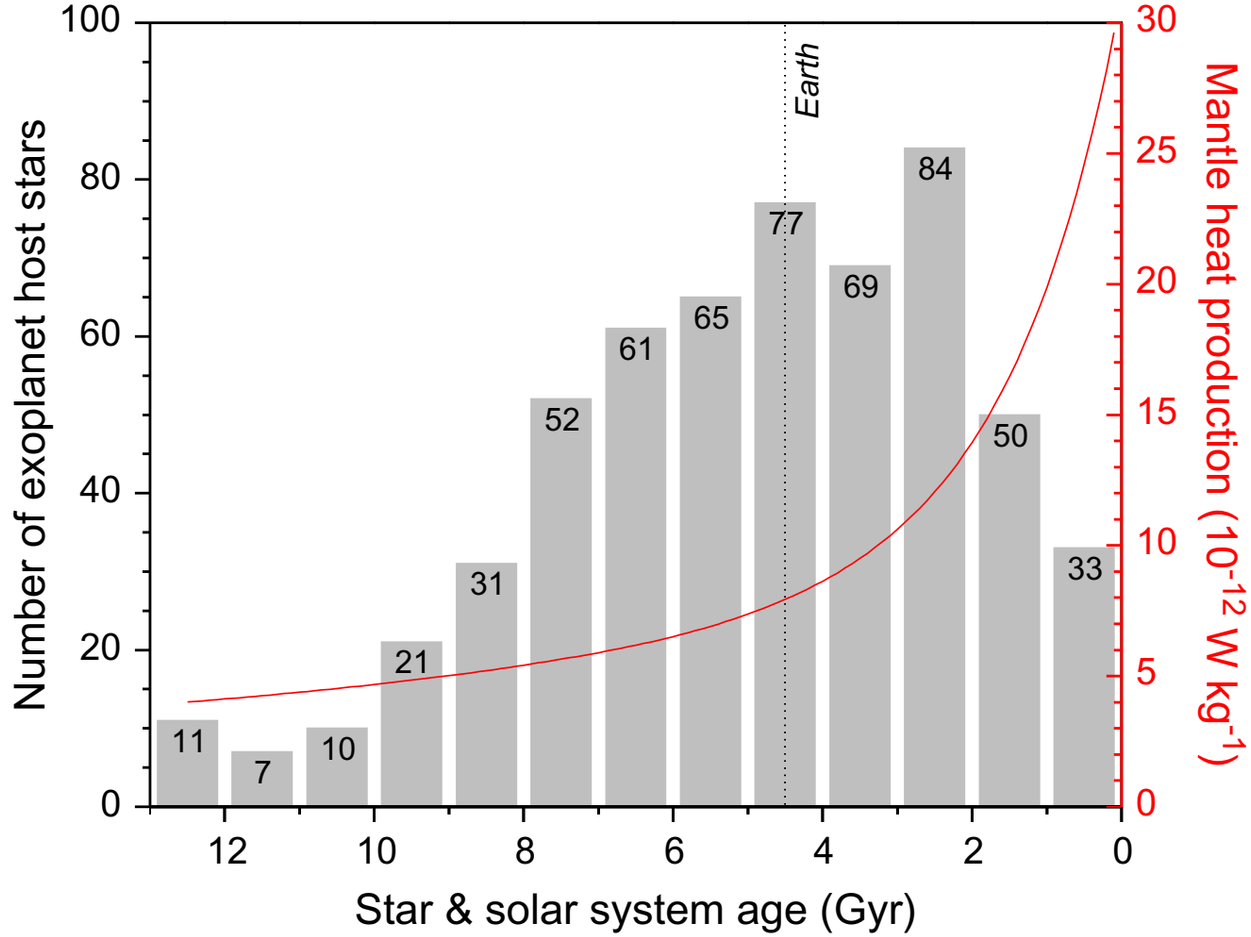

Fig. 14. Number of exoplanet host stars as a function of their age in 2012 superimposed with the predicted current heat production for cosmochemically Earth-like planets. The host stars include those that have either gaseous or rocky planets, and some stars are known to host multiple planets.

Carbon cycling and habitability of Earth-size stagnant lid planets

Bradford J. Foley and Andrew J. Smye

Models of thermal evolution, crustal production, and CO_2 cycling are used to constrain the prospects for habitability of rocky planets, with Earth-like size and composition, in the stagnant lid regime. Specifically, we determine the conditions under which such planets can maintain rates of CO_2 degassing large enough to prevent global surface glaciation, but small enough so as not to exceed the upper limit on weathering rates provided by the supply of fresh rock, a situation which would lead to runaway atmospheric CO_2 accumulation and an inhospitably hot climate. The models show that **stagnant lid planets with initial radiogenic heating rates of 100-250 TW, and with total CO_2 budgets ranging from $\sim 10^{-2}$ – 1 times Earth's estimated CO_2 budget, can maintain volcanic outgassing rates suitable for habitability for ≈ 1 – 5 Gyrs; larger CO_2 budgets result in uninhabitably hot climates, while smaller budgets result in global glaciation. High radiogenic heat production rates favor habitability by sustaining volcanism and CO_2 outgassing longer.** Thus, the results suggest that plate tectonics may not be required for establishing a long-term carbon cycle and maintaining a stable, habitable climate. The model is necessarily highly simplified, as the uncertainties with exoplanet thermal evolution and outgassing are large. Nevertheless, the results provide some first order guidance for future exoplanet missions, by predicting the age at which habitability becomes unlikely for a stagnant lid planet as a function of initial radiogenic heat budget. This prediction is powerful because both planet heat budget and age can potentially be constrained from stellar observations.

5.2 Comparison to plate-tectonic planets. On a plate-tectonic planet CO_2 degassing is easier to maintain. Ridges bring hot mantle all the way to the surface, meaning that volcanism at divergent plate margins will continue until the mantle potential temperature drops below the zero pressure solidus of ≈ 1400 K (Herzberg et al., 2000). Plate tectonics also allows for continual metamorphic degassing through subduction. … Plate tectonics also allows a stabilizing weathering feedback, and thus temperate climates, to be maintained at larger total CO_2 budgets than stagnant lid planets…

6 Conclusions Models of the thermal, magmatic, and degassing history of rocky planets with Earth- like size and composition demonstrate that a carbon cycle capable of regulating atmospheric CO_2 content, and stabilizing climate to temperate surface temperatures, can potentially operate on geologic timescales on planets in the stagnant lid regime. Plate tectonics may not be required for habitability, at least in regards to sustaining a stable, temperate climate on a planet. … Thus, **planets orbiting high thorium or uranium abundance stars or young stars are good targets for searching for biosignatures, because they are more likely to be habitable, even if the mode of surface tectonics is stagnant lid rather than plate tectonics.**

Habitability of Earth-like Stagnant Lid Planets: Climate Evolution and Recovery from Snowball States

ApJ 875 (2019) - Bradford J. Foley

ABSTRACT Coupled models of mantle thermal evolution, volcanism, outgassing, weathering, and climate evolution for Earth-like (in terms of size and composition) stagnant lid planets are used to assess their prospects for habitability. The results indicate that **planetary CO_2 budgets ranging from ≈3 orders of magnitude lower than Earth's to ≈1 order of magnitude larger, along with radiogenic heating budgets as large or larger than Earth's, allow for habitable climates lasting 1–5 Gyr. The ability of stagnant lid planets to recover from potential snowball states is also explored; recovery is found to depend on whether atmosphere–ocean chemical exchange is possible.** For a "hard" snowball with no exchange, recovery is unlikely, as most CO_2 outgassing takes place via metamorphic decarbonation of the crust, which occurs below the ice layer. However, for a "soft" snowball where there is exchange between atmosphere and ocean, planets can readily recover. For both hard and soft snowball states, there is a minimum CO_2 budget needed for recovery; below this limit, any snowball state would be permanent. Thus, there is the possibility for hysteresis in stagnant lid planet climate evolution, where **planets with low CO_2 budgets that start off in a snowball climate will be permanently stuck in this state, while otherwise identical planets that start with a temperate climate will be capable of maintaining this climate for 1 Gyr or more. Finally, the model results have important implications for future exoplanet missions, as they can guide observations to planets most likely to possess habitable climates.**

CONCLUSIONS

… **The initial radiogenic heating rate is also important: heating rates of ≈50 TW are needed for habitable climates to last for at least 1 Gyr, and increasing the heating rate increases the lifetime of volcanism—and hence of temperate climates as well.** Stagnant lid planets are assumed to be dominated by seafloor weathering in this study, and the strong climate buffering ability of seafloor weathering, along with its lower overall weathering rate as compared to continental weathering on Earth, allow a wide range of CO2 budgets to support long-lived habitable climates

A nearby neutron-star merger explains the actinide abundances in the early Solar System

Imre Bartos & Szabolcs Marka - Nature 569, 85 (2May2019)

From the first paragraph: Although short-lived r-process isotopes—with half-lives shorter than 100 million years—are no longer present in the Solar System, their abundances in the early Solar System are known because their daughter products were preserved in high-temperature condensates found in meteorites[5]. Here we report that abundances of short-lived r-process isotopes in the early Solar System point to their origin in neutron-star mergers, and indicate substantial deposition by a single nearby merger event. By comparing numerical simulations with the early Solar System abundance ratios of actinides produced exclusively through the r-process, we constrain the rate of occurrence of their Galactic production sites to within about $1-100$ per million years. This is consistent with observational estimates of neutron-star merger rates[6–8], but rules out supernovae and stellar sources. We further find that **there was probably a single nearby merger that produced much of the curium and a substantial fraction of the plutonium present in the early Solar System. Such an event may have occurred about 300 parsecs away from the pre-solar nebula, approximately 80 million years before the formation of the Solar System.**

My summary: This paper follows the methods of Hotokezaka, K., Piran, T. & Paul, M. Short-lived ^{244}Pu points to compact binary mergers as sites for heavy r-process nucleosynthesis. *Nat. Phys.* **11**, 1042 (2015). Analyzing early solar system (ESS) abundances of short-lived radionuclides ^{244}Pu, ^{247}Cm, and ^{129}I from the literature, they find that most of the ^{247}Cm and about half the ^{244}Pu came from a NSM 300 ± 100 pc away from the pre-solar nebula and 80 ± 40 Myr before its formation. However, they also found that only a very small fraction, about 0.003, of the ^{232}Th came from this NSM, and that this ^{232}Th abundance is only slightly (25%) lower than the uniform production rate with constant $R_{\rm merger}$.

From near the end of the paper:

Given the low Galactic merger rate, a single nearby source stands out as a possible primary origin of short-lived isotopes. This scenario is corroborated by our investigation. We used our Monte Carlo simulations with $R_{\rm merger} = 20$ / Myr to record the properties of the single merger that contributed the most ^{247}Cm to the early Solar System at each time point in our simulation. …

For these time points, we calculated the mean and standard deviation of the dominant event's distance, time and fractional contribution of N_{247} to the pre-solar nebula. We found that the obtained distance of the dominant merger fell within the small range of $d_{dom} = 300 \pm 100$ pc. The time between the dominant merger and the formation of the Solar System was $\Delta t_{\rm dom} = 80 \pm 40$ Myr. This time frame is consistent with the duration that has been considered previously for the isolation time of the pre-solar nebula before the formation of the early Solar System.

The following review by Lugaro+2018 is ref. 16 of Bartos & Marka

Contents lists available at ScienceDirect

Progress in Particle and Nuclear Physics

journal homepage: www.elsevier.com/locate/ppnp

Review

Radioactive nuclei from cosmochronology to habitability

M. Lugaro [a,b,*], U. Ott [c,d], Á. Kereszturi [a]

[a] Konkoly Observatory, Research Centre for Astronomy and Earth Sciences, Hungarian Academy of Sciences, H-1121 Budapest, Hungary
[b] Monash Centre for Astrophysics, Monash University, VIC3800, Australia
[c] Atomki Institute for Nuclear Research, Hungarian Academy of Sciences, H-4026, Debrecen, Hungary
[d] Max-Planck Institute for Chemistry, D-55128 Mainz, Germany

ARTICLE INFO

Article history:
Available online 22 May 2018

This paper is dedicated to the memory of Gerald J. Wasserburg, who pioneered, built up, and inspired the science presented here.

Keywords:
Nuclear reactions
Nucleosynthesis
Abundances
Stars
Sun
Meteorites

ABSTRACT

In addition to long-lived radioactive nuclei like U and Th isotopes, which have been used to measure the age of the Galaxy, also radioactive nuclei with half-lives between 0.1 and 100 million years (short-lived radionuclides, SLRs) were present in the early Solar System (ESS), as indicated by high-precision meteoritic analysis. We review the most recent meteoritic data and describe the nuclear interaction processes responsible for the creation of SLRs in different types of stars and supernovae. We show how the evolution of radionuclide abundances in the Milky Way Galaxy can be calculated based on their stellar production. By comparing predictions for the evolution of galactic abundances to the meteoritic data we can build up a time line for the nucleosynthetic events that predated the birth of the Sun, and investigate the lifetime of the stellar nursery where the Sun was born. We then review the scenarios for the circumstances and the environment of the birth of the Sun, within such a stellar nursery, that have been invoked to explain the abundances in the ESS of the SLRs with the shortest lives — of the order of million years or less. Finally, we describe how the heat generated by radioactive decay and in particular by the abundant ^{26}Al in the ESS had important consequences for the thermo-mechanical and chemical evolution of planetesimals, and discuss possible implications on the habitability of terrestrial-like planets. We conclude with a set of open questions and future directions related to our understanding of the nucleosynthetic processes responsible for the production of SLRs in stars, their evolution in the Galaxy, the birth of the Sun, and the connection with the habitability of extra-solar planets.

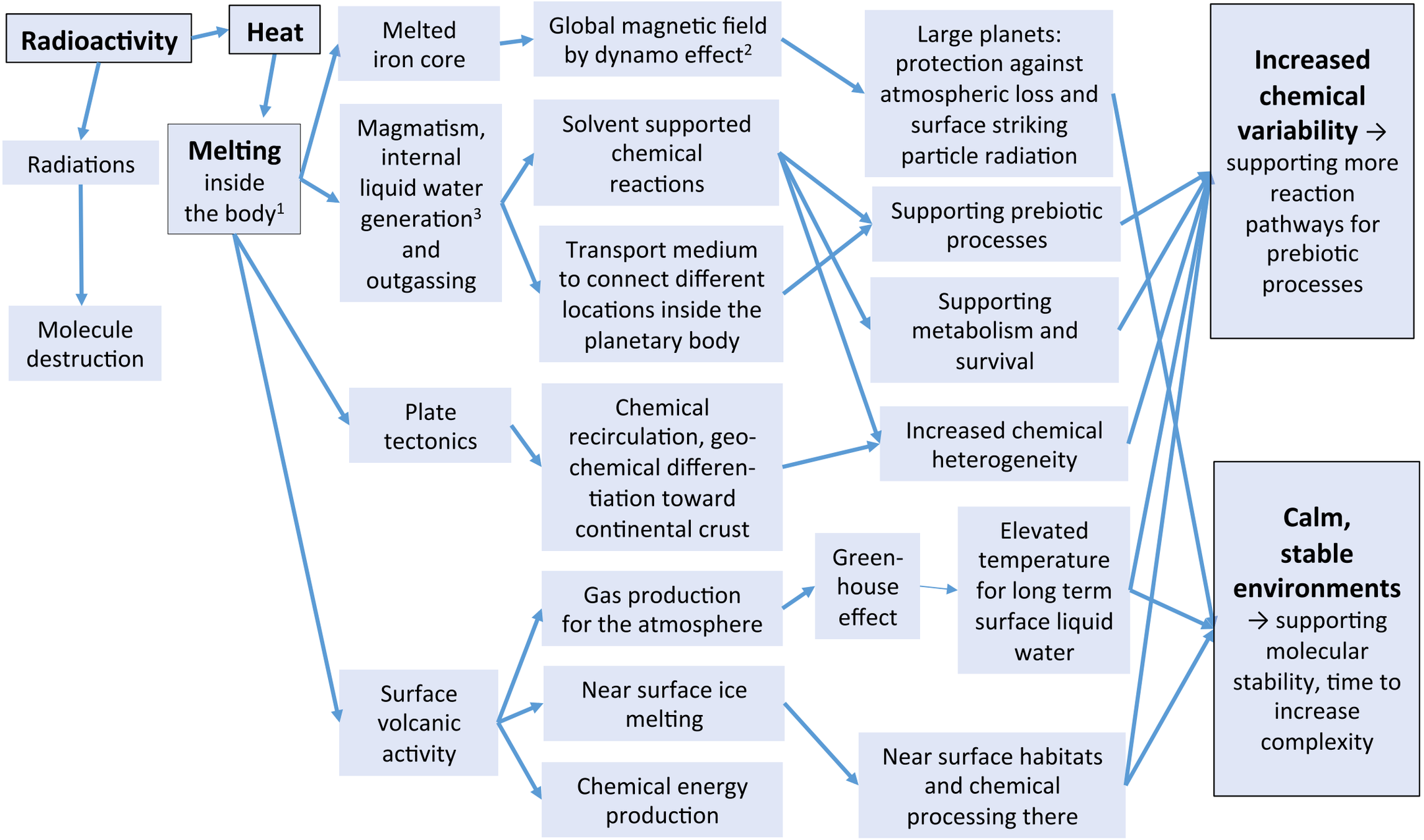

Fig. 6. Possible connections between radioactivity and various factors that influence habitability of solid planetary bodies. Notes according to numbers: 1. Ancient melting was also supported by other processes, including exothermic heat generated by serpentinisation, i.e, the addition of water into the crystal structure of minerals. 2. A very early differentiated iron core is expected to have been present in many planetesimals, based on the paleomagnetic signature of internal magnetic dynamos even in carbonaceous chondrites, where the primitive chondritic material accumulated on the surface of an already differentiated core. 3. Magmatic activity and internal liquid water generation were supported by the SLRs only in the first periods. Later on, long-lived radionuclides became the more important to enable continued activity.

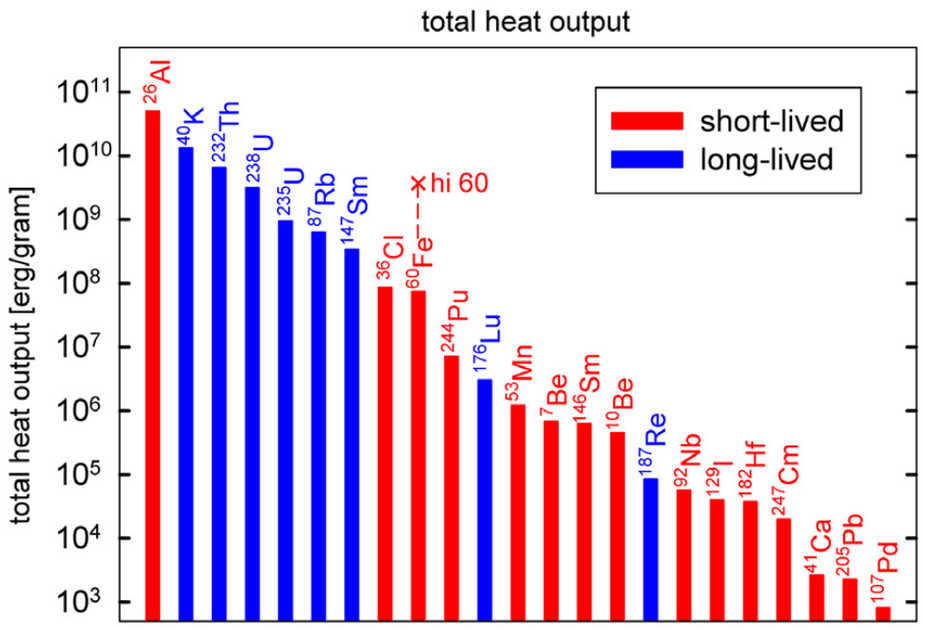

Fig. 15. Total energy available for heating from radioactive decay per gram of material in the Solar System (CI meteorite composition) after the initially present isotope has completely decayed. For ^{10}Be/^{9}Be a value of 1×10^{-3} was used. For ^{60}Fe also the situation for a high abundance (^{60}Fe/^{56}Fe = 5×10^{-7} as compared to 1.01×10^{-8} given in Table 2) is indicated.

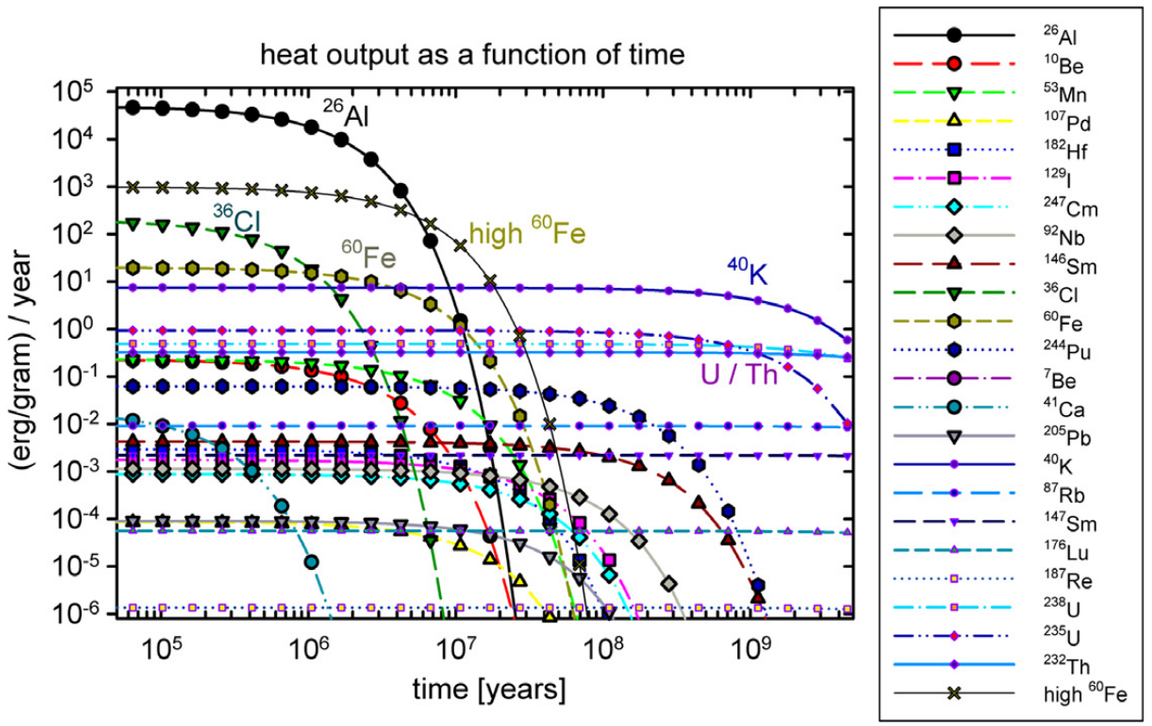

The ^{40}K vs. U/TH curves must be wrong, since ^{40}K half-life is 1.2 Gy, while ^{238}U is 4.5 Gy and ^{232}Th is 14 Gy. Also, much of the ESS potassium must have been lost by the early Earth.

Fig. 16. Net energy output as a function of time, starting 50,000 years after time zero, defined as the time when the nuclei start to decay. For the half-life of ^{146}Sm we used the 103 Myr value. The initial abundances of ^{10}Be and ^{60}Fe are taken as indicated in Fig. 15.

PLANETARY SCIENCE

What makes a planet habitable?

Efforts to identify habitable planets must look beyond atmospheres to planetary interiors

By **Anat Shahar, Peter Driscoll, Alycia Weinberger, George Cody**

The Milky Way Galaxy teems with planetary systems, most of which are unlike our own (*1*). It is tempting to assume that life can only originate on a planet that is similar to Earth, but different kinds of planets may be able to sustain Earth-like features that could be important for habitability. To focus the search for extraterrestrial life, scientists must assess which features of Earth are essential to the development and sustenance of life for billions of years and whether the formation of such planets is common. External effects such as stellar variability and orbital stability can affect habitability, but internal planetary processes that sustain a clement surface are essential to life; these processes are, however, difficult to characterize remotely. A combination of observations, experiments, and modeling are needed to understand the role of planetary interiors on habitability and guide the search for extraterrestrial life.

As exoplanet detection techniques improve, Earth-sized planets are likely to be found in the radiative habitable zone, that is, at distances from their host stars where they could have temperate (about 0° to 100°C) surface temperatures (*2*). This is important because to be habitable, a planet must be able to buffer life from extreme (globally sterilizing) variations in temperature. Launched in 2018, NASA's Transiting Exoplanet Survey Satellite has the capability to find small planets in the habitable zone of nearby stars and measure their radii (*3*). Ground-based telescopes are providing masses for such planets. Their densities provide a first-order constraint on composition, although it is likely that several different possible compositions can be inferred from the same density (*4*). Planets with compositions that differ from those of planets in our Solar System have been largely ignored, even though a wide range of stellar compositions and planetary densities have been discovered. The discovery of life elsewhere in the Solar System, for example on an icy satellite, would also radically expand the types of planets that need to be considered. The James Webb Space Telescope, due to launch in 2021, will attempt to detect atmospheres of the most favorable planets for life, but detailed measurements of atmospheric composition will require future extremely large telescopes on the ground and in space.

Carnegie Institution for Science, Washington, DC, USA. Email: ashahar@carnegiescience.edu

ATMOSPHERIC SIGNATURES OF LIFE

Atmospheric composition will be the primary observable that could imply the presence of life (*5*). However, identifying a biological signature in a planet's atmosphere requires an understanding of the possible compositions of abiotic atmospheres. The presence of free oxygen or an atmosphere out of chemical equilibrium could be signatures of life processes, but neither is definitive because atmospheres change over time and are open systems that are subject to complex sources and sinks. Volcanic eruptions release gases from the planetary interior that are the product of melting and magma migration. Atmospheric weathering can draw down noncondensable species, like carbon dioxide from Earth's atmosphere, to the seafloor, where they can be recycled back into the interior at subduction zones. All these processes are linked to the bulk composition of the planet and will evolve over time.

It remains unclear, therefore, what inferences can be made about the planet's habitability from its atmosphere before understanding more about how the atmosphere is tied to the interior dynamics and evolution of the solid planet. To advance this understanding, exoplanet atmospheres, which give a valuable snapshot of the surface composition, should be combined with experimental and modeling constraints on the interactions between the atmosphere and interior over long time scales.

INTERIOR PROCESSES SUSTAINING LIFE

On Earth, the environment needed for life to exist and be sustained is rooted in the presence of a stable hydrosphere and atmosphere, which are controlled by the planet's bulk composition, interior structure, and dynamics. Plate tectonics plays a crucial role in the long-term moderation of the climate by cycling material between the surface and interior, thereby helping to stabilize the long-term climate, and by cooling the deep interior as hot plumes well up to the surface and cold plates drop down to the core-mantle boundary (*6*). This cooling drives convection and dynamo action (conversion of mechanical to electrical energy) in the liquid-iron outer core, which in turn produces the geomagnetic field that shields the atmosphere and protects the surface from the solar wind (see the figure).

Thus, Earth's interior maintains a stabilizing feedback between the hydrosphere, mantle, and core that is important for long-term habitability (*7*). Climate can also be affected by many external forces, such as stellar variability and orbital fluctuations, but fundamentally, a planet's composition dictates how it responds to these external forces. This prompts the question: Can Earth-like features be produced by planets with alternative compositions?

THE ROLE OF PLANETARY COMPOSITION

The bulk composition of a planet is inherited from the constituents of the protoplanetary disk in which the planet forms, as well as on the planetary building blocks and the mechanisms by which they accumulate to form a planet. Planet-hosting stars are known to span a range of compositions, with considerable variations in the ratios of abundant rocky planet materials such as silicon, magnesium, oxygen, carbon, and iron to hydrogen (*8*). Although the elemental building blocks of planets (such as oxygen, silicon, and iron) are universal, the relative abundances of elements and their processing during planet formation can dramatically alter the ratios of metal, rock, and ice that will set the internal structure of solid bodies (*9*). Compositional variations between exoplanets can arise in a protoplanetary disk when solids coagulate into planetesimals, when the temperature structure of the disk (and therefore locations where ice condenses) change over time, and if the formation of giant planets alters the feeding zones of later-forming rocky planets (10).

These compositional variations will likely produce a range of outcomes for rocky planets. Composition determines the internal material properties associated with heat and mass transport, like melting temperature, thermal and electrical conductivity, viscosity, and the abundance and partitioning of radiogenic isotopes. These properties control the heat budget and thermal evolution of a planet. The amount of water accreted during formation will affect the ocean volume at the surface, which in turn is influenced by water cycling between the surface and the deep Earth. The composition and subsequent partitioning of elements in the interior will determine the oxidation state of the mantle and therefore whether the species that are outgassed to the atmosphere are enriched or reduced (*11*). The physical parameters of high-pressure phases of rock that might exist in deep exoplanetary mantles control their water capacity, rate of heat transfer, likelihood of global convection, and rate of core cooling.

Therefore, the bulk composition and evolution of a planet depend on its formation pathway, accretionary environment, and interior dynamics. However, the implications of planetary composition for the interaction between the surface and interior are almost entirely unexplored.

HOW TO SEARCH FOR HABITABILITY

The physical and chemical changes that a planet undergoes over billions of years—from the composition of the protoplanetary disk, to the differentiation of the planet and the giant impacts it may endure, to the start of plate tectonics and the generation of a magnetic field, and finally to liquid water on a clement surface—are all crucial for understanding habitability. The research needed to coherently investigate these processes cannot be done by scientists in a single discipline in isolation. Observations of stellar, disk, and planetesimal compositions must be combined with experimental studies of mineral physics and melting behavior to serve as inputs to planet formation and geodynamic models. In turn, the results of those modeling efforts will provide feedbacks into the observations and experiments by making predictions and identifying the compositions and material properties that are most important for habitability.

A better understanding of how the bulk composition and the interior of a planet influence habitability is needed to guide the search for the planets and stellar environments where life can thrive and be remotely detected. In the next decade, new extremely large ground- and space-based telescopes will measure the atmospheric compositions of rocky exoplanets and search for biosignatures in the gases (*12*). Humanity will build a library of information about the gaseous envelopes that comprise only a millionth of an exoplanet's mass. To put those measurements in context and to assess which planets may harbor life and sustain it for billions of years, scientists must understand how the bulk of the planet controls the evolution of a stable and clement atmosphere and surface environment. The heart of habitability lies in the planetary interior. ■

Habitable features of exoplanets

On the habitable planet (left), plate tectonics stabilizes the surface climate and cools the interior fast enough to generate a magnetic field that in turn shields the surface from water loss and harmful radiation. On the other planet (right), the stagnant lid insulates the interior, inhibiting magnetic field generation, allowing water loss to space, and rendering the surface too hot and dry for life.

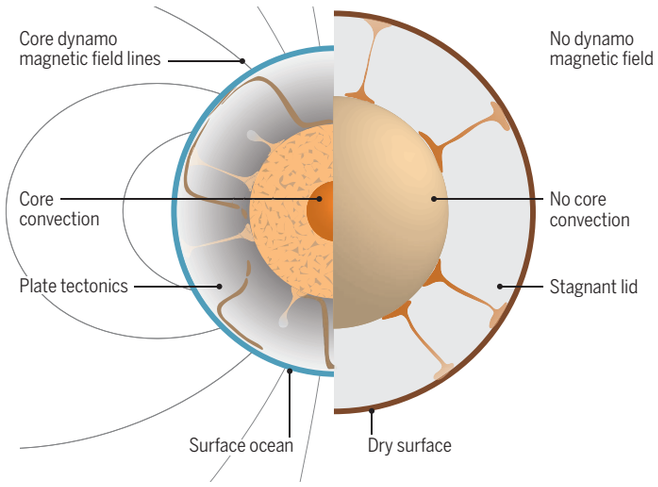

REFERENCES AND NOTES

1. J. N. Winn, in *Handbook of Exoplanets*, H. J. Deeg, J. A. Belmonte, Eds. (Springer, 2018), Volume 1, pp. 1949–1966.
2. G. Anglada-Escudé *et al.*, *Nature* **539**, 437 (2016).
3. L. Kaltenegger, J. Pepper, K. Stassun, K. Oelkers, 2019, *ApJL*, 874:L8 DOI: 10.3847/2041-8213/ab0e8d.
4. L. Zeng, D. D. Sasselov, S. B. Jacobsen, *Astrophys. J.* **819**, 127 (2016).
5. S. Seager, *Science* **340**, 577 (2013).
6. J.C.G. Walker, P.B. Hays, J.F. Kasting, *J. Geophys. Res.* **86** (C10), 9776 (1981).
7. B. J. Foley, P. E. Driscoll, *Geochem. Geophys. Geosyst.* **17**, 1885 (2016).
8. J. M. Brewer, D. A. Fischer, *Astrophys. J. Suppl. Ser.* **237**, 38 (2018).
9. S. Ida, T. Yamamura, S. Okuzumi, *Astron. Astrophys.* **624**, A28 (2019).
10. J. E. Chambers, *ApJ* **825**, 63 (2016).
11. R. D. Wordsworth, L. K. Schaefer, R. A. Fischer, *Astrophys. J.* **155**, 195 (2018).
12. D. Clery, *Science* **358**, 578 (2017).

ACKNOWLEDGMENTS

The authors acknowledge support from the Carnegie Institution for Science.

10.1126/science.aaw4326

Space Sci Rev (2020) 216:37 https://doi.org/10.1007/s11214-020-00656-z

On the Distribution and Variation of Radioactive Heat Producing Elements Within Meteorites, the Earth, and Planets

C. O'Neill[1] · H.S.C. O'Neill[1] · A.M. Jellinek[1] [1] **Planetary Research Centre, Macquarie University, 12 Wally's Walk, Sydney, NSW 2109, Australia**

Abstract The heat production budget of a planet exerts a first order control on its thermal evolution, tectonics, and likelihood for habitability. However, our knowledge of heat producing element concentrations for silicate-metal bodies in the solar system—including Earth—is limited. Here we review the chronicle of heat producing elements (HPEs) in the solar system, from the interstellar medium, to their incorporation in the protoplanetary disk and accreting planetesimals, to later collisional or atmospheric-erosion modifications. We summarise the state of knowledge of the HPEs in terrestrial planets and meteorites, and cur- rent Earth models from emerging constraints, and assess the effect variations may have on the thermal and tectonic history of terrestrial planets.

Some key excerpts: The balance between contemporaneous heat production, and total heat loss, has previously been expressed in terms of the Urey ratio, which is defined as the ratio of internal heat generation, to total system heat loss (Christensen 1985; Lenardic et al. 2011). The most recent estimate for Earth's heat loss is 47 ± 1 TW (Davies and Davies 2010), and for its radiogenic heat production, about 21.5 TW, assuming a geochemical model for the Bulk Silicate Earth (BSE) based on chondrite meteorites (O'Neill 2016). This value gives a planetary Urey ratio of 0.45, implying that less than half of Earth's heat comes from contemporaneous heat production. Non-chondritic BSE models for the concentrations of the HPEs predict even lower values for the Urey ratio (O'Neill and Palme 2008; Jackson and Jellinek 2013).

The three elements contributing to present-day heat production (U, Th and K) share the geochemical characteristic of being incompatible during igneous differentiation of the Earth, and as a result have become concentrated in the Earth's continental crust over geological time, particular into the uppermost continental crust, and perhaps also in deep reservoirs (Labrosse et al. 2007).

Both U and Th are "Refractory Lithophile Elements" (RLEs), which comprise a group of 28 elements that are calculated to condense from the canonical solar nebula at higher temperatures than the main constituents of the rocky planets (i.e. Mg, Si (and associated O) and Fe, the latter initially condensing as metal). The RLEs occur in approximately the same ratios to each other in most undifferentiated meteorites ("chondrites") and, within uncertainty, the solar composition. This observation is assumed to also apply to the Bulk Silicate Earth (known as the "chondritic model" of the Earth's composition), enabling its concentrations of U and Th to be estimated. … By contrast K is not a RLE, but behaves cosmochemically as a moderately volatile element. Therefore, its abundance in the Bulk Silicate Earth is not constrained by the chondritic model, but must be estimated empirically.

Gando et al. (2011) combined results from Borexino and KamLAND to estimate that mantle ^{232}Th and ^{238}U contribute 20.0 +8.8/-8.6 TW to Earth's heat flux. Results from Borexino alone have tended towards higher values (Agostini et al. 2019), and recently, the Borexino team (Agostini et al. 2019) estimated the total radiogenic heat of the Earth at 38.2 +13:6/-12:7 TW (confidence intervals are ±34%), and the total mantle heat contribution of 24.6 TW +11.1/-10.4 from ^{238}U and ^{232}Th. Therefore, even at the 95% confidence interval this estimate would only just be compatible with the largest radiogenic heat production values deduced from geochemistry. We can convert these contributions to mantle concentrations as follows. If we assume the mass of the mantle is 4×10^{24} kg, then a flux of 24.6 TW gives us a mantle heat production from these isotopes of 6.15×10^{-12} W/kg (range of $3.55–8.93 \times 10^{-12}$ W/kg). … Although argued by Agostini et al. (2019) to be marginally consistent with a geodynamic model for mantle heat generation, these values are not consistent with published chondritic or non-chondritic BSE compositions (Table 4). In particular, these results exclude the enstatite-chondrite or non-chondritic Earth models at a high degree of confidence and, thus, more work is required before geoneutrino constraints can be regarded as reliable.

Space Sci Rev (2017) 212:877–898

Water in Extrasolar Planets and Implications for Habitability - Lena Noack[1,2] · Ignas Snellen[3] · Heike Rauer[4,5]

Abstract Exoplanet detection missions have found thousands of planets or planet candidates outside of the Solar System—some of which are in the habitable zone, where liquid water is possible at the surface. We give an overview of the recent progress in observations of water-rich exoplanets, detection of water in the atmosphere of gas giants and less- massive targets, and modelling of the interior and evolution of water layers in exoplanets. We summarise the possible habitability of water-rich planets and discuss the potential of future missions and telescopes towards the detection of water in the atmosphere of low-mass exoplanets or on their surface.

While mass and radius of rocky planets can be observed from space, the interior structure as well as information on thermodynamic properties of the different layers in the interior cannot be observed. Models of possible planet compositions and differentiation processes can help to better understand the thermal evolution of the interior of rocky planets, which influences the subaqueous surface, for example via volcanism and plate tectonics (Noack et al. 2016, 2017).

5.1 Water on Terrestrial Exoplanets

The holy grail in exoplanet research is to discover a potential second Earth. While based on the geophysical definition an Earth-like planet (or rocky planet) would solely require a density indicating a composition of mainly silicate minerals and metals, the "second Earth" is typically expected to have surface oceans like on Earth—and therefore needs to be in the habitable zone. **Just the right mass and radius would not justify to call the detected planet a "second Earth". Some scientists would in addition request the existence of a magnetic field as well as plate tectonics, in other words, a planet that might be able to host complex, Earth-like life (either in its original or present-day form). … Another interesting contribution of plate tectonics is the recycling of water into the mantle and its replenishing at volcanic regions** (Parai and Mukhopadhyay 2012; Höning et al. 2014; Foley 2015), which may be able to lead to stable, shallow ocean layers—even for slightly larger amounts of water than on Earth leading to an enrichment of water in the mantle instead of deeper surface ocean layers for small-massive planets (Schaefer and Sasselov 2015).

L. Noack, D. Breuer, Plate tectonics on rocky exoplanets: influence of initial conditions and rheology. Planet. Space Sci. **98**, 41–49 (2014). doi:10.1016/j.pss.2013.06.020

L. Noack, M. Godolt, P. von Paris, A. Plesa, B. Stracke, D. Breuer, H. Rauer, Constraints for planetary habitability from interior modeling. Planet. Space Sci. **98**, 14–29 (2014)

L. Noack, D. Höning, A. Rivoldini, C. Heistracher, N. Zimov, B. Journaux, H. Lammer, T.V. Hoolst, J.H. Bredehöft, Water-rich planets: how habitable is a water layer deeper than on Earth? Icarus **277**, 215– 236 (2016). doi:10.1016/j.icarus.2016.05.009

L. Noack, D. Höning, A. Rivoldini, C. Heistracher, N. Zimov, B. Journaux, H. Lammer, T. Van Hoolst, J.H. Bredehöft, Water-rich planets: how habitable is a water layer deeper than on Earth? Icarus **277**, 215–236 (2017)

D. Valencia, R.J. O'Connell, D.D. Sasselov, Inevitability of plate tectonics on super-Earths. Astrophys. J. **670**, 45–48 (2007)

H.J. van Heck, P.J. Tackley, Plate tectonics on super-Earths: equally or more likely than on Earth. Earth Planet. Sci. Lett. **310**, 252–261 (2011)

Francis Nimmo's Slide

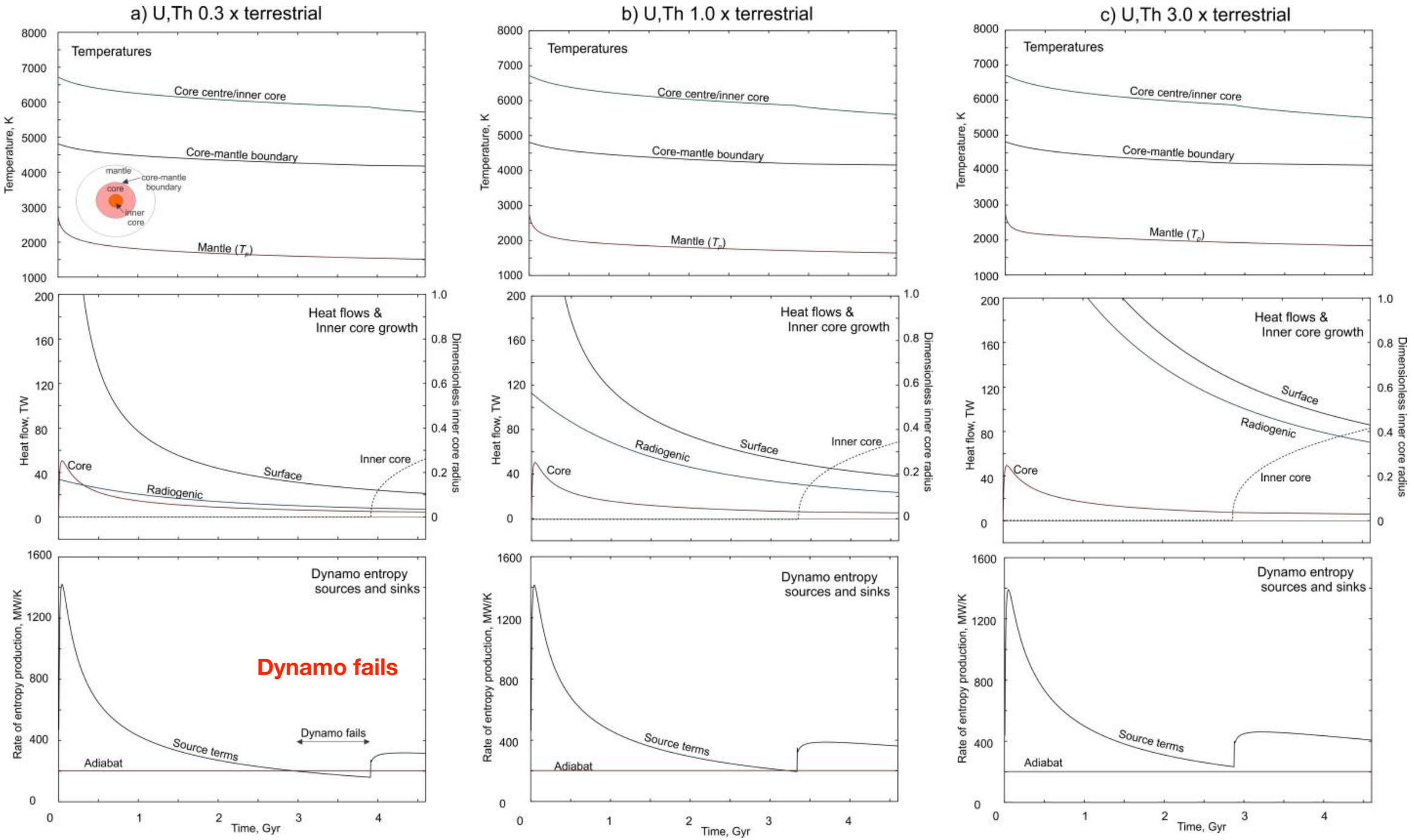

Figures 1a and 1c show how an identical model evolves with the same initial conditions except for 0.3 and 3 times the assumed terrestrial concentrations of U and Th. Less and more radiogenic heating result in colder and warmer present-day mantles (T_p of -133 K and +192 K), respectively. More radiogenic heating results in a slightly larger present-day inner core and a more vigorous dynamo, and vice versa. This effect arises because the strongly temperature-dependent viscosity of the mantle acts as a thermal regulator, as first recognized by [Tozer]. A lower radiogenic heat production results in a cooler, more viscous mantle, with the result that heat fluxes across both the mantle top and bottom are reduced. The reduced heat flux across the base of the mantle results in reduced core cooling and thus a less vigorous dynamo.

- Francis's model shows that Earth may have borderline Th abundance required for a permanent dynamo, if its Eu and Th abundance follows that of the sun and chondrites. Younger (older) thin disk stars have higher (lower) [Eu/Fe], so their younger (older) planets are more (less) likely to have higher radiogenic heat and dynamos.

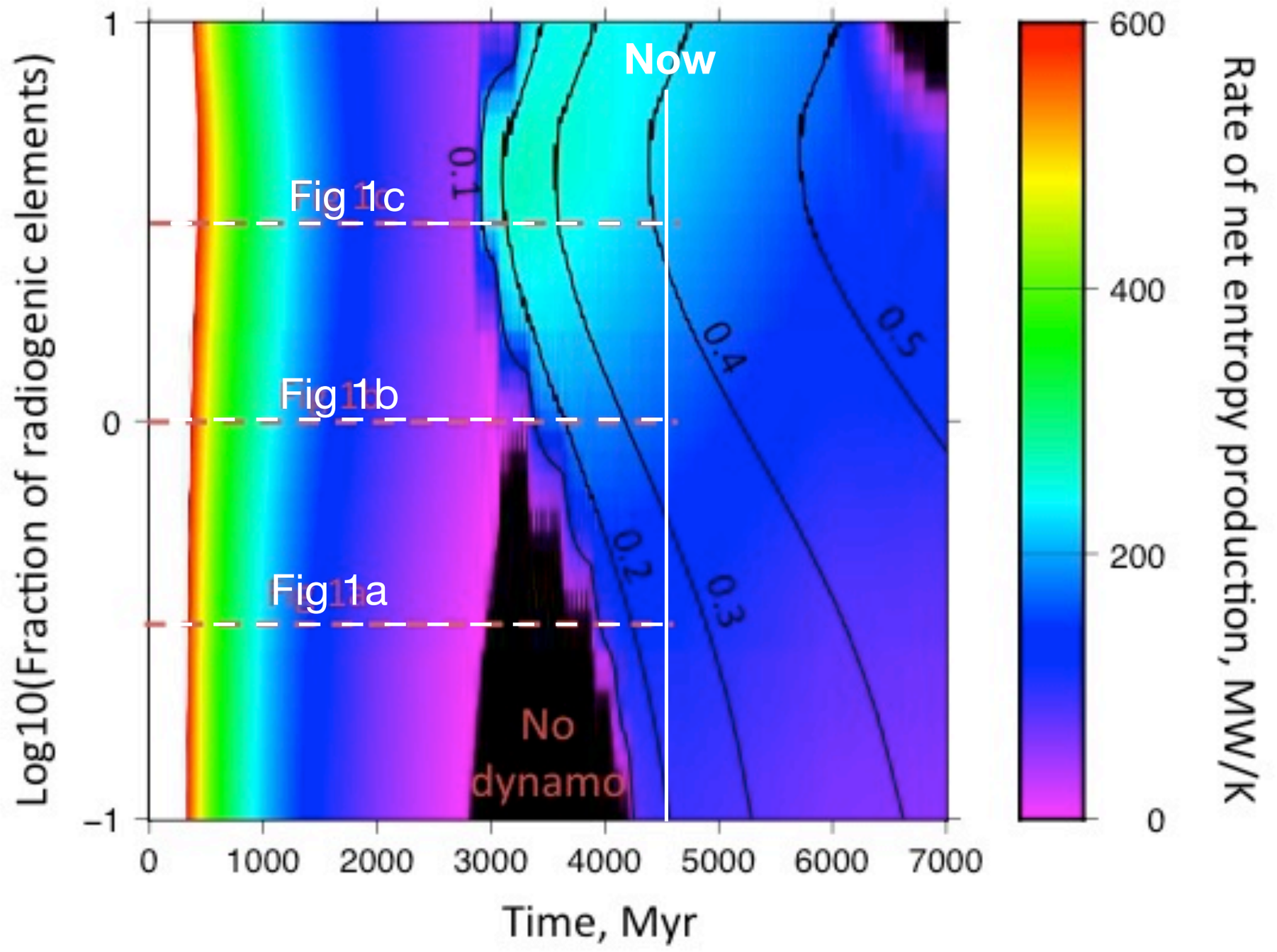

Figure 2. Sensitivity of evolution of core parameters to different radiogenic element concentrations. The colors show the rate of net entropy production, with black indicating a negative value (no dynamo). The contours denote the inner core radius relative to the total core radius. The three dashed red lines show the trajectories of the three evolution scenarios shown in Fig 1. I've added a vertical white line at 4540 Myr, labeled "Now" and changed the red dashed lines to white, for visibility.